Politecnico di Torino

Corso di Laurea Magistrale in Ingegneria Civile
Orientamento Idraulica
A.a. 2025/2026
Sessione di Laurea Luglio 2026

Hydraulic study of filling jet through openings in gate of navigation lock

Relatore:
Prof. Davide Poggi
Prof. dr. ir. Tom De Mulder

Candidato:
Tommaso Baricelli

Il presente progetto di tesi magistrale è stato svolto presso la Ghent University (Università di Gent) nell'ambito del programma di mobilità Erasmus+. La presente versione dell'elaborato è stata adattata ai requisiti del Politecnico di Torino ai fini del conseguimento della Laurea Magistrale.

L'attività di ricerca è stata supervisionata da docenti della Ghent University e da tutor di Flanders Hydraulics, ente di ricerca con il quale il progetto di tesi è stato sviluppato in collaborazione.

Luglio, 2026.

GHENT UNIVERSITY

1859

Politecnico di Torino

Master’s Thesis:

HYDRAULIC STUDY OF FILLING JET THROUGH OPENINGS IN GATE OF NAVIGATION LOCK

Tommaso Baricelli

Student number: 02510216

Supervisor: Prof. dr. ir. Tom De Mulder

Counsellors: Ir. Kristof Verelst (Waterbouwkundig Laboratorium), Dr. ir. Santiago Lopez Castaño (Waterbouwkundig Laboratorium), ir. Alemu Tezera Dessie.

Master's dissertation submitted in order to obtain the degree of Master of Science in Civil Engineering

Academic year 2025-2026

GHENT UNIVERSITY

Politecnico di Torino

May 28, 2026.

GHENT UNIVERSITY

1859

Politecnico di Torino

ACKNOWLEDGEMENTS

First, I would like to sincerely thank my supervisor, Professor Dr. Ir. Tom De Mulder, for proposing this thesis topic, which became more and more fascinating to me throughout my experience here in Belgium. I am deeply grateful for his continuous support, his availability whenever I needed guidance, and for the precise advice and detailed explanations he always provided during the development of this work.

I would also like to thank Ir. Alemu Tezera Dessie for valuable feedback and suggestions received during the thesis process.

A special and heartfelt thanks go to Flanders Hydraulics for opening its doors to me and giving me the opportunity to work inside its laboratories and use its measurement equipment during this research. Being able to carry out the experimental campaign in such an environment has been an incredible experience both academically and personally.

I would like to thank Ir. Kristof Verelst, who was always by my side during all phases of the work. I am grateful to Ir. Jurgen Latte for helping me understand and start the laboratory activities, and I would like to infinitely thank Dr. Ir. Santiago Lopez Castaño, without whom it would not have been possible to begin the measurement campaign. His support was fundamental throughout the experimental work.

I would also like to dedicate a few words to the experience that concluded with this thesis. This year in Belgium has been an incredibly intense experience for me. It feels like a lifetime has passed since I first arrived in a new country, full of curiosity and uncertainty about what this experience would become. In the end, it was “just” one year, but during this time I lived incredible experiences, met special people, and learned that every place can feel like home if you truly live the experience. Maybe one day we will meet again, but for now: *Dankjewel Gent!*

Finally, I would like to thank everyone who supported me throughout this journey, both during the thesis and during my experience in Belgium. Thanks to all the friends I met here, to the many friends who came to visit me and made me feel their closeness, and to those who could not come but were always present regardless of the distance.

A final and enormous thank you goes to my family, and especially to my parents, who support every decision and experience of my life unconditionally. I know that being far away from each other for such a long time has not always been easy, but I am truly grateful for all the incredible opportunities you have given me during these university years.

Vi voglio tanto bene!

Tommaso Baricelli

May 28, 2026.

Hydraulic study of filling jet through openings in gate of navigation lock

Tommaso Baricelli

Supervisors: Prof. dr. ir. Tom De Mulder, ir. Kristof Verelst (Waterbouwkundig Laboratorium), Dr. ir. Santiago Lopez Castaño (Waterbouwkundig Laboratorium), ir. Alemu Tezera Dessie.

Abstract — **The hydraulic behaviour of filling jets inside navigation locks strongly influences momentum redistribution and the hydrodynamic forces acting on vessels during filling operations. Reduced-order numerical tools such as VUL_SLUIS are commonly used to estimate flow conditions while maintaining limited computational requirements. However, the adopted jet schematization does not always reproduce accurately the downstream evolution of the filling jet.**

This research investigates turbulent filling jets generated through concentrated openings in navigation lock gates using a combined numerical and experimental approach. Experimental measurements were performed at Flanders Hydraulics using a physical scale model and Particle Tracking Velocimetry techniques.

Comparisons with the original VUL_SLUIS implementation revealed discrepancies regarding jet spreading, downstream sinking behaviour, and wall-jet development. Based on experimental observations, a modified jet parametrization was proposed combining a LoMo-inspired spreading law, continuous sinking formulation, Gaussian velocity reconstruction, wall-jet transition, and ship-dependent corrections.

The modified model showed improved agreement with the experimental measurements while preserving the reduced-order computational philosophy required for engineering-oriented lock-filling simulations.

Keywords — **Navigation locks, filling jets, VUL_SLUIS, PTV, wall jets, reduced-order hydraulic modelling.**

I. INTRODUCTION

During filling operations in navigation locks, large discharges enter the lock chamber through concentrated openings in the gate and generate highly turbulent jet flows. These jets redistribute momentum inside the chamber and influence the hydrodynamic conditions acting around moored vessels. The downstream development of the jet therefore plays an important role in lock operability and in the prediction of forces acting on ships.

Engineering-oriented numerical tools such as VUL_SLUIS are commonly used to estimate these hydraulic conditions through reduced-order formulations. In the current implementation, the downstream jet development is reconstructed using a simplified schematization derived from classical turbulent jet theory. However, previous studies and preliminary observations indicated that the reconstructed velocity profiles do not always reproduce accurately the experimentally observed behaviour of the filling jet, particularly regarding jet spreading, wall attachment, and downstream sinking toward the bottom boundary.

The present work investigates the downstream evolution of turbulent filling jets generated through openings in navigation lock gates using a combined numerical and experimental approach. Experimental velocity measurements were performed at Flanders Hydraulics using Particle Tracking Velocimetry techniques for different hydraulic and geometrical configurations, both with and without the presence of a vessel inside the lock chamber.

The experimental observations were subsequently compared with the original VUL_SLUIS implementation to evaluate the capability of the current schematization to reproduce the measured flow behaviour. Based on the observed discrepancies, a modified jet parametrization was developed and calibrated against the experimental measurements. The proposed formulation aims to improve the reconstruction of the downstream velocity field while preserving the reduced-order computational philosophy of VUL_SLUIS.

II. SETUP FOR THE SCALE MODEL

The experimental investigations were performed at the hydraulic laboratory of Flanders Hydraulics in Antwerp using the PTV flume facility. The setup consists of a closed-loop hydraulic flume with transparent side walls allowing optical access for Particle Tracking Velocimetry measurements. The flume has a total length of 4.0 m, a width of 0.40 m, and a height of 0.40 m.

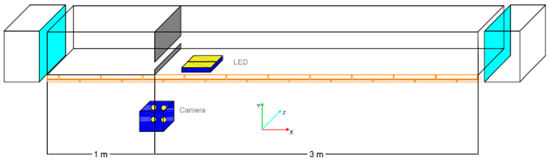

Picture 1. PTV flume setup

The present study focuses on filling jets generated through concentrated openings in the gate of a navigation lock. For this purpose, a simplified lock-gate configuration was installed inside the flume. Two rectangular opening heights were investigated during the experiments, namely 0.03 m and 0.06 m. Different hydraulic conditions were reproduced by varying the hydraulic head difference across the gate.

A simplified vessel geometry was additionally introduced in several configurations to analyse the influence of under-keel confinement on the downstream development of the jet. Different ship positions and keel clearances were tested to investigate the interaction between the jet trajectory and the vessel bottom.

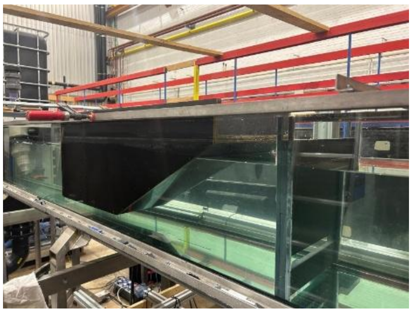

Picture 2. Gate and Ship Setup

The hydraulic conditions inside the flume were controlled through a recirculating pump system. The discharge circulating through the setup was monitored using a flowmeter installed below the flume within the hydraulic circuit, while the corresponding water levels were measured using a graduated water level gauge.

III. MINISHAKER MEASUREMENTS AND RESULTS

The MiniShaker measurements provided detailed insight into the downstream evolution of the turbulent filling jet generated through the gate opening. Averaged velocity fields and vertical velocity profiles were reconstructed for different hydraulic and geometrical configurations in order to analyse the spreading behaviour of the jet, the downstream movement of the velocity core, and the influence of the vessel on the flow structure beneath the hull.

The measurements showed that the filling jet initially propagates almost horizontally after exiting the gate opening. Further downstream, turbulent mixing with the surrounding water causes progressive spreading of the velocity together with a gradual downward movement of the jet toward the bottom boundary. At larger downstream distances, the flow progressively evolves into a wall-jet-like configuration characterized by maximum velocities located close to the bed.

A. Without ship

The measurements performed without the presence of the vessel allowed the fundamental behaviour of the turbulent filling jet to be analysed independently from under-keel confinement effects.

The experimental results showed that smaller gate openings generate thinner jets characterized by stronger relative entrainment and faster downward deflection toward the bottom boundary. Larger openings instead produce thicker jets with larger momentum fluxes, allowing the jet to remain detached from the bottom over longer downstream distances.

The downstream velocity profiles additionally revealed that the jet becomes progressively asymmetric while approaching the bottom boundary, eventually developing into a wall jet with upward velocity decay only.

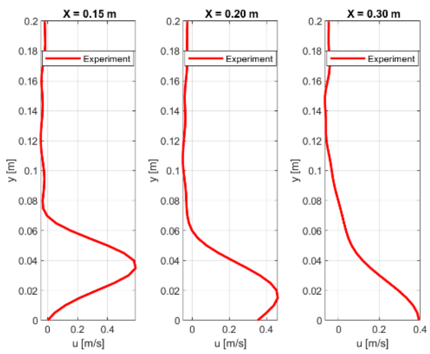

Picture 3. Velocity Profile's behaviour along different positions.

B. With ship

The experiments performed with the presence of the vessel demonstrated that under-keel confinement modifies the downstream development of the filling jet beneath the hull.

The measurements showed that the vessel affects both the trajectory and the concentration of the velocity core. For smaller keel clearances, the jet remained more confined beneath the vessel and the downstream sinking behaviour was reduced compared with the no-ship configurations.

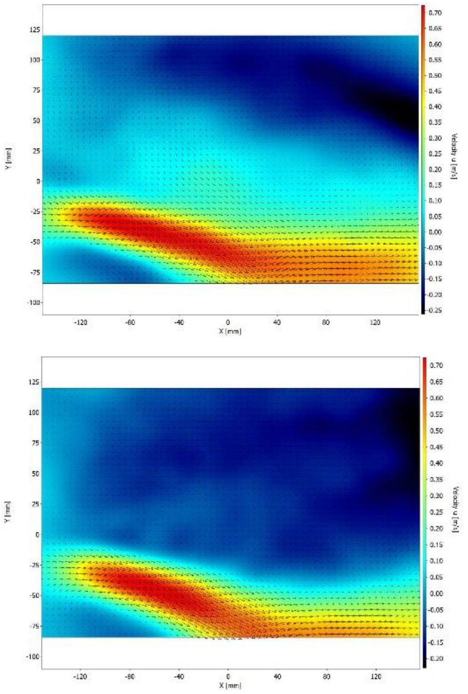

Picture 4. Average velocity fields with and without ship.

The position of the bow relative to the jet trajectory also influenced the downstream velocity distribution, indicating that the vessel should not only be considered during the force calculation stage but also directly within the jet schematization itself.

IV. ANALYSIS OF THE JET ON VUL_SLUIS

The objective of this analysis was to investigate how the software reconstructs the downstream evolution of the filling jet inside the lock chamber and how the resulting velocity profiles change depending on opening height, hydraulic head difference, vessel position, and imposed jet angle.

The original VUL_SLUIS implementation reconstructs the downstream velocity field through a simplified turbulent jet schematization derived from Vrijburcht et al. (1988). The jet spreads progressively downstream according to analytical relations describing turbulent mixing and momentum redistribution. The velocity profiles are reconstructed through a symmetric formulation around the jet centreline, while the downstream sinking behaviour can only be reproduced by manually imposing a non-zero jet inclination angle in the input parameters.

The analyses showed that the reconstructed profiles remain relatively smooth and vertically distributed throughout the water depth. When the jet inclination angle is set equal to zero, the jet remains approximately centred within the water column and does not progressively move toward the bottom boundary.

The analyses additionally highlighted that the presence of the vessel affects the force calculations but does not directly modify the jet schematization itself. Consequently, the reconstructed downstream jet development remains governed by the same geometrical formulation independently from the ship configuration.

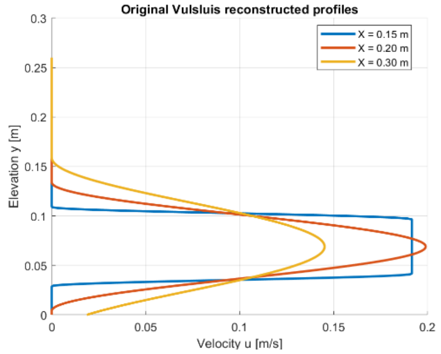

Picture 5. Original VUL_SLUIS profiles.

V. COMPARISON

The comparison between the MiniShaker measurements and the original VUL_SLUIS implementation revealed several systematic differences in the reconstructed velocity profiles. The analysis focused mainly on the downstream spreading of the jet and on the sinking behaviour of the velocity core toward the bottom boundary.

The experimental measurements showed more concentrated velocity cores and stronger velocity gradients compared with the smoother and more vertically distributed profiles reconstructed by VUL_SLUIS. Without imposing a jet inclination angle, the numerical profiles remained approximately centred within the water column and did not reproduce the experimentally observed downward movement of the jet.

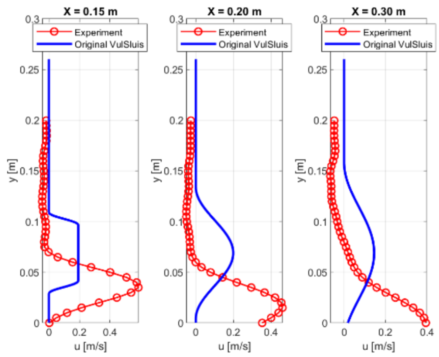

Picture 6. Comparison without jet inclination angle

Additional comparisons were therefore performed by introducing a non-zero jet inclination angle in the VUL_SLUIS input parameters. This modification improved the agreement regarding the downstream jet trajectory, although the reconstructed profiles remained strongly dependent on the selected angle.

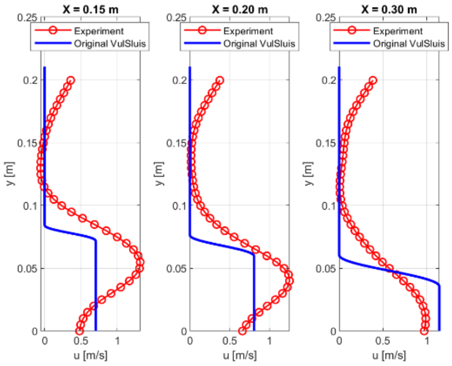

Picture 7. Comparison imposing a jet inclination angle

The comparisons also highlighted that the experimental jet progressively evolves into a wall jet attached to the bottom boundary, whereas the original VUL_SLUIS schematization tends to maintain more symmetric velocity distributions further downstream.

VI. SOLUTION FOR NEW SCHEMATIZATION

A. PARAMETRIZATION

The modified formulation combines a LoMo-inspired spreading law with a continuous sinking parametrization introduced in the present research. The effective jet thickness is expressed as:

$$A_{jet} = c_0 H_{VS} + c_1 c_2 X^{c_3}$$

where H_{VS} represents the opening height, X the downstream distance, and c_2 and c_3 control the downstream spreading behaviour of the jet (Belzner et al, 2018).

The downstream movement of the jet centreline is reconstructed through an exponential sinking formulation:

$$y_c(x) = y_{floor} + (y_0 - y_{floor})e^{-k_s X/H_{VS}}$$

allowing the jet to progressively move toward the bottom boundary and evolve into a wall jet configuration.

The downstream velocity profiles are reconstructed through Gaussian distributions calibrated directly against the experimental measurements:

$$u(y) = u_{max} \exp\left[-\frac{(y - y_c)^2}{2\sigma^2}\right]$$

An opening-dependent correction was introduced to account for the experimentally observed differences between the 0.03 m and 0.06 m opening configurations:

$$factor_{eff} = factor\left(\frac{H_{VS}}{H_{ref}}\right)^{\alpha}$$

with $H_{ref} = 0.03$ m reference to the smallest tested opening height used as reference during the calibration procedure.

When the jet approaches the bottom boundary, the model automatically switches toward a half-Gaussian wall-jet formulation (Schwartz et al., 1960):

$$u(y) \propto \exp\left[-\frac{1}{2}\left(\frac{y}{\sigma_{wall}}\right)^2\right]$$

Finally, additional ship-dependent corrections were introduced to account for the influence of under-keel confinement on the jet trajectory:

$$k_s = k_{s,base} + a_1 k_c + a_2 X_{bow}$$

where k_c represents the keel clearance and X_{bow} the longitudinal distance between the gate and the vessel bow.

B. CALIBRATION

The calibration procedure was performed using the velocity profiles extracted from the MiniShaker measurements. The optimization aimed to identify a single parameter set capable of reproducing the downstream jet evolution for the different hydraulic and geometrical configurations.

The calibration minimized a global objective function combining the error on the velocity profiles, the peak velocity, and the vertical position of the jet core. The errors were normalized using a characteristic velocity scale to compare cases characterized by different hydraulic head differences.

The first calibration stage was performed using the no-ship configurations to determine the fundamental parameters controlling jet spreading and sinking behaviour:

Parameter	Value
c_2	0.010256
c_3	1.999999
$k_{s,0}$	0.500000
$factor$	3.000000
α	1.123021

Table 1. Calibrated Parameters without ship.

A second calibration stage was subsequently performed for the ship configurations in order to determine the ship-dependent correction coefficients:

Parameter	Value
a_1	0.013292
a_2	0.024134

Table 2. Calibrated Parameters with ship

The calibrated parameter set provided improved agreement between the reconstructed and experimental velocity profiles while preserving stable downstream behaviour for all analysed configurations.

C. PROFILES

The new profiles reproduced more realistically the concentration of the velocity core, the progressive sinking behaviour, and the downstream transition toward a wall jet attached to the bottom boundary. The Gaussian reconstruction additionally reduced the excessive vertical spreading observed in the original schematization.

The ship-dependent correction also allowed the downstream jet trajectory to adapt automatically to different vessel positions and under-keel clearances, introducing for the first time a direct influence of the vessel within the jet reconstruction itself.

The following figures compare the experimental measurements, the original VUL_SLUIS profiles, and the profiles reconstructed using the modified parametrization.

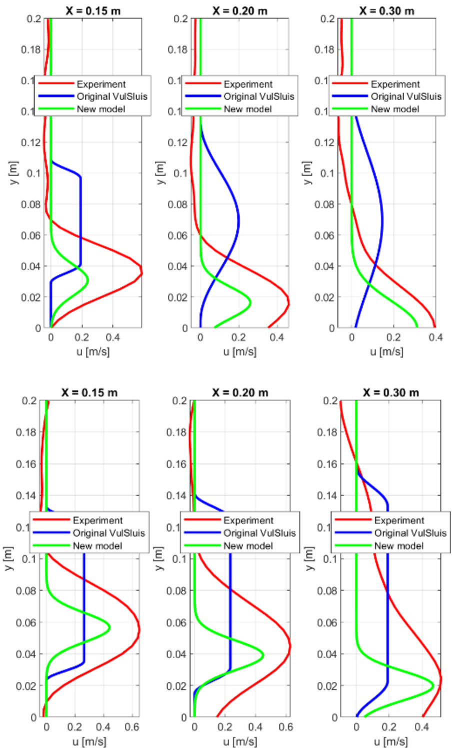

Picture 8. New profile with old and experimental ones without and with ship

VII. CONCLUSIONS & RECOMMENDATIONS

A. CONCLUSIONS

The analyses presented in this research demonstrated that the original VUL_SLUIS jet schematization reproduces the general behaviour of turbulent filling jets but does not accurately capture several important hydraulic characteristics observed experimentally. Discrepancies were identified regarding jet concentration, downstream sinking behaviour, and wall-jet development.

The MiniShaker measurements showed that the filling jet progressively moves toward the bottom boundary and evolves into a wall jet configuration, while the original VUL_SLUIS implementation tends to maintain more symmetric and vertically distributed velocity profiles. The experiments additionally highlighted the influence of the vessel on the downstream jet trajectory beneath the hull.

Based on these observations, a modified jet parametrization was developed combining a LoMo-inspired spreading law, continuous sinking formulation, Gaussian velocity reconstruction, wall-jet transition, and ship-dependent corrections calibrated directly against the experimental measurements.

The modified formulation showed improved agreement with the measured velocity profiles while preserving the reduced-order computational philosophy required for engineering-oriented lock-filling simulations. The force analyses additionally demonstrated that modifications of the jet schematization directly influence the reconstructed jet-related force contributions acting on the vessel.

B. RECOMMENDATIONS

Although the modified parametrization improved the agreement with the experimental observations, additional experimental investigations would be required to further validate and generalize the proposed formulation. In particular, a larger number of ship configurations and hydraulic conditions could improve the stability of the calibrated ship-dependent parameters.

The present research mainly focused on the two-dimensional evolution of the filling jet. Future investigations should therefore analyse possible three-dimensional effects across the lock width and their influence on the downstream momentum redistribution.

Additional measurements closer to the gate opening could also improve the understanding of the initial jet development region, which remained difficult to analyse accurately through the present PTV measurements.

Finally, the proposed methodology could be extended toward more advanced reduced-order hydraulic models capable of directly coupling the downstream jet reconstruction with the resulting hydrodynamic forces acting on the vessel during complete lock-filling operations.

REFERENCES

[1] Belzner Fabian, Simons Franz, and Thorenz Carsten (2018). 'An Application-Oriented Model for Lock Filling Processes'. In proceedings 34th PIANC-World Congress. Pp. 19.

[2] Schwarz, W.H. and Cosart, W.P. (1961) 'The two-dimensional turbulent wall-jet', *Journal of Fluid Mechanics*, 10(4), pp. 481–495.

[3] Vrijburcht, A. (1988). Het vulproces van een schutsluis met een langsvulsysteem. Q176 deel II augustus 1988. Waterloopkundig Laboratorium; Delft Hydraulics Laboratory.

TABLE OF CONTENTS

LIST OF FIGURES

LIST OF TABLES

1 INTRODUCTION

The hydraulic behaviour of filling jets plays a fundamental role in the performance and safety of navigation lock operations. Navigation locks are essential hydraulic structures that allow vessels to move between water bodies characterized by different water levels. During filling and emptying operations, large discharges enter or leave the lock chamber through concentrated hydraulic systems such as gate openings or culverts, generating highly turbulent flow structures inside the chamber. Different filling systems can be adopted in navigation locks, including longitudinal culverts with side ports, bottom filling systems, or concentrated openings located directly in the lock gates. The present research specifically focuses on this latter configuration, namely filling jets generated through concentrated openings in the gate of a navigation lock.

The hydraulic behaviour of these flows strongly influences both operational efficiency and navigational safety. Concentrated filling jets generate complex velocity distributions and momentum redistribution processes that may induce significant longitudinal and transverse forces on vessels moored inside the lock. Excessive velocities or unfavourable flow patterns can compromise mooring stability and reduce the operability of the lock system.

For this reason, numerical tools are used during the design and assessment phases of navigation locks to estimate flow conditions and vessel forces during filling and emptying operations. Among these tools, reduced-order hydraulic models occupy an important position because they provide computationally efficient approximations of complex hydraulic phenomena while remaining suitable for engineering applications and operational studies.

VUL_SLUIS belongs to this class of engineering-oriented reduced-order models. Developed as a MATLAB-based computational framework, the software simulates hydraulic processes occurring during lock filling and emptying operations by combining simplified formulations for discharge, momentum redistribution, velocity distributions, and force calculations acting on vessels inside the lock chamber. Within VUL_SLUIS, the filling jet generated through concentrated gate openings is reconstructed through a simplified turbulent jet schematization derived from Vrijburcht et al. (1988).

Although this formulation captures the general behaviour of turbulent filling jets, several limitations emerge when the numerical reconstruction is compared with physical observations. In particular, the current implementation tends to generate velocity profiles that remain excessively symmetric and vertically diffused compared with experimentally observed flow fields. Furthermore, the downward movement of the jet towards the bottom boundary, commonly observed in physical filling jets developing into wall jets, can only be reproduced by manually imposing a jet inclination angle within the model input parameters.

An additional limitation concerns the interaction between the filling jet and the vessel inside the lock chamber. In the current VUL_SLUIS implementation, the vessel influences the subsequent force calculations but does not directly modify the jet reconstruction itself. Consequently, the under-keel confinement generated by the ship is not explicitly included in the downstream evolution of the velocity field. Experimental observations nevertheless indicate that the presence of the vessel affects the spreading, concentration, and sinking behaviour of the jet beneath the hull.

The present thesis originates from the need to improve the physical representation of filling jets within reduced-order hydraulic models while preserving the computational efficiency required for engineering applications. The research focuses on the downstream development of turbulent filling jets and on the introduction of experimentally calibrated corrections within the VUL_SLUIS jet schematization.

The study combines numerical analyses performed with VUL_SLUIS and experimental investigations carried out through physical scale model tests at the hydraulic laboratory of Flanders Hydraulics in Antwerp. The experimental campaign is based on Particle Tracking Velocimetry (PTV) measurements performed using the MiniShaker system and the DaVis processing environment. These measurements allowed detailed velocity fields to be reconstructed for different hydraulic and geometrical configurations and made it possible to analyse experimentally the downstream behaviour of the filling jet.

Focus is given to the spreading behaviour of the jet, the progressive sinking of the velocity core toward the bottom boundary, the transition towards wall-jet behaviour, and the influence of under-keel confinement generated by the vessel. The experimental measurements are subsequently compared with the velocity profiles reconstructed through the original VUL_SLUIS implementation in order to identify the principal discrepancies between the numerical schematization and the observed hydraulic behaviour.

Based on these observations, a modified jet parametrization is proposed for implementation within VUL_SLUIS. The proposed formulation combines a LoMo-inspired spreading law with a new sinking parametrization introduced within the present research. The downstream velocity profiles are reconstructed through Gaussian distributions calibrated directly against the experimental measurements. Attention is devoted to replacing the manually imposed jet inclination angle currently required by VUL_SLUIS with a continuous sinking formulation emerging directly from the calibration against the experimental data.

The proposed methodology does not aim to reproduce the complete turbulent flow field in detail, as would be possible through high-fidelity CFD simulations. Instead, the objective is to improve the physical realism of the reduced-order jet schematization while maintaining compatibility with the existing VUL_SLUIS computational structure and preserving its computational efficiency.

The present work is partially inspired by previous investigations conducted at Delft University of Technology concerning lock-filling hydraulics and longitudinal ship forces, particularly the work of Van Loon involving LOCKFILL simulations and physical scale model tests (Van Loon, TU Delft, 2017). Whereas these earlier studies focused primarily on the forces acting on the vessel, the present research concentrates directly on the hydraulic behaviour and parametrization of the filling jet itself through detailed velocity measurements obtained using PTV techniques.

The broader objective of this thesis is therefore to establish a better understanding of the interaction between turbulent filling jets and vessels inside navigation locks and to provide a first step toward an improved reduced-order representation of filling jets within VUL_SLUIS. The proposed approach demonstrates how experimental velocity measurements can be integrated into engineering-oriented hydraulic models to improve the reconstruction of filling jets while still preserving the computational efficiency required for practical lock-filling simulations.

1.1 Problem Definition

The present research addresses the limitations associated with the current representation of filling jets within VUL_SLUIS. At present, the software reconstructs the downstream velocity field through simplified analytical relations derived from idealized turbulent jet theory. Although this formulation reproduces the general spreading behaviour of the jet, it does not fully capture several important hydraulic phenomena observed experimentally.

Comparisons with physical measurements reveal that the current VUL_SLUIS implementation tends to overestimate the vertical spreading of the jet while underestimating the progressive downward deflection of the velocity core. In addition, the sinking behaviour of the jet depends strongly on a manually imposed inclination angle, making the reconstruction highly sensitive to a case-specific external input parameter.

The vessel additionally does not directly influence the jet reconstruction itself. Consequently, under-keel confinement effects observed experimentally are not represented explicitly within the downstream evolution of the velocity field.

The research problem can therefore be formulated as follows:

Does the presence of a vessel influence the hydraulic behaviour of filling jets inside a navigation lock chamber, and how can this interaction be incorporated into the VUL_SLUIS jet schematization through a physically consistent reduced-order parametrization?

1.2 Objective and Research Questions

The primary objective of this thesis is to improve the understanding and numerical representation of filling jets inside navigation locks through a combined numerical and experimental investigation.

The study focuses on:

- analysing the current jet representation implemented in VUL_SLUIS;
- investigating the hydraulic behaviour of filling jets through scale model experiments;
- comparing numerical and experimental velocity fields;
- proposing modifications to the existing jet parametrization.

The following research questions are defined:

1. How are filling jet velocities currently calculated in VUL_SLUIS?
2. How does the presence of a vessel modify the jet structure and velocity distribution inside the lock chamber?
3. What differences can be identified between the numerical results produced by VUL_SLUIS and the experimental measurements obtained through PTV analysis?
4. How can the current jet schematization in VUL_SLUIS be improved in order to better reproduce the observed hydraulic behaviour?

1.3 Research Methodology

The methodology adopted in this thesis combines numerical analyses and experimental investigations.

The first phase consists of analysing the current VUL_SLUIS implementation and the assumptions governing the reconstruction of filling jets inside the lock chamber. Particular attention is devoted to the downstream evolution of the velocity profiles and to the role of the jet inclination angle currently required by the software.

The second phase involves experimental investigations performed on a physical scale model at Flanders Hydraulics in Antwerp. Velocity measurements are conducted using Particle Tracking Velocimetry through the MiniShaker system and the DaVis processing environment. Different hydraulic and geometrical configurations are analysed both with and without the presence of the vessel inside the lock chamber.

The third phase consists of comparing the experimental velocity profiles with the numerical profiles reconstructed through VUL_SLUIS. The analysis focuses primarily on jet spreading, velocity concentration, downstream sinking behaviour, and wall-jet development.

Finally, a modified jet parametrization is proposed and integrated conceptually within the VUL_SLUIS framework. The modified formulation is calibrated against the experimental measurements in order to improve the agreement between the numerical reconstruction and the observed hydraulic behaviour while preserving the computational efficiency of the original model.

1.4 Thesis Outline

The remainder of this thesis is organized as follows.

Chapter 2 describes the experimental setup developed at Flanders Hydraulics, including the scale model configuration, hydraulic conditions, MiniShaker setup, and PTV measurement methodology.

Chapter 3 presents the experimental measurements and analyses the downstream behaviour of the filling jet under different hydraulic and geometrical configurations.

Chapter 4 introduces the current VUL_SLUIS implementation and describes the existing jet schematization used to reconstruct velocity profiles inside the lock chamber.

Chapter 5 presents the comparison between the experimental measurements and the original VUL_SLUIS velocity profiles, highlighting the principal discrepancies between the numerical reconstruction and the observed hydraulic behaviour.

Chapter 6 introduces the modified jet parametrization proposed within the present research, including the calibration methodology and the comparison between the new schematization and the experimental profiles.

Chapter 7 discusses the overall results of the research, analyses the principal improvements introduced by the modified parametrization, and evaluates the limitations of the present work.

Finally, Chapter 8 summarizes the main conclusions of the thesis and provides recommendations for future developments and further research.

2 SETUP FOR THE SCALE MODEL

2.1 PTV Flume

The experimental measurements performed within the framework of this research were conducted in the PTV flume facility at Flanders Hydraulics, located in Antwerp, Belgium (Waterbouwkundig Laboratorium). The flume is specifically designed for advanced optical flow visualisation techniques, including Particle Tracking Velocimetry (PTV) and Particle Image Velocimetry (PIV), making it particularly suitable for detailed hydraulic investigations involving complex flow structures.

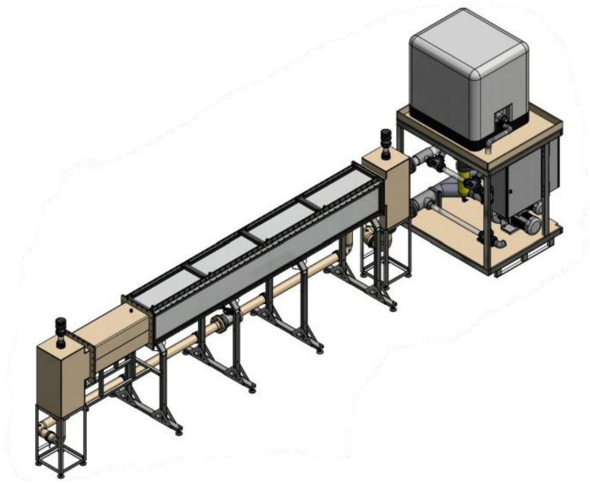

Figure 1. PTV flume in Waterbouwkundig Laboratorium in Antwerp.

The facility consists of a small closed-loop hydraulic flume with high visual accessibility, allowing accurate optical measurements of particle motion within the flow field. The transparent and accessible configuration of the setup is specifically intended to facilitate non-intrusive velocity measurements through laser-based and image-based techniques. The flume has a total length of 4.0 m, a width of 0.40 m, and a height of 0.40 m. The discharge capacity ranges from approximately 1.6 l/s up to 32 l/s, enabling the reproduction of a wide range of hydraulic conditions relevant for laboratory-scale investigations.

The hydraulic conditions inside the flume can be controlled through the regulation of the recirculating pump system. The discharge circulating through the setup depends on the pump power and is monitored using a flowmeter installed below the flume within the hydraulic circuit. Different flow rates can therefore be imposed to reproduce the desired hydraulic conditions for the experiments.

The corresponding upstream and downstream water levels inside the flume were subsequently measured experimentally using a water level gauge consisting of a graduated vertical measuring rod. By adjusting the discharge and measuring the resulting water levels, different hydraulic head differences were established for the various test configurations analysed in the present research.

The flume is equipped with a LaVision MiniShaker system for performing three-dimensional time-resolved PTV measurements. The optical rail integrated into the setup also permits the installation of additional measurement devices, such as high-speed cameras and laser systems, enabling detailed analyses of turbulent flow behaviour and transient hydraulic phenomena.

Within the context of the present thesis, the PTV flume was selected because of its capability to accurately reproduce the hydraulic behaviour of filling jets under controlled laboratory conditions. The optical accessibility of the facility and the integration with advanced PTV instrumentation enabled detailed measurements of the velocity field generated by the filling jets. This provided the experimental basis necessary for comparing the measured flow behaviour with the numerical schematisation implemented in VUL_SLUIS.

Importance was given to the analysis of the jet development at different distances from the lock gate and to the influence of the vessel on the velocity distribution inside the lock chamber. The experimental configuration therefore allowed the investigation of flow characteristics that cannot easily be captured through simplified numerical approaches alone.

The combination of controlled hydraulic conditions, high-resolution optical measurements, and flexible experimental configuration makes the PTV flume an effective facility for investigating the complex interaction between filling jets and vessels in navigation locks.

2.2 PTV Operations

Particle Tracking Velocimetry (PTV) is an optical flow measurement technique used to reconstruct the motion of fluid particles in time and space by tracking the displacement of tracer particles between consecutive images. In contrast to traditional intrusive measurement methods, PTV allows a non-invasive investigation of complex flow structures with high spatial and temporal resolution. Within the framework of this research, the technique was employed to analyse the hydraulic behaviour of the filling jets generated inside the navigation lock scale model.

The experimental setup was based on the LaVision MiniShaker system integrated with the DaVis 10.0 software environment. The MiniShaker is an integrated multi-camera imaging system specifically developed for volumetric PTV and Tomographic PIV applications. The system used in this study consists of four synchronised cameras assembled within a compact stereoscopic configuration, allowing simultaneous acquisition of particle motion from different viewing angles (LaVision, 2019).

Figure 2. Multi-camera imaging system.

The four-camera arrangement was positioned in side-view configuration relative to the flume to capture the development of the jet along the longitudinal section of the lock chamber model.

In addition to the cameras, the setup included two LaVision LED-Flashlight 300 illumination units placed underneath the flume. These high-power LED systems provide pulsed illumination specifically designed for volumetric flow measurements in air and water applications. The LEDs generate short and intense light pulses capable of illuminating the tracer particles suspended within the flow, enabling accurate particle detection by the cameras (LaVision, 2019).

Figure 3. LED-Flashlight 300 illumination unit.

The DaVis 10.0 software acted as the central acquisition and processing environment of the measurement system. The software integrates camera control, illumination synchronisation, image acquisition, calibration procedures, and post-processing operations within a single platform. Furthermore, DaVis supports advanced volumetric PTV method called Shake-the-Box (STB), which is specifically designed for time-resolved three-dimensional particle tracking (LaVision, 2019).

For the PTV measurements, the flow was seeded using microplastic tracer particles characterised by a density sufficiently close to that of water to accurately follow the fluid motion. These particles become visible when illuminated by the LED light sources positioned beneath the flume, allowing the cameras to record their displacement throughout the measurement volume. The use of these particles is essential for reconstructing the velocity field, since the PTV algorithm tracks the motion of individual tracers between consecutive frames.

Before performing the measurements, a calibration procedure was required to establish the geometric relationship between the physical measurement volume and the camera coordinate system. This operation was performed using a calibration plate placed inside the measurement domain. The calibration plate contains a predefined pattern of reference markers with known geometric coordinates. By recording the calibration target simultaneously with all four cameras, the software can determine the spatial orientation and optical distortion characteristics of each camera.

Figure 4. Calibration Plate

The perspective calibration procedure is fundamental because it allows the transformation of the recorded two-dimensional image coordinates into real three-dimensional spatial coordinates. In other words, the calibration process enables the reconstruction of particle positions inside the physical measurement volume rather than simply within the image plane of each individual camera.

Following the perspective calibration, a volume self-calibration procedure was performed. Volume self-calibration is an optimisation process used to reduce residual calibration errors caused by small misalignments, optical distortions, or imperfections in the experimental setup. The procedure uses the recorded particle images themselves to iteratively improve the camera mapping functions and increase the consistency between the different camera views.

The volume self-calibration is particularly important in volumetric PTV measurements because even small calibration inaccuracies may lead to substantial errors in the reconstructed particle positions and velocity fields. By refining the optical transfer function and improving the stereo reconstruction accuracy, the procedure increases the reliability of the final measurements.

Once the calibration procedures were completed, the actual recording phase could begin. The MiniShaker cameras were configured to acquire 300 images over a total duration of 3 seconds, producing time-resolved recordings of the particle motion inside the flow field.

Initially, the measurements were performed without the presence of the lock gate and vessel in order to familiarise with the instrumentation and verify the reliability of the setup. During this preliminary phase, the measured particle velocities were used to calculate the discharge through the cross-sectional area of the flume. The obtained values were subsequently compared with the discharge indicated by the flowmeter to validate the consistency of the measurements.

After verifying the correct functioning of the system, the lock gate and vessel model were installed inside the flume. The corresponding configurations and scaling choices adopted for these elements will be discussed in the following sections of this chapter.

The recordings obtained from the cameras do not directly provide velocity fields and therefore require several post-processing operations. These include particle identification, particle tracking, stereo reconstruction, filtering procedures, and vector field generation. The detailed post-processing methodology adopted in this research will be presented in the following chapter before discussing the experimental results. Particular attention will be devoted to the extraction of velocity profiles at different distances from the gate and to the generation of average velocity vector fields in side-view configuration.

2.3 Physical Model

This section describes the design choices adopted for the lock gate and vessel models used during the experimental campaign. The geometry of the physical was developed to ensure both hydraulic representativeness and compatibility with the constraints imposed by the PTV measurement system and the dimensions of the experimental flume.

2.3.1 Gate Design

The preliminary design of the gate geometry was initially inspired by the work previously presented in the thesis of Van Loon (Van Loon, TU Delft, 2017), which was used as a methodological reference to maintain a comparable experimental approach and facilitate possible analogies with previous investigations on lock filling jets.

At the beginning of the design phase, attention was also given to the recently constructed Lock of Sint-Baafs-Vijve in Flanders as a modern example of inland navigation lock design. The initial intention was therefore to reproduce a realistic lock geometry through geometric scaling.

In real navigation locks, including the Saint-Baafs-Vijve lock, breaking bars are often installed downstream of the filling openings to dissipate the incoming jet and reduce the concentration of the flow entering the lock chamber. The presence of these elements can also be included within the VUL_SLUIS input parameters. For the present research, however, only a simplified configuration without breaking bars was considered. The analysis therefore focuses on a rectangular opening without additional dissipation bars, allowing the downstream jet behaviour and its parametrization to be investigated under simplified and controlled hydraulic conditions.

A geometric scale factor equal to $\lambda = 18$ was considered during the early stages of the design process. This approach was used for gate opening height and generally for ship's dimensions. However, after evaluating the physical limitations imposed by the dimensions of the PTV flume and the optical constraints associated with the MiniShaker measurements, it became necessary to adapt the geometry to dimensions more suitable for the experimental facility. For instance, the flume width of 0.4 meters obliged to deeply change the scale factor. Consequently, the final model dimensions were not obtained through a strict geometric scaling of the real lock, but rather through a compromise between hydraulic representativeness and laboratory feasibility.

In particular, the longitudinal dimensions of the real lock could not be reproduced within the available flume length. For this reason, the gate was positioned approximately 1 m downstream from the upstream inlet section of the flume and approximately 3 m upstream from the downstream outlet section (Figure 5). This configuration created a fictitious lock chamber sufficiently long to accommodate the vessel model while still preserving an adequate downstream development length.

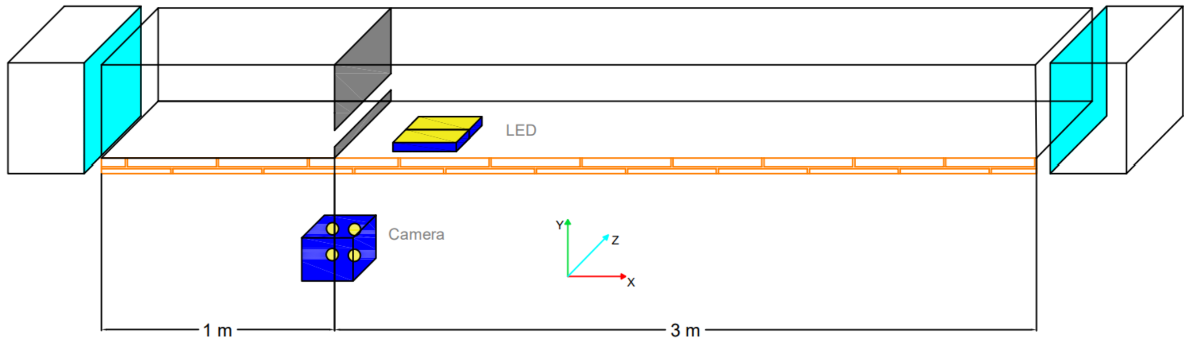

Figure 5. Overview of the scale model test setup.

The gate opening was designed as a rectangular submerged opening extending over the entire width of the flume. Consequently, the gate width w_f was assumed equal to the flume width to generate a quasi-two-dimensional jet structure and simplify the interpretation of the velocity field.

In Table 3 are shown values of Sint-Baaf Vijve prototype thar are still scaled according to the original assumptions (Vercruysse et al., 2016).

	Prototype	**Scale factor λ**	**Physical Model**
Opening height	1.05 m	18	0.058 m
Sill height	0.18 m	18	0.01 m

Table 3. Prototype and Physical Model values.

In the prototype lock there are 6 different openings and 8 breaking bars for each opening. In the case of this research they are not considered and there is just one opening without any bar.

Initially, the opening position was selected to closely reproduce modern lock filling systems, where the jet outlet is generally located near the bottom sill. By scaling the dimensions of the Sint-Baafs-Vijve lock (λ=18), the corresponding sill distance resulted approximately equal to 0.01 m from the bottom of the flume. Nevertheless, preliminary tests highlighted significant optical issues associated with this configuration. In particular, the LED-Flashlight illumination system positioned underneath the transparent flume generated reflections that interfered with the visibility of the jet region when observed through MiniShaker cameras. Since the PTV measurements strongly depend on the correct illumination and tracking of tracer particles, these reflections reduced the quality of the recorded images close to the bottom wall.

To overcome this limitation, the opening was repositioned slightly higher, placing the sill of the opening at a distance $h_s = 0.06$ m from the flume bottom. This modification considerably improved the visibility of the jet while maintaining a sufficiently realistic submerged jet configuration. In addition to the sill elevation, two different opening heights were selected to investigate the influence of jet thickness on the spreading behaviour and the resulting velocity distribution inside the lock chamber. The use of multiple opening heights allows a comparative analysis of jet development, turbulent diffusion, and interaction with the surrounding flow.

The geometry of the physical model gate is illustrated in the dedicated drawings included in the following pages, while the main geometric parameters are summarised in Table 4 and the gates with two different heights are sketched in Figure 6.

Parameter	Symbol	Value	
Opening height	h_o	0.03 m	0.06 m
Flume width	w_f	0.40 m	
Plate 1 height	h_1	0.10 m	
Plate 2 height	h_2	0.15 m	
Sill height	h_s	0.06 m	

Table 4. Parameters for lock gate design.

The heights $h_1$and h_2 were introduced to facilitate the movement and replacement of the upper gate plates during the measurement procedures, allowing rapid transitions between different experimental configurations. Since the upper plates were physically separated elements, a small leakage flow was present between them during the experiments. However, preliminary observations indicated that the resulting discharge was negligible compared to the main jet flow and therefore did not significantly influence the hydraulic behaviour analysed in this study.

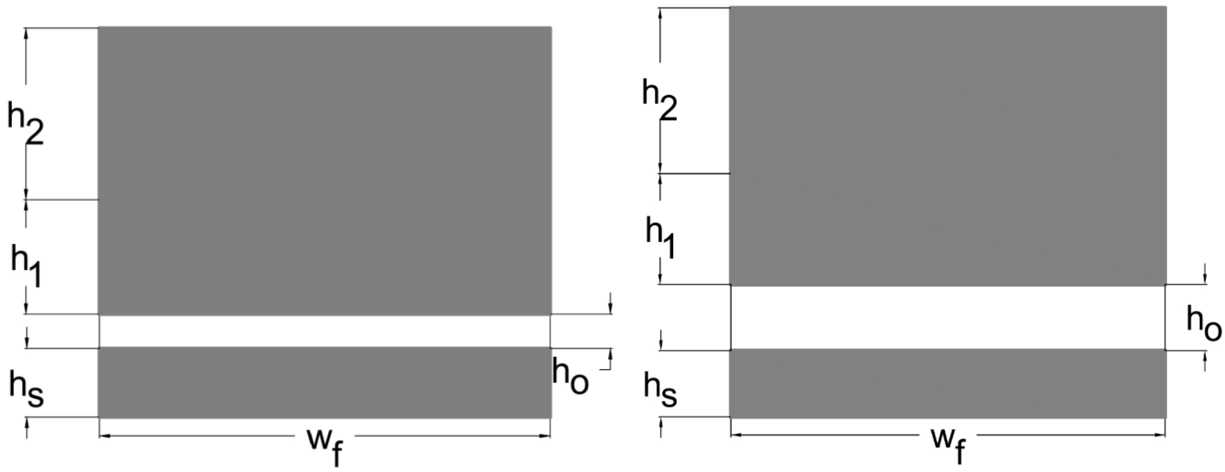

Figure 6. Sketch of designed gates

The different gate configurations analysed in this study varied one parameter at a time to isolate the influence of each geometric modification on the generated flow field. This approach allowed a clearer interpretation of the effects associated with opening height, sill elevation, and vessel presence on the jet evolution and velocity distribution inside the lock chamber.

2.3.2 Ship Design

The vessel model adopted during the experimental campaign was designed to reproduce the main geometric characteristics of inland navigation barges typically operating in European waterways (Waterway Guidelines, 2020). Attention was devoted to the bow geometry because the interaction between the filling jet and the upstream part of the vessel constitutes one of the principal focuses of this research. In particular, the selected bow inclination angle α corresponds to the geometry of an average pushing barge according to Deltares (2016).

At the same time, the geometry was adapted to the physical limitations imposed by the PTV flume dimensions and by the requirements of the optical measurement system. As for the gate design, the prototype vessel was loosely inspired by the dimensions of inland navigation vessels belonging to the EMCT Vb class (Waterway Guidelines, 2020), which represents the vessel categories for which the Lock of Sint-Baafs-Vijve was designed. Nevertheless, the final dimensions of the model were adjusted to guarantee compatibility with the available experimental space and to do that only the bow of the ship was designed. The ship model is showed in the Appendix A.

The principal geometric dimensions of the vessel physical model are illustrated in

Figure 7 and Figure 8. The corresponding fixed geometric parameters are summarised in Table 5.

Parameter	Symbol	Value
Total ship length	L_t	0.9304 m
Ship beam	B	0.39 m
Vertical bow angle	α	30°
Ship height	D	0.25 m
Bow length	L_{bow}	0.4304 m
Length at keel plane	L_k	0.50 m
Gate thickness	t	0.01 m

Table 5. Fixed bow parameters

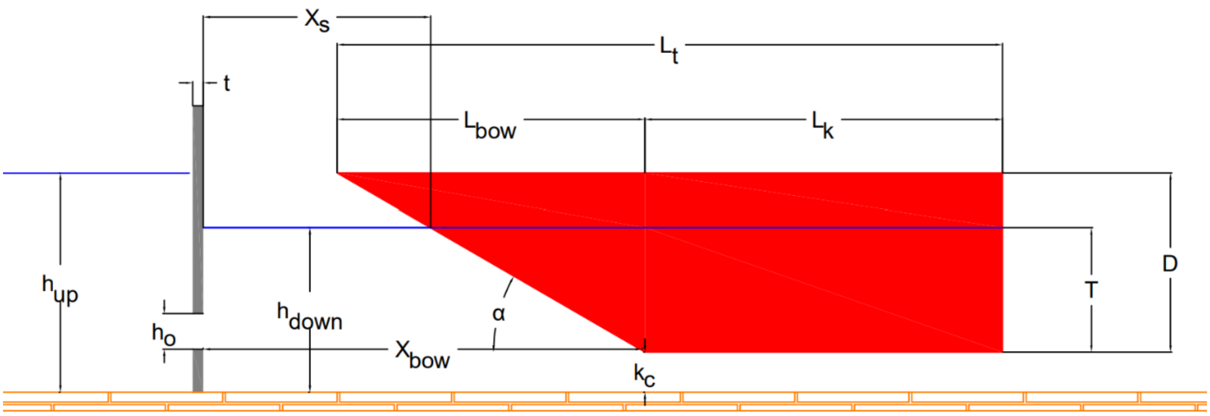

Figure 7. Side view of the lock within the presence of a ship

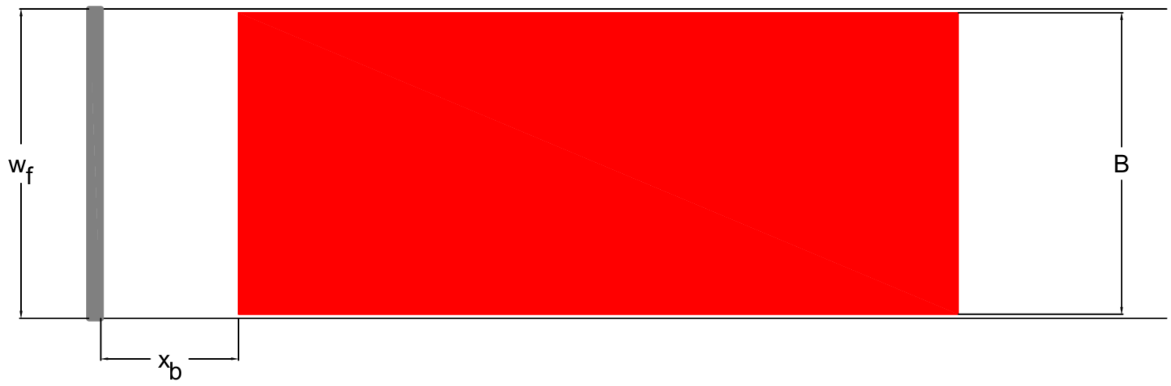

Figure 8. Top view of the lock within the presence of a ship

Some geometric parameters were not fixed but were instead derived for each experimental condition. In particular, the ship draught T was determined as a function of the downstream water depth and the imposed keel clearance according to:

$$T = h_{downstream} - k_c$$

where $h_{downstream}$ represents the water depth in the lock chamber and k_c the keel clearance between the vessel bottom and the flume bed.

Since different hydraulic and geometric conditions were investigated during the experimental tests, several combinations of keel clearance, upstream-downstream water level difference, and ship position were analysed. The complete list of experimental cases is summarised in Table 6, where the varying parameters include the longitudinal ship position X_{bow}, the keel clearance k_c, and the hydraulic head difference: $\Delta h = h_{upstream} - h_{downstream}$ used to generate the filling jet.

Parameter	Value
k_c	0.03 m
	0.08 m
X_{bow}	0.505 m
	0.60 m
Δh	0.02 m
	0.045 m
	0.09 m

Table 6. Variable Parameters

Concerning the vessel width, the beam B was intentionally selected equal to the width of the flume. This choice was made to reproduce a two-dimensional hydraulic configuration. Since the objective of the present research is the investigation of the jet behaviour in a two-dimensional framework, eliminating lateral flow bypasses around the vessel allows a clearer interpretation of the measured velocity fields. Furthermore, the MiniShaker measurements provide an averaged velocity vector field over the entire width of the flume. Consequently, adopting a vessel beam equal to the flume width ensures consistency between the physical configuration and the assumptions underlying the optical measurements and subsequent data analysis.

The positioning of the vessel relative to the gate required particular attention. The selected distances were chosen not only to investigate different jet-vessel interaction scenarios, but also to allow a meaningful comparison with the VUL_SLUIS numerical schematisation discussed in the following chapters.

At this stage, the imposed geometric parameter was the distance between the gate and the bottom intersection point of the vessel bow, denoted as X_{bow}. Subsequently, the corresponding distance measured at the water surface level between the gate and the ship was also determined experimentally and analytically.

Assuming a linear bow inclination, this surface distance can be calculated as:

$$X_s = \frac{h_{downstream} - k_c}{\tan(\alpha)}$$

The relationship between these geometric quantities will become particularly relevant in the comparison with VUL_SLUIS, where the representation of the vessel position relative to the filling jet requires a consistent definition of the characteristic interaction distance. This aspect will be discussed in detail in Section 4.1.1 concerning the numerical modelling approach.

2.4 Important Measurement Parameters

The hydraulic behaviour observed during the experimental campaign was strongly influenced by several operational parameters associated with the generation of the filling jet and the definition of the hydraulic conditions inside the flume. Among these parameters, the pumping system configuration and the downstream water level definition played a central role in determining the characteristics of the measured velocity fields.

2.4.1 Pumping System

The hydraulic conditions inside the experimental setup were controlled through the recirculating pumping system of the PTV flume. The pump generated the discharge circulation through the flume and consequently established the hydraulic head difference between the upstream and downstream sides of the gate opening. Since the filling jet is directly driven by the pressure gradient across the gate, the upstream-downstream water level difference represents one of the governing parameters controlling the velocity and development of the jet inside the lock chamber.

The hydraulic head difference is defined as Δh and directly determines the amount of momentum transferred through the opening. According to the submerged sluice-gate flow formulations presented by Swamee (1992), the discharge through a submerged opening can be expressed as:

$$Q = C_d ab\sqrt{2g(h_u - h_d)}$$

where Q is the discharge, C_d the discharge coefficient, a the opening height, b the opening width, g the gravitational acceleration, and $h_u - h_d$ the hydraulic head difference across the gate.

This relation highlights the intrinsic coupling between gate opening, discharge, and hydraulic head difference. For a fixed gate geometry, the flow rate that can pass through the opening depends on the pressure difference established between the upstream and downstream sections of the gate.

Within the present experimental setup, the pumping system allowed the regulation of different flow rates by adjusting the pump power. Once the system reached steady-state conditions, both the upstream and downstream water levels remained stable, and no net accumulation of water occurred within the flume. Under these conditions, the continuity principle implies that the discharge measured by the flowmeter inside the recirculating system corresponds to the discharge effectively passing through the opening of the gate. Under steady-state conditions, the measured flow rate therefore controls the hydraulic head difference across the gate.

This relationship remains valid only for fixed opening geometry. Changing the opening height modifies the hydraulic resistance imposed by the gate and consequently alters the relation between discharge and hydraulic head difference. For this reason, different combinations of discharge and Δh were analysed separately for each opening configuration investigated during the experimental campaign.

An alternative methodology could have consisted in modifying the downstream water level through the introduction of hydraulic obstacles or flow restrictions downstream of the lock chamber. Although this solution would have allowed additional control over the hydraulic head difference, it would also have significantly altered the optical conditions inside the MiniShaker measurement domain.

The accuracy of the volume self-calibration procedure depends strongly on maintaining stable optical conditions during the measurements. Significant water level variations inside the camera field of view would have altered the refraction conditions and reduced the reliability of the stereoscopic reconstruction process. For this reason, the hydraulic conditions were controlled primarily through discharge regulation rather than through downstream flow obstruction.

Figure 9. Flume in steady-state condition.

Although the absolute upstream and downstream water levels varied slightly between different experimental configurations, the procedure was designed to maintain constant values of Δh for cases intended to be directly compared. This aspect became particularly important when analysing the influence of geometric parameters such as vessel position or keel clearance, since maintaining the same hydraulic forcing conditions ensured that the observed differences in the velocity fields could primarily be associated with geometric effects rather than variations in discharge conditions.

The complete hydraulic parameters associated with each experimental case are presented together with the corresponding measurement results in the dedicated results chapter.

2.4.2 Downstream Water Level

The definition of the downstream water level represents an important aspect in the analysis of submerged filling jets. In turbulent submerged flows generated through gate openings, the downstream flow region cannot be described by a single uniform water depth immediately after the opening. Instead, the flow is characterised by the formation of a high-momentum turbulent jet that progressively develops downstream while interacting with the surrounding fluid and the bottom boundary of the flume.

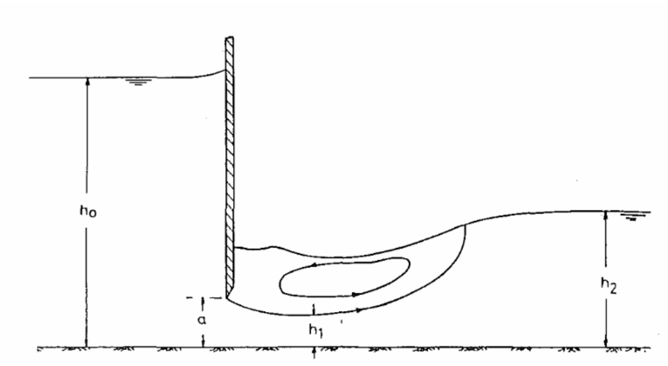

Figure 10. Downstream water level influenced by turbulent behaviour of the jet (Swamee, 1992).

The hydraulic behaviour of submerged jets downstream of sluice gates has been extensively discussed in the literature concerning turbulent wall jets and submerged gate flows. Once the flow exits the opening, the jet undergoes contraction and acceleration, producing strong turbulence generation and entrainment mechanisms. The jet subsequently spreads downstream due to turbulent momentum diffusion, progressively transferring momentum from the high-velocity jet core towards the surrounding fluid. (Schwarz et al., 1960)

As described by Swamee (1992), submerged sluice-gate flows are characterised by different hydraulic regions immediately downstream of the gate opening. The local water depth close to the gate is governed primarily by the jet development itself and by the concentrated momentum of the discharged flow. Further downstream, turbulent mixing and energy dissipation gradually redistribute momentum throughout the flow depth, leading to a different and more stable downstream water level.

This behaviour is closely related to the physics of turbulent wall jets. Experimental investigations on turbulent wall jets show that the maximum velocity region remains concentrated close to the wall during the initial development stage, while turbulent entrainment progressively increases the jet thickness and reduces the local velocity magnitude further downstream. Consequently, the hydraulic conditions immediately downstream of the opening differ substantially from those observed after the jet has undergone significant turbulent spreading (Launder and Rodi, 1983).

Within the framework of the present research, the discharge through the gate openings is evaluated using the hydraulic head difference between the upstream water level and the downstream water level at the end of the lock chamber, consistently with conventional lock hydraulic formulations.

However, the analysis presented in this thesis is primarily focused on the behaviour of the filling jet and on its interaction with the vessel geometry. For this reason, particular attention is given to the local flow conditions immediately downstream of the gate opening, where the jet is still highly coherent and where the principal hydraulic phenomena governing the velocity distribution occur.

The MiniShaker measurement domain is concentrated in this near-field region downstream of the gate. Furthermore, the optical measurement volume does not extend up to the free water surface further downstream. The recorded velocity fields are therefore mainly focused on the submerged jet region and on the interaction between the jet, the bottom wall, and the vessel bow.

Consequently, although the global hydraulic head controlling the discharge is defined using the downstream water level at the end of the lock chamber, the local water level immediately downstream of the gate is adopted as a reference for the interpretation of the measured flow field. This approach ensures consistency between the hydraulic parameters used to describe the local flow conditions and the physical region effectively captured by the PTV measurements.

3 MINISHAKER MEASUREMENTS AND RESULTS

3.1 Post processing procedure

Following the acquisition phase, the recorded images were processed within the DaVis 10.0 software. DaVis provides an integrated platform for volumetric particle tracking, vector field reconstruction, filtering operations, and statistical post-processing of PTV measurements.

The post-processing workflow adopted in the present research was specifically designed to obtain reliable velocity fields describing the behaviour of the filling jet downstream of the gate opening. Since the final objective of the study is the comparison between different hydraulic configurations and the analysis of the jet evolution, the processing sequence focused on improving particle visibility, reconstructing particle trajectories, and generating averaged two-dimensional velocity fields representative of the measured flow.

The first processing operation applied to the recorded images consisted of a background subtraction procedure using the *Subtract Gaussian Average* time filter available in DaVis. This operation removes stationary image components and background illumination effects by subtracting a temporally averaged Gaussian-filtered image from the original recordings. The procedure significantly improves the contrast between the tracer particles and the background, facilitating particle identification during the tracking phase. This operation is particularly important in optical measurements performed under submerged conditions, where reflections and non-uniform illumination may reduce particle visibility (LaVision, 2019).

After the background subtraction, a smoothing operation was applied using a 3×3 Gaussian smoothing filter. The objective of this step was to reduce high-frequency image noise while preserving the shape and intensity distribution of the tracer particles. Gaussian smoothing improves the robustness of the subsequent particle detection procedure by reducing local pixel fluctuations not associated with physical particles.

Once the image pre-processing operations were completed, the particle tracking phase was performed using the *Shake-The-Box* (STB) algorithm. The Shake-The-Box method is a volumetric particle tracking technique specifically developed for time-resolved Lagrangian flow measurements. The algorithm identifies individual tracer particles in the images recorded by the multiple cameras and reconstructs their three-dimensional trajectories over time (LaVision, 2019).

To evaluate the reliability and accuracy of the reconstructed velocity fields, an additional validation procedure was performed and is discussed in Annex B. Measurements Accuracy. The validation was based on a reference configuration consisting of flow measurements inside the flume without the presence of the gate model or the vessel. For this configuration, the discharge obtained by integrating the reconstructed velocity profiles over the water depth was compared with the discharge measured independently through the flowmeter installed in the hydraulic circuit. This comparison provided an indication of the consistency between the PTV-derived velocity fields and the imposed hydraulic conditions, thereby allowing the overall accuracy of the post-processing procedure to be assessed.

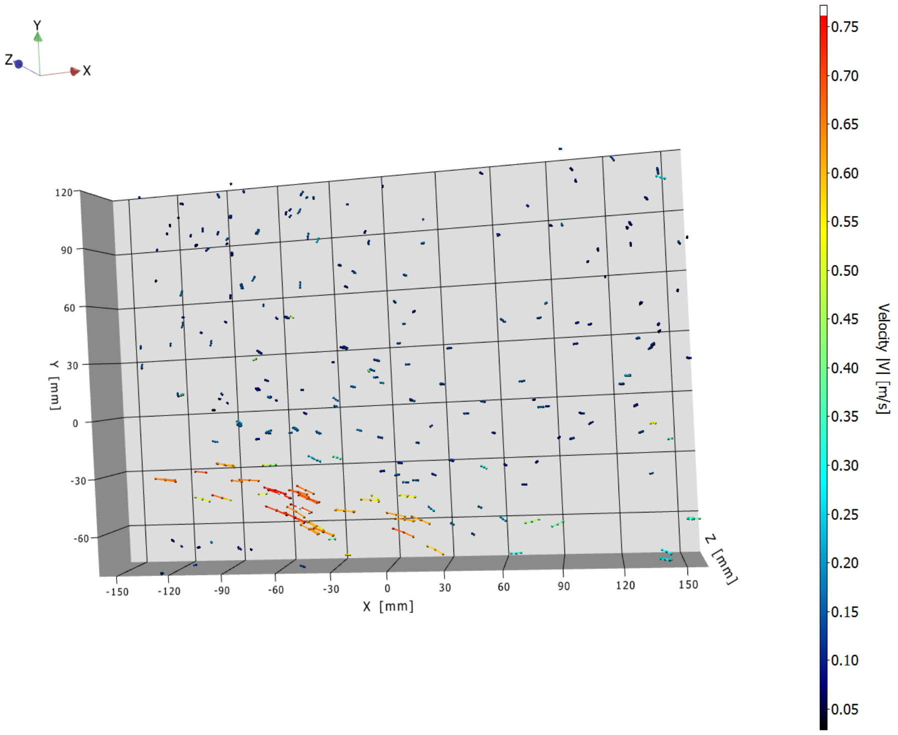

Figure 11. Example of particle trajectories performed by ShakeTheBox.

Within the present study, the Shake-The-Box processing was configured to perform both particle detection and particle tracking while storing the reconstructed tracks for subsequent vector field generation. The reconstruction volume was defined according to the coordinate system established during the calibration procedure using the calibration plate. The origin of the coordinate system was located at the centre of the calibration plate.

The selected processing volume was defined as: $x = [-160 \text{ mm}, 160 \text{ mm}]$, $y = [-80 \text{ mm}, 120 \text{ mm}]$, and $z = [40 \text{ mm}, 80 \text{ mm}]$.

The selected domain corresponds to the region of interest where the filling jet develops downstream of the gate and interacts with the vessel geometry. Although the measurements were reconstructed volumetrically in three dimensions, the present research focuses on a quasi-two-dimensional analysis of the jet behaviour. For this reason, the velocity fields corresponding to the different z-planes were subsequently averaged to obtain representative two-dimensional flow fields.

Following the Shake-The-Box reconstruction, the *Fine Scale Reconstruction* procedure was applied. The resulting vector fields provide the local velocity distribution inside the measurement domain and constitute the basis for the hydraulic analysis performed in this thesis.

Subsequently, a *Vector Statistics* operation was performed to calculate averaged velocity fields and statistical quantities from the reconstructed vectors. During this phase, the velocity data corresponding to all reconstructed z-planes were averaged together to obtain a single representative two-dimensional velocity field for each experimental case. In addition to the mean velocity field, the standard deviation of the velocity components was also calculated, providing an indication of the local flow variability and turbulence intensity.

The final stage of the post-processing procedure focused on the extraction of velocity profiles from the averaged vector fields. Since the objective of the research is the investigation of the filling jet evolution downstream of the gate, velocity profiles were extracted at three different longitudinal positions inside the flume.

The selected profile locations, referred to the coordinate system associated with the calibration plate and referred to the physical flume reference system starting from immediately downstream of the gate are showed in Table 7.

	Plate reference system	Flume reference system
X_1	-50 mm	0.15 m
X_2	0 mm	0.20 m
X_3	100 mm	0.30 m

Table 7. Velocity profile's locations.

The vertical coordinate system follows the same calibration reference. Within the calibration plate system, the visible measurement domain extends from $y = -80$ mm up to $y = 120$ mm. Consequently, the coordinate $y = -80$ mm corresponds to the bottom of the flume, while the remaining vertical positions are measured upward from the flume bottom. This reference system is adopted consistently throughout the averaged vector fields and the extracted velocity profiles presented in the following sections.

These locations were selected to analyse the spatial evolution of the jet as it propagates downstream and interacts with the vessel geometry. The extracted velocity profiles, together with the averaged vector fields obtained from the MiniShaker measurements, constitute the principal results used in the following sections to compare the different experimental configurations characterised by varying opening heights, hydraulic head differences, keel clearances, and vessel positions.

A large number of measurements were performed during the experimental campaign using different hydraulic and geometrical configurations, including variations in opening height, hydraulic head difference, vessel position, and keel clearance. In the present thesis, only the most relevant cases are discussed and compared in detail to focus on the principal hydraulic behaviours observed during the experiments and on the comparison with the numerical schematization implemented in VUL_SLUIS. A complete overview of all the performed measurements and tested configurations is provided in Appendix C.

3.2 Without ship

The first series of measurements was performed without the presence of the vessel inside the lock chamber. These tests provide a reference description of the filling jet behaviour under different hydraulic and geometric conditions without introducing additional disturbances caused by the ship geometry. The measurements therefore allow the isolated analysis of the jet development downstream of the gate opening and establish the baseline conditions required for the subsequent comparison with the cases including the vessel.

The analysis presented in this section focuses on two main characteristics of the jet evolution: the spreading of the jet and its progressive attachment towards the bottom of the flume. The spreading behaviour is evaluated through the evolution of the velocity distribution downstream of the gate, while the sinking behaviour refers to the progressive downward displacement of the jet core caused by the interaction between the turbulent jet and the bottom boundary.

3.2.1 Different opening height

The first comparison concerns the influence of the opening height on the development of the filling jet. Two configurations characterised by the same hydraulic head difference, but different opening heights were analysed (Table 8).

	Case 1	**Case 2**
Q (flow rate)	0.0052 m³/s	0.0097 m³/s
$\mathbf{h_u}$	0.28 m	
$\mathbf{h_d}$	0.26 m	
Δh	0.02 m	
$\mathbf{h_o}$	0.03 m	0.06 m

Table 8. Parameters for comparison 1

The averaged velocity vector fields (Figure 12) obtained from the PTV measurements show that the opening height directly influences the initial structure of the jet and its downstream evolution. For the smaller opening height, the discharged flow is more vertically concentrated and therefore generates a thinner jet characterised by stronger local velocity gradients immediately downstream of the gate. In contrast, the larger opening produces a thicker jet with a broader initial velocity distribution. Since these cases have the same hydraulic head, they present same velocity intensities inside the filling jets.

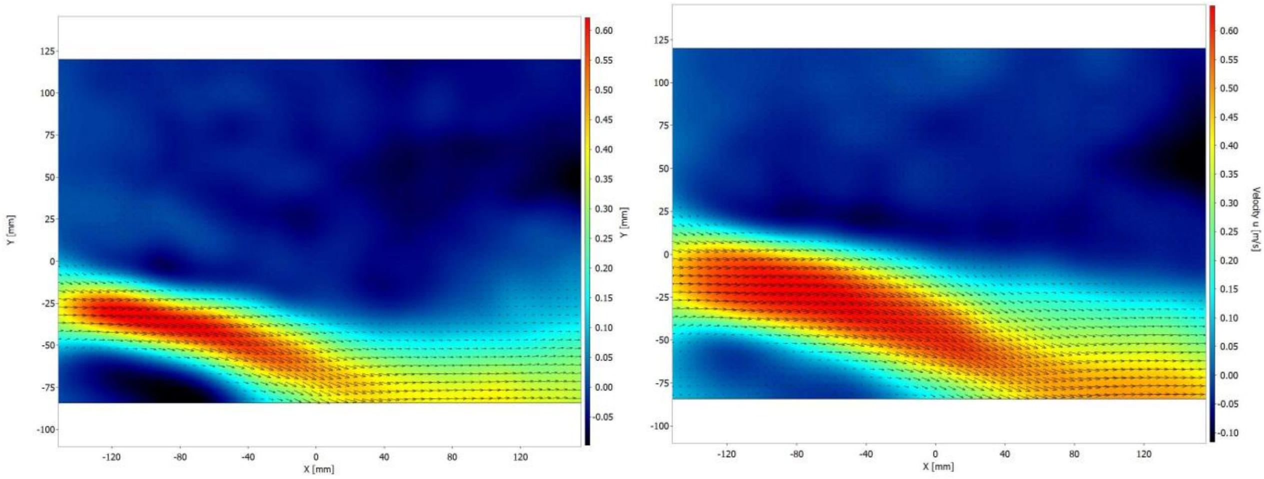

Figure 12. Average vector fields of Case 1 (0.03 m opening) and Case 2 (0.06 m opening).

The spreading behaviour of the jet becomes evident from the velocity profiles extracted at increasing downstream distances from the gate. In the case of the smaller opening height (Figure 13), the jet initially remains relatively concentrated and maintains a confined high-velocity core close to the gate. As the flow propagates downstream, turbulent entrainment progressively redistributes momentum towards the surrounding fluid, increasing the vertical extension of the velocity profile.

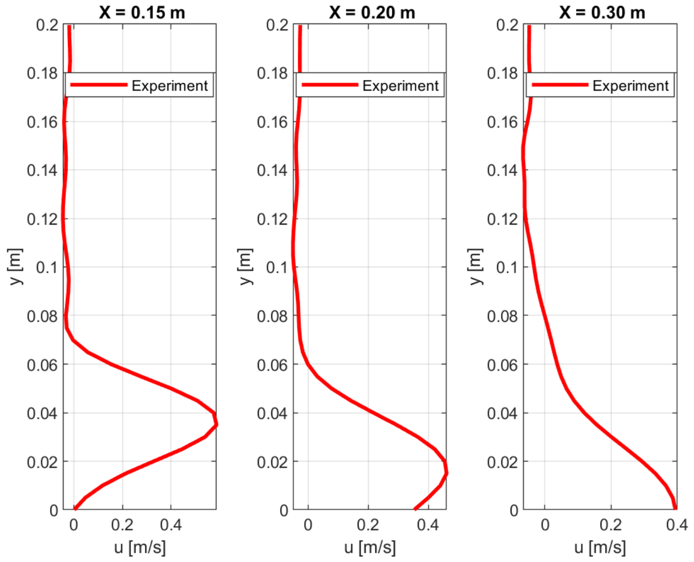

Figure 13. Vertical velocity profile at different distances from the gate for opening height 0.03 m (visualized on MATLAB for better understanding).

For the larger opening height (Figure 14), the spreading process begins earlier because the jet already exits the opening with a greater vertical thickness. The velocity distribution therefore appears less concentrated in the near-field region, while the downstream evolution is characterised by a smoother redistribution of momentum throughout the flow depth.

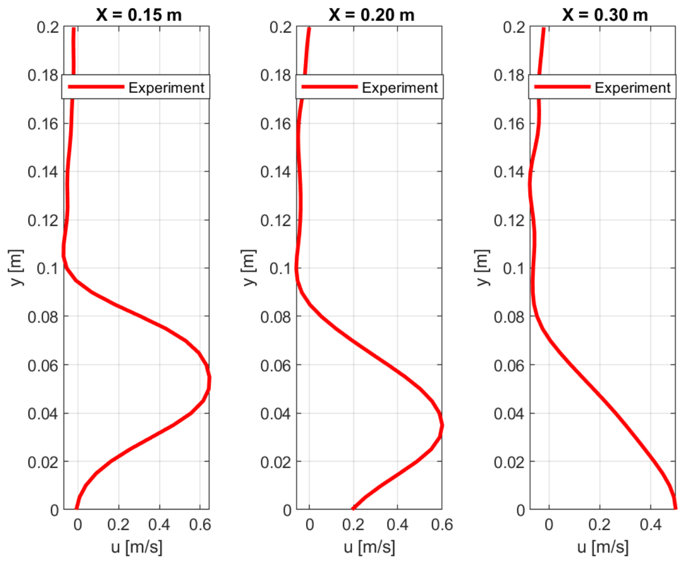

Figure 14. Vertical velocity profile at different distances from the gate for opening height 0.06 m.

The measurements also provide insight into the sinking behaviour of the jet. The interaction between the turbulent jet and the bottom wall progressively causes the high-velocity core to move downward and attach to the flume bed. This effect becomes visible in the velocity profiles extracted at increasing downstream distances, where the location of the maximum velocity progressively shifts closer to the bottom boundary.

The comparison between the two gate openings suggests that jet attachment to the bottom is strongly influenced by the opening geometry. For the smaller opening, the jet is thinner and the relative shear with the surrounding water is stronger; this can enhance turbulent entrainment and promote a faster downward deflection, leading to earlier attachment to the bed. Conversely, the larger opening produces a thicker jet with a greater total momentum flux, $M \sim \rho A V^2$, where M represents the jet momentum flux, ρ is the water density, A is the effective jet cross-sectional area, and V is the characteristic jet velocity (Albayrak, Hopfinger, and Lemmin 2008). Even if the characteristic jet velocity is similar for the same hydraulic head, the larger jet carries more momentum over a wider flow area, which may allow it to remain detached over a longer downstream distance before sinking toward the bottom.

These observations confirm that the opening geometry significantly affects both the spreading rate and the wall attachment characteristics of the filling jet. Such effects are particularly relevant for the numerical schematisation implemented in VUL_SLUIS, where the opening geometry directly influences the predicted velocity distribution inside the lock chamber.

3.2.2 Different hydraulic head

The second comparison investigates the influence of the hydraulic head difference on the development of the filling jet. In this case, the opening geometry was kept constant with an opening height equal to 0.03 m, while two different hydraulic head differences were analysed, corresponding approximately to 0.045 m and 0.09 m respectively (Table 9).

	Case 1	**Case 2**
Q (flow rate)	0.0074 m^3/s	0.010 m^3/s
h_u	0.29 m	0.315 m
h_d	0.245 m	0.225 m
Δh	0.045 m	0.09 m
h_o	0.03 m	

Table 9. Parameters for comparison 2

Since the hydraulic head difference directly governs the pressure gradient across the gate, increasing Δh produces substantially higher discharge velocities through the opening. This effect is clearly visible in the measured velocity fields (Figure 16) where the larger hydraulic head generates higher velocity magnitudes throughout the jet region. Although the averaged vector fields reveal a qualitatively similar jet structure in both cases, the increased momentum associated with the larger hydraulic head significantly modifies the downstream flow evolution. The stronger velocity gradients enhance turbulent shear production and entrainment with the surrounding water, which may promote faster lateral spreading of the jet and a more rapid loss of flow coherence downstream.

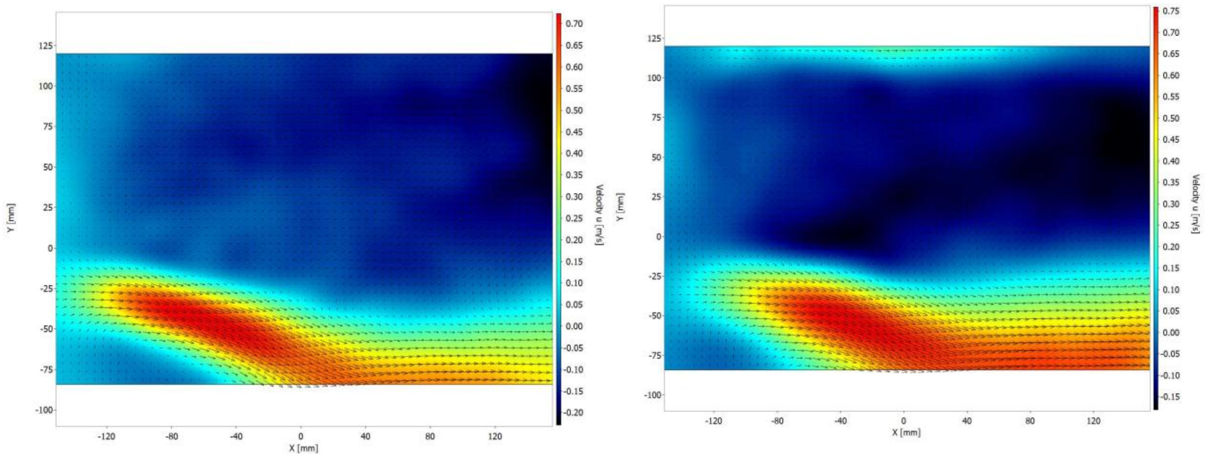

Figure 15. Average vector fields of Case 1 (Δh = 0.045 m) and Case 2 (Δh = 0.09 m).

Turbulence production in shear flows is commonly related to the Reynolds stress and to the mean velocity gradient:

$$P = -\overline{u'v'}\,\frac{\partial U}{\partial y}$$

where P is the turbulent kinetic energy production, $-\overline{u'v'}$ is the Reynolds shear stress, and $\frac{\partial U}{\partial y}$ is the mean velocity gradient. Therefore, the higher velocities generated by the larger hydraulic head intensify shear-layer turbulence and mixing processes within the submerged jet. (Rajaratnam, 1968).

It should be noted that the PTV measurements presented limitations in the region immediately downstream of the gate opening. Within approximately the first part immediately downstream of the gate, the high particle concentration and the strong local velocity gradients made the particle tracking procedure less reliable. The reconstructed velocity fields in this near-gate region should be interpreted with caution.

Similarly, the measurements in the upper part of the flow domain close to the free surface are characterized by lower accuracy, as discussed previously. For this reason, the analyses presented in the following sections focus primarily on the central and lower regions of the jet, where the velocity reconstruction proved to be more reliable and representative of the downstream jet behaviour.

The velocity profiles extracted at different downstream locations show only moderate differences in peak velocity magnitude between the two hydraulic-head configurations. Although the larger hydraulic head (Figure 17) generates slightly higher velocities, the overall sinking behaviour of the jet remains qualitatively similar in both cases, with no substantial variation in the attachment of the velocity core toward the flume bed.

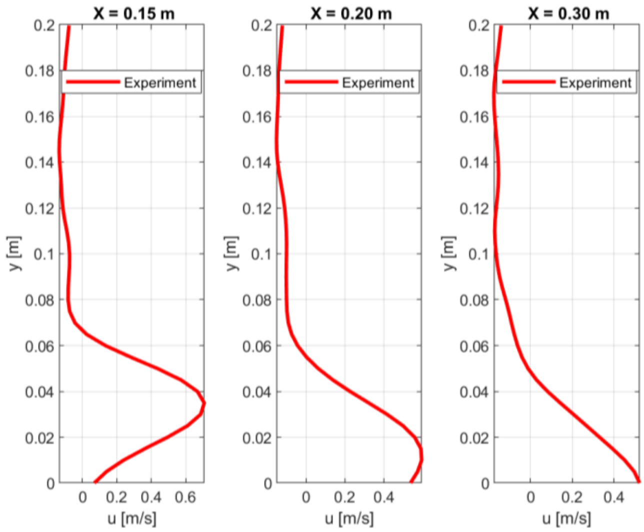

Figure 16. Vertical velocity profile at different distances from the gate for Δh = 0.045 m.

The primary difference is instead observed in the spreading behaviour of the jet. Under the larger hydraulic head, the stronger velocity gradients enhance turbulent entrainment and mixing with the surrounding water, leading to a wider and more diffused jet structure downstream. Conversely, the lower-head configuration (Figure 16) produces a more confined jet with reduced spreading in the vertical direction and weaker turbulent diffusion.

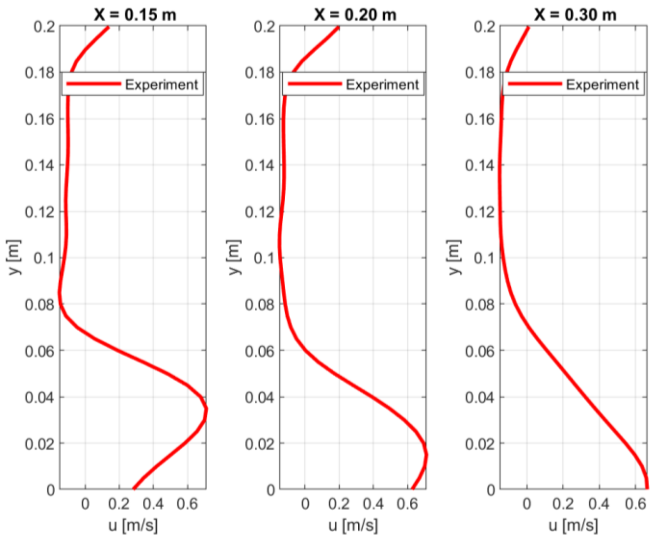

Figure 17. Vertical velocity profile at different distances from the gate for Δh = 0.09 m.

The comparison demonstrates that the hydraulic head difference mainly affects the downstream spreading of the jet.

3.3 With ship

Following the analysis of the filling jet without the presence of the vessel, the second part of the experimental campaign focused on the interaction between the jet and the ship geometry. The introduction of the vessel inside the lock chamber modifies the available flow area and alters the pressure distribution downstream of the gate, consequently influencing the development of the jet and the resulting velocity field.

3.3.1 Interaction with the bow of the ship

The first comparison investigates the influence of the vessel presence on the downstream development of the filling jet. Two cases are considered: the first one without the vessel and the second one including the ship inside the lock chamber (Table 10).

	Case 1 (without ship)	**Case 2 (with ship)**
Q (flow rate)	0.0074 m^3/s	0.0068 m^3/s
h_u	0.29 m	
h_d	0.245 m	
Δh	0.045 m	
h_o	0.03 m	
k_c	n.a.	0.03 m
X_{bow}	n.a.	0.505 m

Table 10. Parameters for Comparison 3 (n.a. = not applicable).

The average vector fields (Figure 18) indicate that the presence of the ship primarily affects the downstream development of the jet rather than its initial generation at the gate opening. Since both the gate geometry and the hydraulic head difference remain unchanged between the two configurations, the maximum jet velocities immediately downstream of the opening are comparable in magnitude. The principal differences therefore emerge further downstream, where the interaction between the jet and the vessel geometry becomes dominant.

The confinement imposed by the reduced under-keel region modifies the natural spreading behaviour of the turbulent wall jet. In the configuration without the vessel, the jet progressively expands while interacting with the surrounding fluid and develops larger recirculation regions above the high-velocity core. This behaviour becomes visible in the averaged vector fields through the formation of broader low-velocity and reverse-flow regions surrounding the jet trajectory.

When the ship is introduced inside the lock chamber, the available flow area beneath the hull becomes restricted and the downstream evolution of the jet changes substantially. The under-keel confinement limits the vertical expansion of the jet and suppresses the formation of larger recirculation structures. Consequently, the jet follows a more direct and less curved trajectory towards the under-keel region while maintaining a more coherent downstream-oriented momentum distribution.

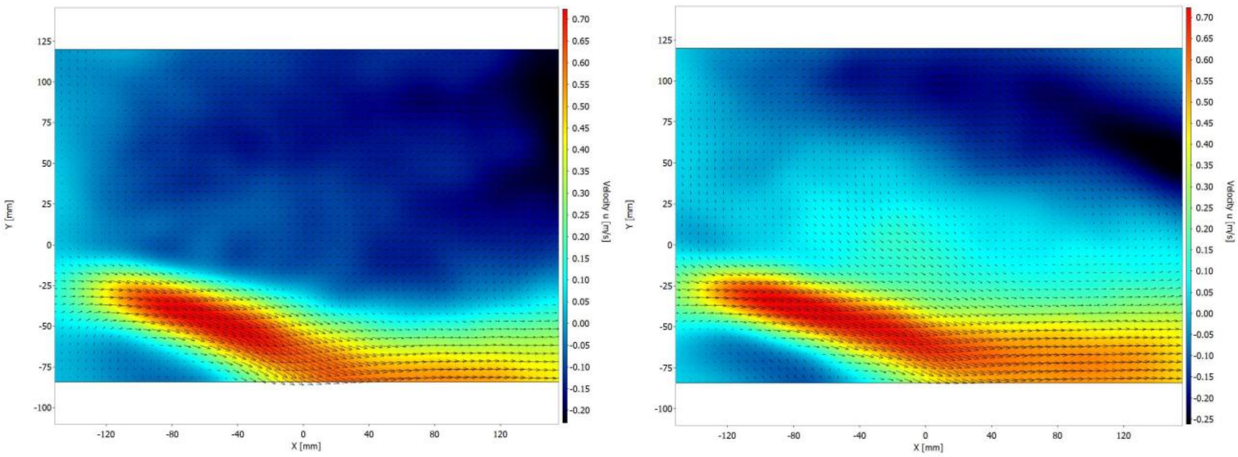

Figure 18. Average vector fields of Case 1 (without ship) and Case 2 (with ship).

The surrounding flow field also becomes significantly more organised in the presence of the vessel. Compared with the no-ship configuration, the velocity fields exhibit fewer regions characterised by negative streamwise velocities and weaker reverse-flow motion. The interaction between the jet and the vessel geometry therefore reduces the development of large-scale recirculation zones and constrains the redistribution of momentum around the jet.

This behaviour is further confirmed by the extracted velocity profiles (Figure 20), particularly at the section located approximately $X = 0.3$ m downstream of the gate. The profiles show that the presence of the vessel modifies the spatial distribution of the streamwise velocity and alters the downstream decay of the jet momentum.

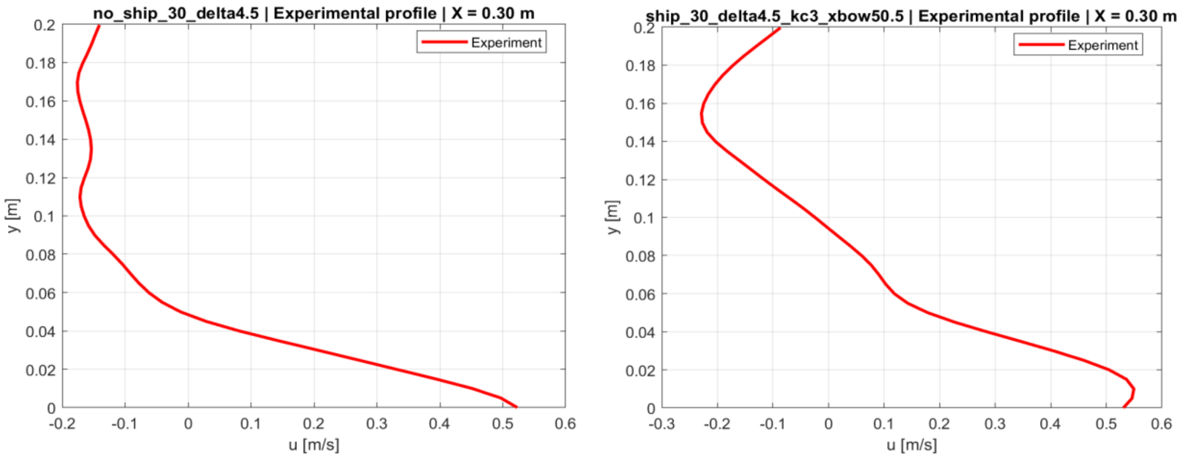

Figure 19. Vertical velocity profiles for Case 1 (with ship) and Case 2 (without ship).

In the configuration without the ship, the velocity profile transitions relatively rapidly towards negative values above the jet core, indicating the presence of stronger recirculation structures surrounding the main flow. This behaviour is consistent with the larger spreading and entrainment processes observed in the averaged vector fields.

Conversely, in the configuration with the vessel, positive streamwise velocities persist over a significantly larger portion of the profile. The downstream momentum therefore remains more aligned with the principal jet direction and the formation of reverse-flow regions is substantially reduced. The confinement generated beneath the hull limits the transverse redistribution of momentum and forces the flow to remain concentrated within the available under-keel section.

The comparison demonstrates that the presence of the vessel does not simply alter the magnitude of the velocity field but rather changes the entire downstream organisation of the turbulent jet. The interaction between the jet and the under-keel confinement modifies the balance between turbulent spreading, entrainment, and recirculation development, resulting in a more channelled and directionally coherent flow structure downstream of the gate.

3.3.2 Different keel clearances

The second comparison analyses the influence of the keel clearance on the development of the filling jet. Two configurations characterised by different keel clearances were investigated while maintaining all other geometric and hydraulic parameters constant. The considered cases correspond to keel clearances of 0.03 m and 0.08 m respectively (Table 11).

	Case 1	**Case 2**
Q (flow rate)	0.020 m^3/s	
h_u	0.34 m	0.29 m
h_d	0.25 m	0.20 m
Δh	0.09 m	
h_o	0.06 m	
k_c	0.03 m	0.08 m
X_{bow}	0.505 m	

Table 11. Parameters for comparison 4

Before analysing the post-processed velocity fields, a difference between the two keel-clearance configurations was already observable directly during the experiments. Although the same flow rate was imposed in both cases to maintain approximately the same hydraulic head difference across the gate, the configuration characterised by the smaller keel clearance (k_c = 0.03 m) required a higher upstream water level compared to the case with k_c = 0.08 m.

This behaviour is directly related to the reduction of the available flow area beneath the vessel. For the smaller keel clearance, the under-keel region imposes a stronger hydraulic confinement on the downstream flow, increasing the overall hydraulic resistance experienced by the jet while propagating beneath the hull. Therefore, a larger upstream water level was required to maintain the same discharge through the system and preserve the target hydraulic head difference.

The comparison between the two different configurations subsequently shows that the overall wall-jet structure remains qualitatively similar in both cases (Figure 20). The jet still develops as a bottom-attached turbulent wall jet characterised by a high-velocity core propagating downstream beneath the vessel. The maximum velocity magnitudes immediately downstream of the gate remain comparable, indicating that the change in keel clearance does not significantly modify the initial momentum generated at the opening. Similarly, the general downstream sinking behaviour of the jet remains present in both configurations, with the high-velocity core progressively moving towards the flume bottom as the flow develops downstream.

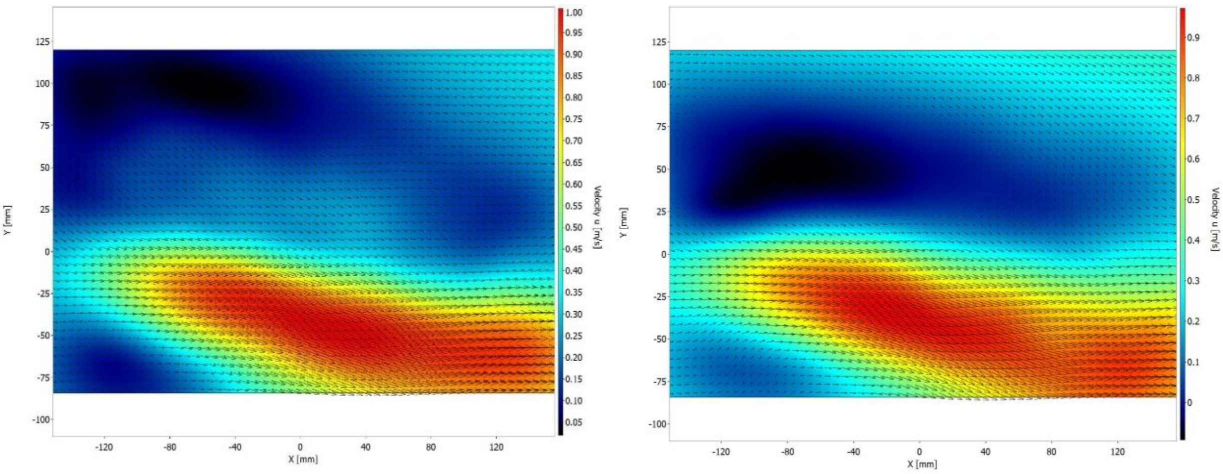

Figure 20. Average vector fields of Case 1 (k_c = 0.03 m) and Case 2 (k_c = 0.08 m).

The principal differences between the two cases are instead associated with the degree of confinement imposed by the under-keel region and with the resulting redistribution of the momentum around the jet.

For the smaller keel clearance configuration, the reduced available flow area beneath the vessel forces the jet to remain more confined along the bottom region of the flume. The averaged vector fields show that the high-velocity core maintains a more compact structure and that the surrounding recirculation region above the jet remains relatively limited in size. The reduced vertical space constrains the turbulent spreading of the jet and suppresses part of the large-scale recirculation structures that would otherwise develop above the main flow.

Therefore, the velocity gradients surrounding the jet become locally stronger and the flow field appears more channelled beneath the vessel. The redistribution of momentum towards the upper part of the flow domain is therefore reduced, resulting in a more concentrated downstream-oriented velocity field.

In the vertical profile plots it is possible to highline difference behaviour of the line immediately upper the core of the jet. Lines for the Case 1 (Figure 21) show a gradual decay to smaller velocities without going into negative velocity fields. Lines of the second case (Figure 22) instead are steeper and goes into the field of negative velocities.

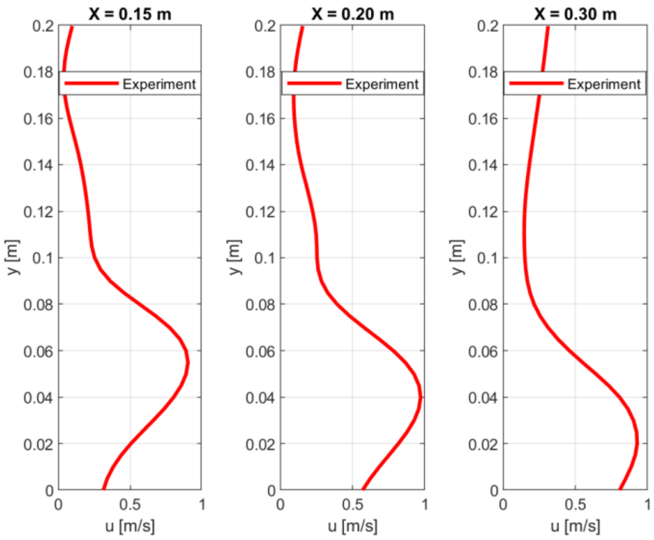

Figure 21. Vertical velocity profiles at different distances from the gate for kc = 0.03 m.

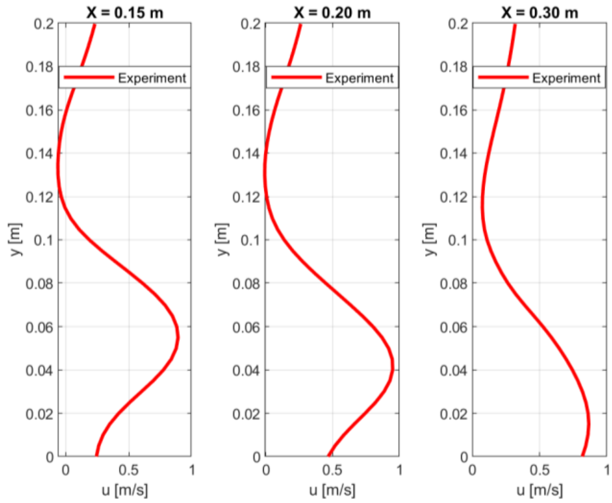

Figure 22. Vertical velocity profiles at different distances from the gate for k_c = 0.08 m.

3.3.3 Different distances from the gate

The final comparison investigates the influence of the longitudinal distance between the gate, and the vessel bow on the development of the filling jet. Two configurations were analysed, corresponding to ship positions located approximately 0.505 m and 0.65 m downstream of the gate respectively (Table 12).

	Case 1	Case 2
Q (flow rate)	0.0052 m^3/s	
h_u	0.27 m	
h_d	0.25 m	
Δh	0.02 m	
h_o	0.03 m	
k_c	0.08 m	
X_{bow}	0.0505 m	0.65 m

Table 12. Parameters for Comparison 5

The comparison between the two ship positions shows that the longitudinal location of the vessel affects not only the surrounding recirculation field, but also the local structure and concentration of the filling jet itself. Although the overall trajectory of the jet and its general sinking behaviour remain qualitatively similar in both configurations, differences can be noticed in the degree of jet concentration and in the redistribution of momentum within the downstream flow.

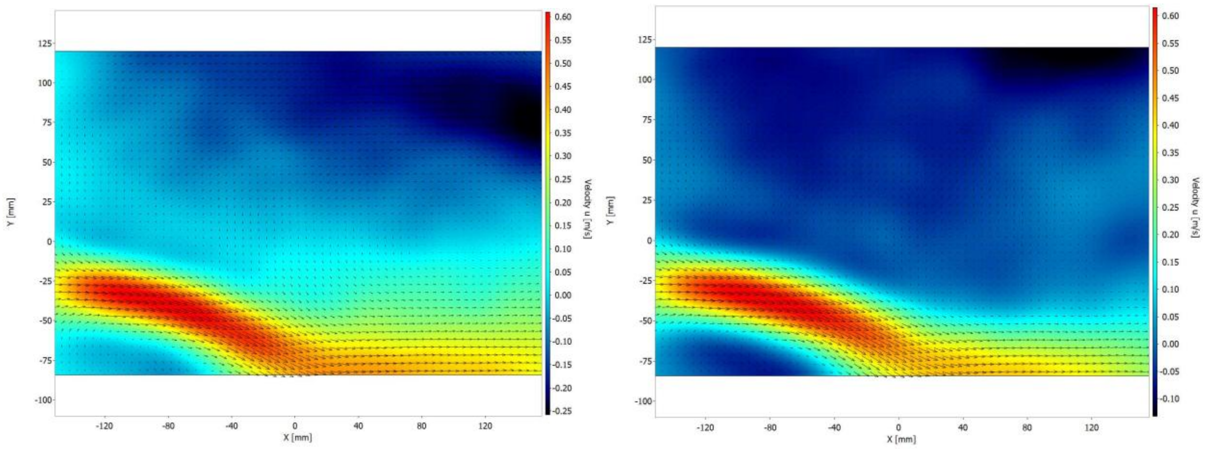

Figure 23. Average vector fields of Case 1 (Xbow = 0.505 m) and Case 2 (Xbow = 0.65 m).

The average vector fields (Figure 23) indicate that moving the vessel further downstream modifies the interaction between the developing turbulent wall jet and the under-keel confinement region. In both configurations, the jet initially exits the gate with comparable momentum and follows a similar downstream-oriented trajectory. However, the distance available for the free development of the jet before interacting with the ship strongly influences the subsequent organisation of the flow.

For the configuration characterised by the larger ship distance ($X_{bow} = 0.65$ m), the jet is allowed to develop over a longer free-stream region before encountering the confinement imposed by the vessel bottom. Consequently, the high-momentum core remains more coherent and concentrated when reaching the under-keel region. This behaviour becomes particularly visible in the velocity profiles extracted at $X = 0.30$ m downstream of the gate, where the streamwise velocity distribution appears more channelled and localised around the jet core.

The profiles (Figure 25) show that the positive streamwise velocities remain concentrated within a narrower vertical region, while the surrounding flow exhibits weaker momentum redistribution. This indicates that the jet maintains a more organised structure and that the interaction with the vessel occurs after the jet has already developed a relatively stable wall-jet configuration. The resulting flow therefore appears more canalised beneath the vessel.

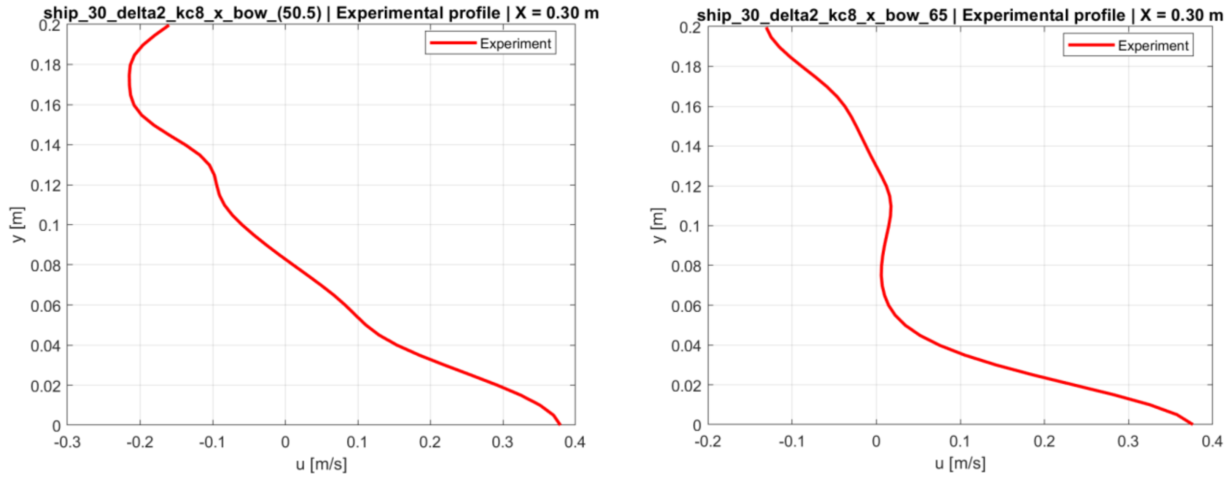

Figure 24. Vertical velocity profiles for Case 1 and Case 2.

The selected geometric scale factor and the physical dimensions of the vessel model imposed minimum allowable distances between the gate and the ship bow. Therefore, the experimental configurations could not reproduce extremely small gate-to-ship distances where even stronger interaction effects between the developing jet and the vessel would likely become more pronounced.

In addition, the spatial extent of the MiniShaker measurement domain limited the possibility of capturing a larger portion of the downstream flow field for the configurations characterised by greater ship distances. A wider camera focus and a larger measurement volume would have allowed a more complete observation of the interaction between the jet development and the further downstream vessel position. Due to experimental and optical constraints associated with the setup, such an extended measurement configuration was not possible within the present campaign.

Nevertheless, the obtained results remain physically consistent and sufficiently reliable for analysing the influence of ship position on the jet behaviour. The measurements clearly show modifications in the concentration and redistribution of the jet momentum associated with variations in the gate-ship distance, particularly in the downstream velocity profiles and in the degree of jet canalisation beneath the vessel.

Although the interaction could have been investigated in greater detail using a larger observation domain, the present results still provide valuable information regarding the evolution of the turbulent wall jet in the presence of the ship. In particular, the observed differences between the configurations constitute useful experimental evidence for the future parametrisation and improvement of the jet schematisation implemented in VUL_SLUIS.

4 ANALYSIS OF THE JET ON VUL_SLUIS

4.1 Introduction to VUL_SLUIS

VUL_SLUIS is a numerical tool developed at Flanders Hydraulics for the simulation of hydraulic processes occurring during the filling and emptying operations of navigation locks. The software was conceived as the Flemish counterpart of the Dutch program LOCKFILL (Deltares, 2016).

The program is entirely implemented in MATLAB and consists of a sequence of interconnected scripts and functions that solve the hydraulic problem through a one-dimensional schematisation of the lock system. Unlike fully three-dimensional CFD approaches, VUL_SLUIS adopts a simplified representation of the flow field to significantly reduce computational time while still retaining the principal hydraulic phenomena governing lock filling processes. This makes the software particularly suitable for preliminary design studies, parametric analyses, and operational assessments where multiple simulations are required.

The numerical workflow begins with the definition of the lock geometry, hydraulic conditions, vessel characteristics, and levelling system configuration within an input file. The input parameters are subsequently processed by different calculation modules responsible for solving the discharge evolution, water level variation, jet characteristics, and longitudinal force components acting on the vessel.

The lock system is schematised as a hydraulic domain connecting the upstream and downstream basins through openings located in the lock gates. Both rectangular and circular openings can be implemented within the model together with different gate operation systems such as lifting gates and butterfly valves. The flow through the openings is governed by classical hydraulic formulations derived from Bernoulli's equation and discharge coefficients accounting for hydraulic losses.

The discharge through the gate opening is generally expressed as (Verelst et al., 2014):

$$Q = C_d A \sqrt{2g\Delta h}$$

The filling and emptying process is solved transiently, meaning that the discharge and the hydraulic head difference evolve continuously during the simulation. The temporal variation of the water level inside the lock chamber is determined through the continuity equation:

$$\frac{dV}{dt} = Q$$

which, for a lock chamber of constant cross-sectional area, becomes:

$$A_c \frac{dh}{dt} = Q$$

where A_c is the chamber cross-sectional area and h is the water level inside the lock chamber.

At every time step, VUL_SLUIS calculates the hydraulic head difference, the resulting discharge through the openings, and the corresponding velocity distribution associated with the filling jet. The software subsequently uses these hydraulic quantities to estimate the longitudinal forces acting on the vessel.

The vessel itself is represented through a simplified geometrical schematisation. Instead of reproducing the complete hull geometry, VUL_SLUIS models the ship as a block-shaped body characterised by a limited number of geometric parameters such as length, beam, draught, and bow geometry. This simplified representation allows the software to calculate the hydraulic interaction between the vessel and the filling flow while maintaining a relatively low computational complexity.

The total longitudinal force acting on the vessel is subdivided into several physical contributions. According to the VUL_SLUIS methodology, the total force is composed of contributions associated with translatory waves, momentum reduction, friction effects, and direct jet action. The force balance is therefore written schematically as (Verelst et al., 2016):

$$F_{tot} = F_{wave} + F_{mom} + F_{fric} + F_{jet}$$

where F_{wave} represents the force associated with translatory waves, F_{mom} corresponds to momentum-related forces, F_{fric} is the friction force acting on the hull, and F_{jet} represents the direct force generated by the filling jet.

The present research focuses specifically on the jet-related contribution and on the hydraulic schematisation used by VUL_SLUIS to represent the downstream development of the filling jet. The software currently models the jet evolution using simplified wall-jet formulations and empirical spreading relations derived from previous hydraulic studies and laboratory measurements.

Several variables associated with the jet are internally calculated and stored during the simulation. These include the maximum jet velocity, jet thickness, spreading parameters, momentum flux, and velocity distribution along the lock chamber. These quantities subsequently enter the force calculations and determine the predicted hydraulic interaction between the jet and the vessel.

One of the principal limitations of the present VUL_SLUIS schematisation is that the development of the jet is calculated largely independently from the actual presence of the ship inside the lock chamber. Although the vessel geometry enters the force balance equations, the jet itself is assumed to evolve according to predefined wall-jet relations that do not fully account for the modifications induced by under-keel confinement and bow interaction.

As demonstrated in the previous experimental chapters, however, the presence of the vessel significantly alters the downstream organisation of the jet, particularly in terms of spreading behaviour, momentum redistribution, confinement effects, and recirculation development. The following sections therefore analyses into detail the present jet schematisation implemented in VUL_SLUIS and compare it with the experimental observations obtained from the MiniShaker PTV measurements.

4.1.1 Ship Schematization and Definition of X_{bow}

Within VUL_SLUIS, the vessel is represented through a simplified block-shaped schematisation rather than through a detailed hull geometry. The ship is therefore described using a limited number of geometrical parameters capable of reproducing the principal hydraulic interaction mechanisms between the vessel and the filling flow. In addition to the vessel length, beam, and draught, the bow geometry is introduced through two angular parameters, namely α and β, representing the bow inclination in the vertical and horizontal planes respectively.

The simplified bow representation plays an important role in the calculation of the longitudinal forces generated by the filling jet. VUL_SLUIS evaluates the hydraulic interaction between the jet and the bow through control-volume momentum balances in which the incoming jet momentum is redistributed around the vessel geometry. The force calculation assumes that the velocity downstream of the bow is horizontally distributed over the available wetted section, while hydrostatic pressure conditions are applied on the bow surface itself.

A critical parameter within this schematisation is the longitudinal distance between the gate and the vessel bow, denoted as X_{bow}. Although the parameter is generally defined as the distance between the gate and the bow of the vessel, the exact physical definition becomes less straightforward when dealing with an inclined bow geometry such as the one adopted in the present physical model.

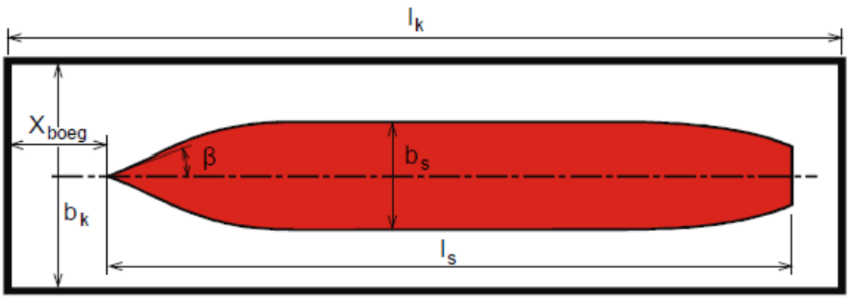

Figure 25. Sketch of the ship inside the lock chamber according to VUL_SLUIS (Verelst, 2014).

Because the ship used in the experiments possesses an inclined bow rather than a vertical block-shaped front, the effective interaction points between the jet and the vessel depends on the vertical position considered along the bow. In practice, the distance may be measured at the bottom of the vessel, at the waterline, or at an intermediate location along the inclined bow surface.

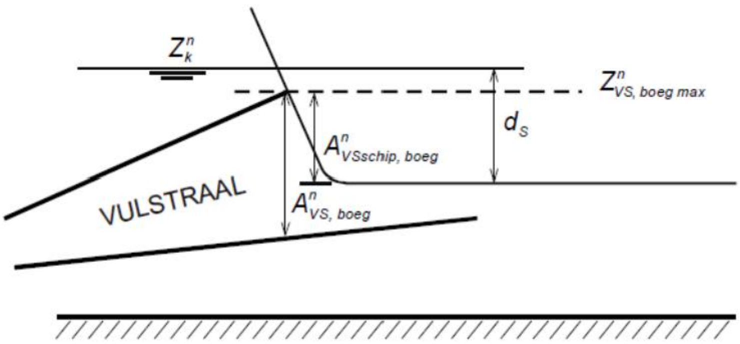

Figure 26. Impacting jet area on the bow of the ship according to VUL_SLUIS (Verelst, 2014).

From a hydraulic perspective, these different definitions are not equivalent. Measuring X_{bow} at the bottom of the ship corresponds to the location where the lower part of the jet first encounters the vessel geometry. However, the upper part of the jet interacts with the bow further downstream due to the bow inclination. Since VUL_SLUIS calculates the force contribution based on the projected bow geometry and the local jet velocity, the exact interaction location between the upper part of the jet and the bow cannot be uniquely determined within the simplified schematisation.

For this reason, defining X_{bow} at the waterline provides a more conservative interpretation of the gate-to-bow distance. The jet velocities evaluated closer to the gate are generally higher because turbulent spreading and momentum dissipation are less developed in the near-field region. Using the waterline distance therefore leads to larger calculated jet velocities acting on the bow compared to a definition based on the bottom intersection point.

The present research adopts the waterline definition of X_{bow} when translating the physical model geometry into VUL_SLUIS input parameters. The waterline value was measured for each case of the physical tests and used on each case on the software. This choice is consistent with the interpretation suggested by the LOCKFILL (Deltares, 2016) schematisation and provides a conservative representation of the jet–ship interaction.

4.1.2 Comparison Between Experimental and Numerical Hydraulic Conditions

An important distinction must nevertheless be made between the physical conditions simulated by VUL_SLUIS and those reproduced within the experimental setup adopted in the present research. VUL_SLUIS is inherently designed to simulate the transient filling or emptying process of a closed lock chamber. During a standard simulation, the software continuously updates the water level inside the chamber as the filling process evolves in time. Consequently, the hydraulic head difference, discharge, and jet velocities progressively vary throughout the levelling operation until equilibrium conditions between upstream and downstream water levels are reached.

In contrast, the physical experiments performed in the PTV flume do not reproduce a completely closed lock chamber undergoing a real transient filling process. Within the experimental setup, the flow is generated through a recirculating hydraulic system operating under approximately steady-state conditions. The upstream and downstream water levels therefore remain essentially constant during each measurement, while the flow rate through the gate opening remains stable over time.

Consequently, the experimental measurements effectively correspond to the initial stage of a lock-filling operation, namely the instant immediately after the gate opening when the hydraulic head difference is still fully developed and the jet velocities are close to their maximum values. The measured flow fields therefore represent a quasi-stationary approximation of the initial filling jet developing inside the lock chamber.

This distinction is particularly important when comparing the MiniShaker measurements with the VUL_SLUIS simulations. For the purposes of the present research, the comparison between the numerical model and the physical experiments is performed by considering the initial phase of the VUL_SLUIS filling process, corresponding to the time interval in which the hydraulic head difference remains approximately equal to the constant values imposed in the experimental setup.

The jet visualisations and velocity profiles extracted from the current version of VUL_SLUIS are therefore analysed with reference to this initial filling stage, ensuring consistency between the transient numerical calculations and the quasi-steady hydraulic conditions reproduced within the physical model experiments.

4.2 Jet Schematization in VUL_SLUIS

The representation of the filling jet in VUL_SLUIS is based on the formulations developed by Vrijburcht et al. (1988), implemented in the MATLAB subroutines *vul_sluis_impuls_straal.m and vul_sluis_impuls_straal_LvH.m*. The objective of this schematization is to describe the downstream evolution of the jet generated at the gate opening and to calculate the associated discharge and momentum distributions used in the subsequent force calculations.

The jet is modelled as a two-dimensional turbulent plane jet developing in the longitudinal vertical plane of the lock chamber under steady-flow conditions. The formulation assumes that no vessel is present during the calculation of the jet development itself and that the downstream flow initially behaves as a free turbulent jet entering a large body of still water.

Immediately downstream of the opening, two turbulent mixing layers develop at the boundaries of the jet. Between these mixing layers, a central region exists where the outlet velocity remains approximately constant. This region is referred to as the potential core. According to Vrijburcht et al. (1988) and Figure 27. Mixing layers schematization according to Vrijburcht et al. (1988).Figure 27, the mixing layers initially expand with slopes approximately equal to 1:6 and 1:12 relative to the jet axis, while the potential core extends over a longitudinal distance equal to twelve times half the initial jet height:

$$X_B = 12 \cdot \frac{h_{VS}}{2}$$

where h_{VS} is the initial height of the jet immediately downstream of the gate opening.

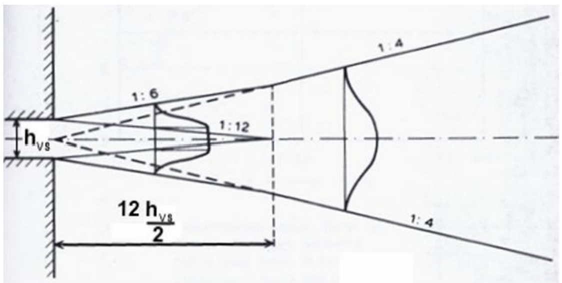

Figure 27. Mixing layers schematization according to Vrijburcht et al. (1988).

Beyond this transition region, the potential core disappears and the jet spreads with a constant spreading angle corresponding to a slope of approximately 1:4 measured from the jet centreline. The velocity profile progressively evolves into a bell-shaped turbulent distribution on both sides of the symmetry axis.

The schematization distinguishes between the behaviour of a free jet in unbounded water and that of a confined jet inside a lock chamber. In the free-jet region, turbulent entrainment causes the jet discharge to increase downstream due to the continuous suction of surrounding water into the jet core. Inside the lock chamber, however, the available surrounding water is limited by the bottom and the free surface. Consequently, recirculation regions develop between the jet and the lock boundaries.

Within the region where the jet does not yet interact with the bottom boundary, the downstream evolution of the discharge inside the jet is calculated through empirical relations derived by Vrijburcht et al. (1988). In the transition region, the discharge inside the jet is expressed as:

$$Q_{VS,X} = Q_{VO}\left(1{+}0.321\frac{X}{h_{VS}/2}\right)$$

while further downstream the relation becomes:

$$Q_{VS,X} = Q_{VO}\left(0.4\frac{X}{h_{VS}/2}\right)$$

where Q_{VO} represents the discharge through the gate opening and $Q_{VS,X}$ the discharge within the jet at a downstream distance X.

Within the initial development region, the jet impulse is assumed to remain constant:

$$I_{VS,X} = I_{VO}$$

where I_{VO} denotes the impulse directly downstream of the gate opening.

When the spreading jet reaches the bottom boundary, the influence of the wall is introduced through the development of a wall jet. The portion of the velocity profile that would geometrically penetrate the bottom is reflected and superimposed onto the existing velocity distribution. The resulting wall-jet profile is represented as a half bell-shaped distribution attached to the bottom boundary.

The downstream velocity field is therefore reconstructed through the calculation of several geometrical points defining the limits of the jet profile, the mixing layers, the potential core, and the wall-influence region. Variables such as $h_{XA,VS}$, $h_{XB,VS}$, $h_{XC,VS}$, $h_{XD,VS}$, $X_{B,VS}$, $X_{G,VS}$, and $X_{R,VS}$ are internally stored in the code and define the geometrical evolution of the velocity profile along the lock chamber.

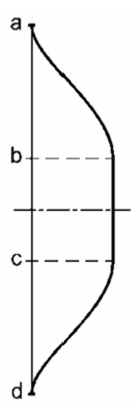

Figure 28. Velocity profile of the jet at location X (Verelst, 2014).

The formulation additionally allows the jet to develop with an inclination relative to the bottom. This inclination is represented through the angle Φ, corresponding to the angle between the jet axis and the horizontal bottom boundary. Depending on the value of Φ and on the downstream location where the jet reaches the wall, different wall-interaction cases are considered in the implementation.

Although the schematization reproduces the principal features of turbulent wall-jet development, it remains fundamentally based on idealised two-dimensional assumptions. The jet evolution is calculated independently from the actual downstream confinement generated by the vessel geometry. Consequently, the spreading behaviour, recirculation structures, and redistribution of momentum observed experimentally beneath the hull are not dynamically included within the current implementation.

As shown in the MiniShaker measurements, however, the presence of the vessel significantly alters the downstream organisation of the jet, particularly in terms of confinement effects, reduction of recirculation zones, and modification of the velocity distribution beneath the hull. These discrepancies between the idealised VUL_SLUIS schematization and the experimental observations constitute the basis for the modified jet parametrisation proposed in the following chapters.

4.3 Velocity Profiles

In order to evaluate the behaviour of the present jet schematization implemented in VUL_SLUIS, some numerical cases corresponding to the hydraulic and geometric configurations investigated experimentally were analysed. The objective of this section is not yet to perform a direct comparison with the MiniShaker measurements, which will be discussed in the following chapter, but rather to illustrate how the current VUL_SLUIS implementation reproduces the downstream evolution of the filling jet under conditions analogous to the physical model tests.

It should be noted that the coordinate system adopted for the velocity profile plots differs from the one originally associated with the calibration plate and used for the averaged vector fields. As discussed previously, the averaged velocity fields are initially reconstructed in the calibration plate reference system, where the bottom of the flume corresponds to $y = -80$ mm.

For the velocity profile analyses, however, the coordinate system was converted into the physical flume reference system to facilitate a more direct comparison between the experimental measurements and the VUL_SLUIS profiles. Consequently, for all velocity profile plots presented in the following sections, the origin *(0,0)* corresponds to the bottom of the flume at the gate location, with the vertical coordinate measured upward from the flume bottom and the longitudinal coordinate measured downstream from the gate opening. This transformed reference system is therefore consistent with the coordinate system adopted for the VUL_SLUIS reconstructions and allows a more intuitive interpretation of the downstream jet evolution.

4.3.1 Without ship

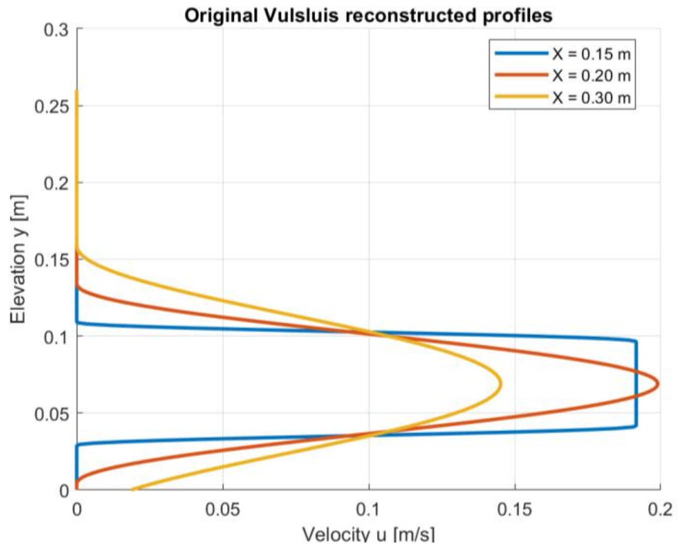

Figure 29. Reconstructed original VUL_SLUIS profiles for case without ship, opening height 0.03 m and hydraulic head of 0.02 m.

Figure 29 shows the velocity profiles reconstructed from the original VUL_SLUIS jet schematization for the configuration characterised by an opening height equal to 0.03 m and a hydraulic head difference $\Delta h = 2$ cm. The profiles are extracted at three downstream locations corresponding to $X = 0.15$ m, $X = 0.20\ m$, and $X = 0.30$ m from the gate opening. The reconstructed profiles presented in this section are based on an imposed value of $\Phi = 0°$, corresponding to a jet initially aligned parallel to the bottom boundary. One of the objectives of the present research is precisely to reduce the dependence of the jet schematization on predefined input parameters such as Φ, replacing them with a parametrization more directly derived from experimentally observed jet behaviour.

Although this configuration is intended to represent the case without vessel discussed in the experimental campaign, it should be noted that VUL_SLUIS intrinsically requires the presence of a ship geometry within the simulation setup. Consequently, a fictitious vessel configuration was introduced in the numerical model solely to allow the execution of the calculations while minimising its influence on the downstream jet development. The selected configuration therefore approximates the behaviour of a free jet inside the lock chamber as closely as possible within the constraints of the software implementation.

The calculated profiles reproduce the classical downstream evolution of the wall-jet schematization implemented in VUL_SLUIS. Immediately downstream of the gate, at $X = 0.15$ m, the velocity profile still exhibits a relatively compact structure characterised by an almost uniform high-velocity region corresponding to the remaining potential core of the jet. The profile presents relatively sharp velocity gradients at both the upper and lower boundaries of the jet, indicating that the turbulent spreading process is still limited at this location.

Further downstream, at $X = 0.20$ m, the profile progressively evolves into a smoother bell-shaped distribution. The maximum velocity decreases compared to the near-field section, while the vertical extension of the profile increases due to turbulent entrainment and momentum redistribution. This behaviour directly reflects the empirical spreading relations described in the previous section.

At $X = 0.30$ m, the spreading process becomes even more pronounced. The maximum velocity is further reduced, and the profile becomes significantly wider, indicating that the jet momentum has been redistributed over a larger portion of the flow depth. The profile also shows the progressive downward displacement of the high-velocity core associated with the wall-jet development along the bottom boundary.

4.3.2 With ship

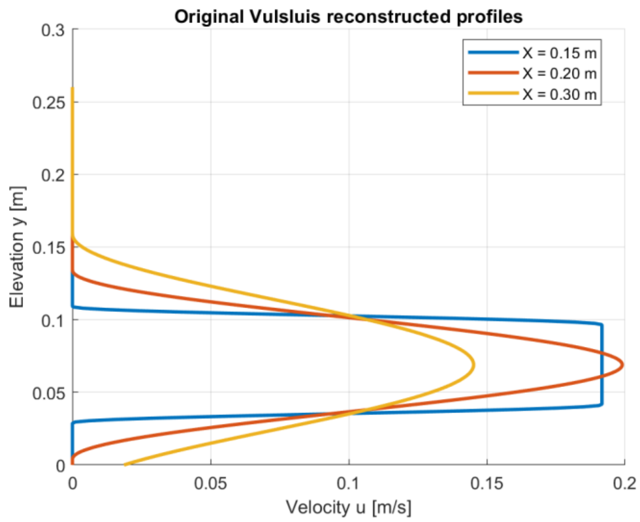

Figure 30. Reconstructed original VUL_SLUIS profiles for case with ship, opening height 0.03 m, hydraulic head of 0.02 m, k_c = 0.03 m and X_{bow} = 0.505 m

The profiles presented in Figure 30 correspond to the ship configuration with a gate opening of 0.03 m, a hydraulic head difference $\Delta h = 0.02$ m, a keel clearance $k_c = 0.03$ m, and a bow position $X_{bow} = 0.505$ cm. As explained in the previous section, the ship position was imposed through the free-surface parameter X_s, set equal to 0.11 m.

For the ship configuration, the vessel mass was additionally included in the model setup. The ship mass was estimated from the displaced water volume assuming floating equilibrium:

$$m = \rho LBT$$

where $L\ [m]$, $B\ [m]$, and $T\ [m]$ are the ship length, beam, and draft, respectively. Using $L = 0.9304$ m, $B = 0.39$ m, $T = 0.23$ m, and $\rho = 1000\ \mathrm{kg/m^3}$, the resulting ship mass is approximately 83 kg.

The comparison between these velocity profiles obtained for the configurations without ship and with ship under identical opening height and hydraulic head conditions shows that the profiles remain essentially unchanged in the current VUL_SLUIS implementation. The downstream velocity distributions, the spreading behaviour, and the position of the jet core are practically identical in both cases.

This result directly reflects one of the principal assumptions of the original VUL_SLUIS schematization. Although the vessel geometry is included in the subsequent force calculations, the development of the filling jet itself is calculated independently from the actual presence of the ship inside the lock chamber.

For this reason, the next chapter will focus on the direct comparison between the velocity profiles reconstructed by VUL_SLUIS and the experimentally measured profiles obtained from the physical model tests. This comparison will allow the limitations of the current schematization to be identified more clearly and quantified through the observed differences between numerical and experimental jet behaviour. Subsequently, the following chapter will introduce a modified jet schematization specifically developed to account for the influence of the vessel on the downstream jet evolution. The objective of the new parametrization is precisely to overcome the present limitation of the original VUL_SLUIS implementation, ensuring that the reconstructed velocity profiles differ between the configurations without ship and with ship in a manner consistent with the experimental observations.

4.4 Force Predictions with the Original Jet Schematization

Although the main objective of the present research is the analysis and improvement of the jet schematization implemented in VUL_SLUIS, it is also important to evaluate how the current velocity distributions influence the longitudinal force calculations performed by the software.

In VUL_SLUIS, the total longitudinal force acting on the vessel is composed of different physical contributions, including forces generated by translatory waves, momentum reduction, friction effects, and direct jet action (Section 4.1). The jet schematization mainly affects the force components associated with jet action and momentum reduction, since both depend directly on the calculated downstream evolution of the filling jet and on the corresponding momentum distribution.

For this reason, representative force calculations obtained with the original VUL_SLUIS implementation are presented in this section for configurations analogous to the experimental cases previously analysed. The objective is not to validate the calculated forces experimentally, since no direct force measurements were performed during the physical model campaign, but rather to establish a reference framework for the original jet schematization.

This baseline will subsequently be compared with the force predictions obtained using the modified jet parametrization proposed in the following chapters. In this way, the influence of the new jet schematization on the calculated longitudinal forces can be directly evaluated.

Table 13 shows cases for which forces are calculated with the present version of VUL_SLUIS.

Case	**Ship Configuration**	**h_o [m]**	**Δh [m]**	**k_c [m]**	**X_{bow} [m]**	**X_s [m]**
1	With ship	0.03	0.02	0.03	0.505	0.11
2	With ship	0.03	0.09	0.03	0.505	0.16
3	With ship	0.06	0.02	0.33	0.505	0.125

Table 13. Different cases for which longitudinal forces are calculated with the present version of VUL_SLUIS in the lock filling operation.

Case 1

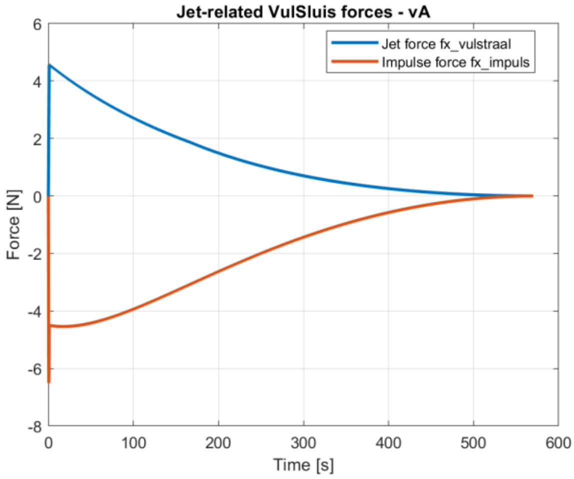

Figure 31. Jet-Related forces on original VUL_SLUIS for Case 1.

Case 2

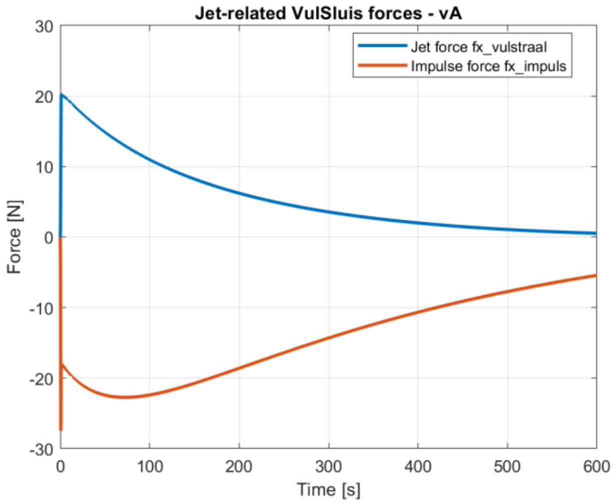

Figure 32. Jet-Related forces on original VUL_SLUIS for Case 2.

Case 3

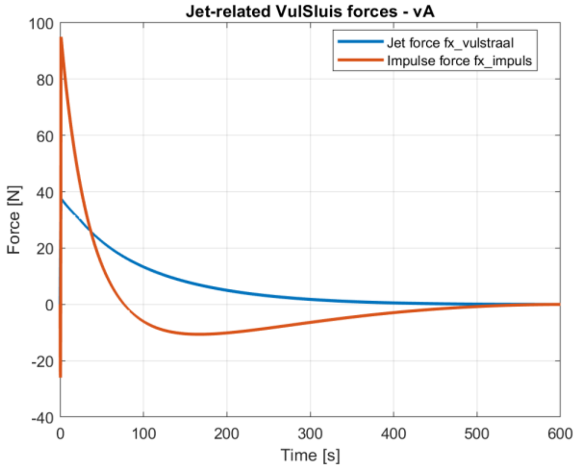

Figure 33. Jet-Related forces on original VUL_SLUIS for Case 3.

Figure 31, Figure 32 and Figure 33 present the force components that are directly influenced by the jet schematization implemented in VUL_SLUIS. Only the jet-related contributions are analysed, namely the impulse force $f_{x,\text{impuls}}$ and the jet force $f_{x,\text{vulstraal}}$. Other forces, such as the translational wave force and the friction force, are not included in this comparison because they are mainly governed by global lock hydraulics, water-level gradients, and resistance effects, rather than by the detailed structure of the filling jet itself.

The component $f_{x,\text{impuls}}$ represents the contribution associated with the global momentum balance of the filling flow. This term depends on the discharge and on the overall downstream transport of momentum generated by the jet. Although it is influenced by the jet development, it mainly reflects the integral behaviour of the flow rather than the local velocity distribution beneath the vessel. During the filling process, recirculation zones, flow redistribution, reflected waves, and confinement effects may generate longitudinal momentum components opposite to the main jet direction.

The other contribution $f_{x,\text{vulstraal}}$, on the other hand, is directly linked to the reconstructed jet velocity profile. This force depends on the spatial distribution of velocity within the jet and is therefore strongly affected by the adopted jet schematization. Modifications to the jet spreading, jet sinking trajectory, and vertical velocity distribution directly alter this contribution. By plotting these two force components separately, it becomes possible to distinguish between changes affecting the global momentum transport of the flow and changes specifically associated with the local redistribution of the jet beneath the ship. This distinction is essential for assessing how the jet reconstruction influences the hydrodynamic loading predicted by VUL_SLUIS.

5 COMPARISON BETWEEN SCALE MODEL AND VUL_SLUIS

The previous chapters presented separately the experimental results obtained from the MiniShaker PTV measurements and the velocity profiles reconstructed through the original VUL_SLUIS jet schematization. The objective of the present chapter is to directly compare these two approaches to evaluate how accurately the current VUL_SLUIS implementation reproduces the physical behaviour of the filling jet observed in the scale model experiments.

The comparison focuses primarily on the downstream velocity distributions and on the evolution of the turbulent wall jet inside the lock chamber. Attention is paid to the spreading behaviour of the jet and the downstream sinking of the high-velocity core. The redistribution of momentum associated with particle recirculation will not constitute the primary focus of the present analysis. The main objective of this thesis is the investigation of the filling jet behaviour itself, whereas the velocity measurements obtained in the recirculation regions above the jet core are characterised by lower accuracy, as previously discussed in Chapter 2.

Similarly, the influence of the vessel on the velocity profiles will not be analysed extensively in this section, since this aspect was already investigated in detail in the previous chapter. Moreover, as previously demonstrated, the original VUL_SLUIS implementation does not directly account for the effect of the vessel on the downstream development of the jet.

To facilitate a direct interpretation of the differences, the velocity profiles extracted from VUL_SLUIS and from the MiniShaker measurements are plotted together at identical downstream locations from the gate. This combined representation allows a detailed comparison between the numerical and experimental profiles and makes it possible to identify both qualitative and quantitative discrepancies between the two approaches.

5.1 Spreading of the jet

One of the principal aspects analysed in the comparison is the downstream spreading behaviour of the filling jet. The spreading process governs the redistribution of momentum inside the lock chamber and strongly influences the downstream evolution of the velocity field.

For different geometric and hydraulic configurations analysed (Figure 34, Figure 35), similar characteristics can be observed in the comparison between the experimental measurements and the original VUL_SLUIS profiles. Independently of the opening height and hydraulic head difference, the experimental jet core appears significantly more concentrated than the one predicted by VUL_SLUIS. The measured profiles show higher local velocity gradients around the jet core, indicating a sharper transition between the high-momentum region and the surrounding flow.

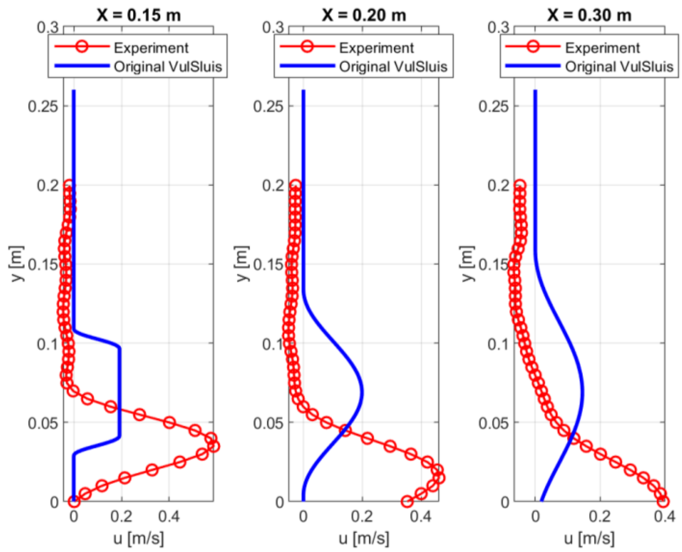

Figure 34. Comparison between experimental data and VUL_SLUIS reconstructed profiles. (Without ship, h_o = 0.03 m and Δh = 0.02 m).

In contrast, the profiles reconstructed by VUL_SLUIS are smoother and show a wider vertical spreading of the jet. This behaviour is a direct consequence of the analytical wall-jet formulation implemented in the original schematization, where the velocity distribution is governed by predefined spreading laws. As a result, the numerical model tends to redistribute the jet momentum over a larger portion of the flow depth than observed in the scale model measurements.

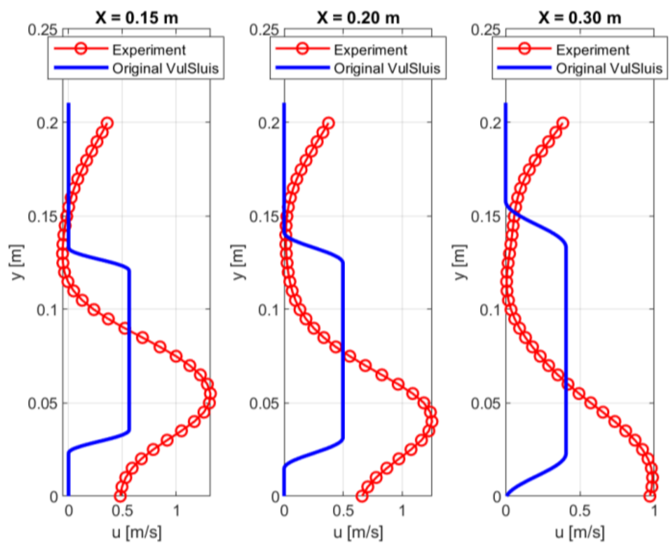

Figure 35. Comparison between experimental data and VUL_SLUIS reconstructed profiles. (Without ship, h_o = 6 cm and Δh = 9 cm).

In the present subsection, all VUL_SLUIS profiles are reconstructed using a jet inclination angle $\Phi = 0°$. This choice is intentional, since the objective here is to isolate the spreading behaviour of the jet from the effects associated with its downward inclination. The role of Φ, together with the limitations of defining a different inclination angle for each individual case, is discussed separately in the section dedicated to the sinking behaviour of the jet.

This distinction is important because the purpose of the present analysis is not to improve the agreement by manually adjusting the jet angle, but rather to identify the systematic differences in spreading between the measured jet and the original VUL_SLUIS schematization. The comparison therefore shows that, even when the jet is assumed to remain horizontal, the original model tends to predict a smoother and more vertically diffused velocity distribution than the one observed experimentally.

5.2 Sinking

To analyse the sinking behaviour of the jet, the same two hydraulic configurations previously discussed for the spreading analysis were considered, namely the cases characterised by an opening height of 3 cm with $\Delta h = 2$ cm and an opening height of 6 cm with $\Delta h = 9$ cm. In contrast with the previous subsection, the VUL_SLUIS simulations presented here were reconstructed by imposing a jet inclination angle derived from the experimental observations.

The inclination angle was estimated directly from the experimental jet trajectory using the geometrical relation:

$$\theta = \tan^{-1}\left(\frac{\Delta x}{\Delta y}\right)$$

where Δx and Δy represent the longitudinal and vertical displacement of the jet core extracted from the MiniShaker measurements. The estimated angle was around $\Phi = -18°$.

The introduction of the inclination angle significantly improves the agreement between the numerical and experimental profiles, particularly regarding the downstream position of the jet core. Compared with the results presented in the spreading analysis, the reconstructed VUL_SLUIS profiles now reproduce more accurately the downward evolution of the jet and the progressive displacement of the high-velocity region towards the bottom boundary.

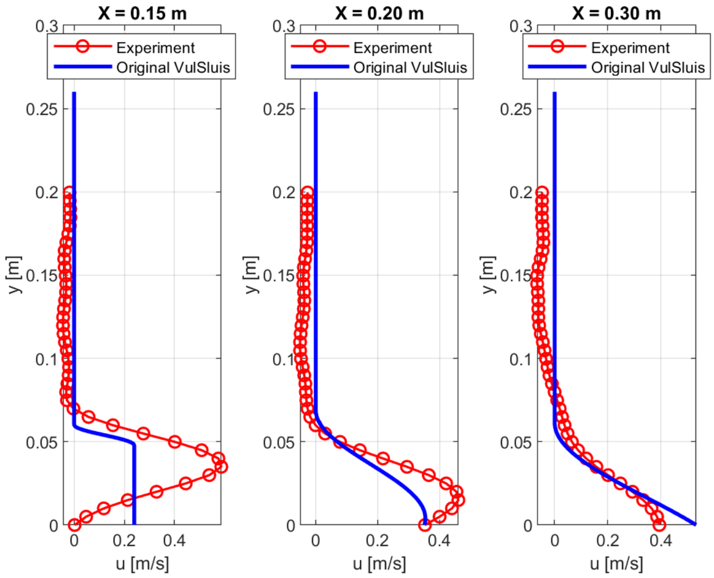

Figure 36. Comparison between experimental data and VUL_SLUIS reconstructed profiles with an input jet angle. (Without ship, h_o = 3 cm and Δh = 2 cm).

This effect becomes especially visible in the downstream sections at $X = 0.20$ m and $X = 0.30$ m, where the numerical profiles follow the experimentally observed sinking tendency much more closely than in the $\Phi = 0°$ configuration. The comparison therefore confirms that the inclination angle constitutes one of the dominant parameters controlling the downstream position of the jet within the current VUL_SLUIS schematization.

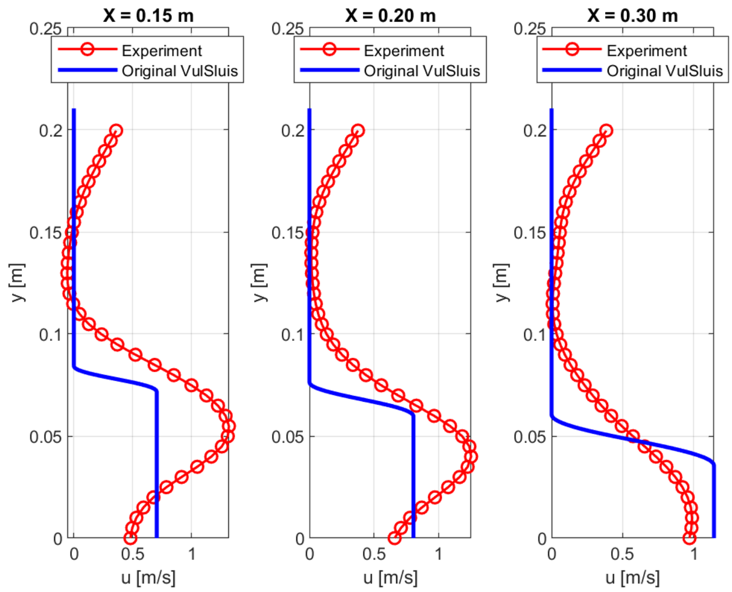

Figure 37. Comparison between experimental data and VUL_SLUIS reconstructed profiles with an input jet angle. (Without ship, h_o = 6 cm and Δh = 9 cm).

At the same time, the analysis also highlights one of the principal limitations of the original implementation. The quality of the agreement between numerical and experimental profiles becomes strongly dependent on the selected value of Φ introduced in the input file. Small variations in the imposed inclination angle can significantly modify the downstream jet trajectory and therefore alter the reconstructed velocity profiles.

This dependency represents a major limitation for practical applications because the inclination angle cannot be considered a universal parameter. The experimental results suggest that the sinking behaviour depends simultaneously on multiple hydraulic and geometrical conditions, including opening height, hydraulic head difference, turbulent entrainment, and downstream confinement. Consequently, determining a different Φ value manually for each individual case would not provide a sufficiently generalised approach for the numerical schematization of the filling jet.

For this reason, the modified jet parametrization proposed in the following chapter will not rely on externally imposed inclination angles. Instead, the new schematization will aim to incorporate the sinking behaviour directly within the parametrization itself, allowing the downstream evolution of the jet to develop more naturally as a function of the governing hydraulic conditions without requiring a case-dependent definition of Φ. The objective of the proposed modification is therefore to improve the physical realism of the jet representation while preserving the computational efficiency and the original philosophy of VUL_SLUIS.

6 SOLUTION FOR NEW JET SCHEMATIZATION

6.1 Idea

The comparison between the MiniShaker measurements and the original VUL_SLUIS implementation demonstrated that the current jet schematization cannot accurately reproduce the downstream evolution of the filling jet inside the lock chamber. Although the original formulation captures the general behaviour of a turbulent wall jet, important discrepancies remain regarding the spreading of the velocity profile and the downward movement of the jet core.

The experimental results showed that, after exiting the gate opening, the filling jet initially propagates almost horizontally, progressively spreads due to turbulent mixing, and gradually moves downward toward the bottom of the lock chamber, eventually developing into a wall jet attached to the bottom boundary. Similar behaviour is commonly described in turbulent jet theory, where entrainment of surrounding fluid modifies both the jet width and its trajectory (Rajaratnam, 1976).

The current VUL_SLUIS implementation instead relies on a geometrical reconstruction derived from Vrijburcht et al. (1988), where the spreading of the jet is governed by predefined analytical relations. As discussed in the previous chapters, this formulation tends to produce velocity profiles that are excessively smooth and vertically diffused compared with the experimental measurements. Furthermore, the sinking behaviour of the jet can only be reproduced by manually imposing an inclination angle Φ, which strongly affects the resulting profiles and cannot be considered a universal parameter.

Rather than replacing the entire VUL_SLUIS framework, the proposed approach modifies only the internal reconstruction of the jet geometry and velocity distribution. In this way, the existing routines for discharge evolution, momentum calculation and force estimation can still be preserved.

The proposed schematization is based on a parametric reconstruction of the jet using experimentally calibrated relationships. The approach combines simplified turbulent jet theory with empirical relations derived from the MiniShaker measurements. The intention is not to reproduce the complete turbulent flow field in detail, but rather to obtain a reduced-order representation capable of reproducing the most relevant hydraulic characteristics of the filling jet.

The calibration philosophy adopted in the present research is based on the use of the entire experimental dataset rather than on individual isolated cases. The objective is therefore not to obtain a perfect reconstruction for a single configuration, but to identify a set of parameters capable of reproducing the general behaviour of the filling jet under different hydraulic and geometrical conditions. To achieve this, a global objective function is defined to minimize the discrepancy between the reconstructed numerical profiles and the experimental velocity measurements across all available cases.

The calibration process is conducted in two successive stages. A first calibration is performed using only the configurations without vessel, allowing the spreading behaviour and the sinking trajectory of the turbulent jet to be analysed independently from confinement effects beneath the hull. This initial stage provides the base parametrization governing the downstream development of the jet inside the lock chamber.

Subsequently, a second calibration stage is introduced for the configurations including the vessel. In this phase, the keel clearance k_c and the longitudinal distance between the gate and the ship bow X_{bow} become governing parameters influencing the downstream evolution of the jet. The experimental measurements showed that both quantities significantly affect the confinement of the flow and the downward deflection of the jet beneath the hull.

This second calibration stage represents one of the principal innovations of the proposed schematization. Unlike the original VUL_SLUIS implementation, where the jet evolution is calculated independently from the vessel position, the modified parametrization introduces a direct dependency between the jet behaviour and the ship configuration inside the lock chamber. Consequently, the new formulation allows the jet evolution to adapt not only to the hydraulic conditions imposed at the gate, but also to the presence and position of the vessel within the lock chamber.

6.1.1 Parametrization

The proposed jet schematization is based on a reduced-order parametric reconstruction of the filling jet aimed at reproducing the principal hydraulic behaviours observed in the MiniShaker measurements while preserving the computational efficiency and engineering-oriented philosophy of VUL_SLUIS. The formulation combines concepts derived from existing lock-filling models with new parametrizations introduced specifically within the framework of the present research.

The first component of the model concerns the downstream spreading of the jet. In the original VUL_SLUIS implementation, the geometry of the jet is reconstructed through predefined characteristic elevations derived from the analytical formulation proposed by Vrijburcht et al. (1988). Although this approach provides a simplified representation of turbulent wall jets, the comparison with the experimental measurements showed that the resulting velocity profiles remain excessively smooth and vertically diffused.

To overcome this limitation, the present research adopts a spreading formulation inspired by LoMo (BAW Lock Model), the German software developed by the Federal Waterways Engineering and Research Institute (BAW) for the simulation of lock filling and emptying processes. In the LoMo approach, the downstream development of the jet is represented through an empirical law describing the increase of the jet cross-sectional area as a function of the distance from the gate (Belzner, Simons and Thorenz, 2018).

In its general form, the LoMo parametrization is expressed as:

$$A_{jet} = c_0 + c_1 A_{valve}(t) + c_2 x^{c_3}$$

where A_{valve} represents the opening area at the gate, while c_0, c_1, c_2, and c_3 are empirical coefficients controlling the initial jet dimensions and the downstream spreading behaviour. As discussed in the LoMo documentation, the coefficients c_0 and c_1 can be simplified to $c_0 = 0$ and $c_1 = 1$ when the initial jet section is assumed to coincide directly with the physical opening area.

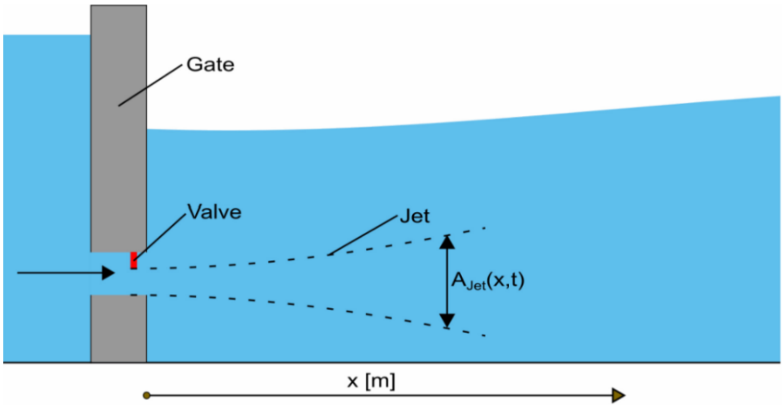

Figure 38. Propagation of the filling jet inspired by LoMo (Belzner et al. 2018.).

The same assumption is adopted in the present work. Physically, this means that no additional empirical correction is imposed at the gate section and that the initial jet thickness corresponds directly to the opening height used in the experiments. Consequently, the proposed formulation can be written as:

$$A_{jet}(x) = H_{VS} + c_2 x^{c_3}$$

where H_{VS} represents the effective gate opening height. The coefficients c_2 and c_3 govern the magnitude and downstream evolution of the spreading process. This parametrization allows the jet thickness to evolve continuously along the lock chamber and provides considerably greater flexibility than the original geometrical reconstruction adopted in VUL_SLUIS.

A second and more substantial modification concerns the vertical trajectory of the jet centreline. The experimental measurements consistently showed that the jet progressively moves downward after exiting the gate and eventually develops into a bottom-attached wall jet. This behaviour was not reproduced adequately by the original VUL_SLUIS implementation unless an inclination angle Φ was manually imposed. However, the comparison with the experiments demonstrated that the appropriate value of Φ strongly depends on the hydraulic and geometrical conditions and therefore cannot be considered a universal parameter.

For this reason, the present research introduces a new parametrization for the downstream evolution of the jet centreline:

$$y_{core}(x) = y_{floor} + (y_0 - y_{floor})\exp\left(\frac{-k_s X_{sink}}{H_{VS}}\right)$$

where y_0 denotes the initial jet centreline elevation, y_{floor} represents the elevation the bottom of the lock camber, and k_s controls the sinking intensity.

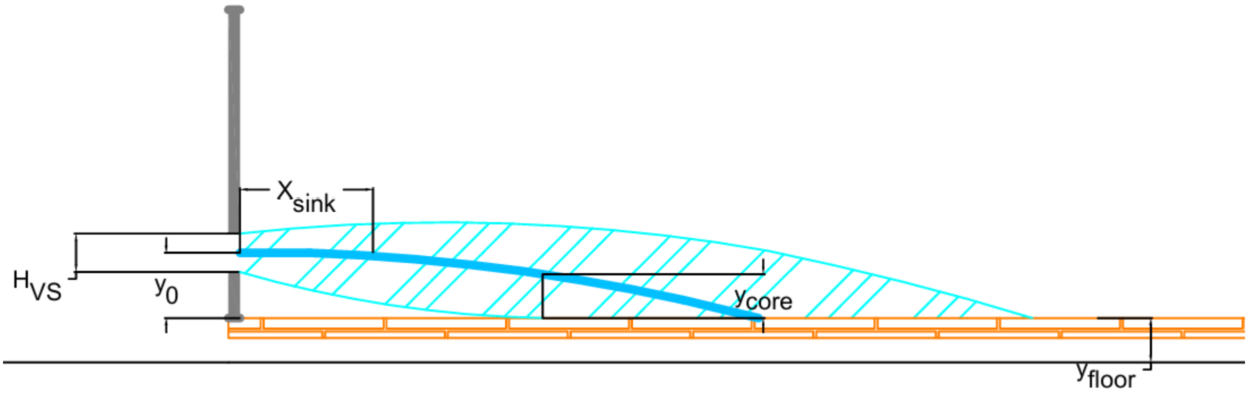

Figure 39. Sketch of the new jet trajectory.

This exponential formulation constitutes one of the principal contributions of the present work. Rather than imposing an arbitrary inclination angle, the jet trajectory evolves naturally through a continuous parametrized relation calibrated against the MiniShaker measurements. The exponential form was selected because it provides a smooth asymptotic transition between the initial jet trajectory and the bottom boundary while naturally reproducing the progressive reduction of the sinking rate downstream. Furthermore, the normalization by H_{VS} preserves geometric similarity between different gate openings and ensures that the sinking behaviour scales consistently with the initial jet dimensions.

The experimental comparison additionally showed that applying the sinking immediately downstream of the gate produced excessive downward deflection at short downstream distances, particularly for the smaller openings. Physically, the jet initially retains a strong horizontal inertia and behaves similarly to a developing potential-core region before progressively transitioning toward a wall jet. To account for this behaviour, a delayed sinking formulation was introduced:

$$X_{sink} = \max(0, X - X_0)$$

with:

$$X_0 = 3H_{VS}$$

This modification delays the onset of the exponential sinking mechanism over an initial development length proportional to the gate opening height. The selected value of $3H_{VS}$ is consistent with the order of magnitude of the potential-core region represented in the original VUL_SLUIS schematization and significantly improved the agreement with the experimental profiles at $X = 0.15$ m.

Once the downstream spreading and centreline trajectory are reconstructed, the vertical velocity distribution is computed. In contrast with the original VUL_SLUIS formulation, the present model does not assume a central region with constant velocity. The MiniShaker measurements consistently showed that the experimental profiles exhibit smooth continuous distributions without a uniform potential core. The measured profiles instead resemble Gaussian-type turbulent distributions characterised by gradual velocity decay away from the jet centre.

For this reason, the velocity profile is reconstructed using a Gaussian formulation:

$$u(y) \propto exp\left(-\frac{1}{2}\left(\frac{y - y_{core}}{\sigma}\right)^2\right)$$

where the profile width is linked to the LoMo-inspired jet thickness through:

$$\sigma = \frac{A_{jet}}{factor_{eff}}.$$

An additional calibration parameter, α, was introduced to account for the influence of the opening height on the concentration of the reconstructed velocity profile. The experimental measurements showed that larger gate openings tend to generate more concentrated velocity cores compared with smaller openings. To reproduce this behaviour, the effective concentration factor is expressed as:

$$factor_{eff} = factor\left(\frac{H_{VS}}{H_{ref}}\right)^{\alpha}$$

where H_{VS} represents the gate opening height and H_{ref} is a reference opening height introduced for normalization purposes. In the present research:

$$H_{ref} = 0.030\ m$$

corresponding to the smallest opening configuration used during the experimental campaign. This value was selected as the reference opening used to express the concentration correction in dimensionless form and to ensure consistency between the different opening configurations considered in the calibration procedure.

Positive values of α therefore produce larger values of $factor_{eff}$ for larger openings, resulting in smaller values of σ and consequently more concentrated velocity profiles. This empirical correction significantly improved the agreement between the reconstructed and experimental profiles across the different opening configurations.

The downstream measurements also demonstrated that once the jet approaches the bottom boundary, the flow progressively evolves into a wall jet characterized by a maximum velocity located close to the bottom. To reproduce this behaviour, the model automatically switches from the full Gaussian formulation to a half-Gaussian wall-jet profile whenever the jet centreline becomes sufficiently close to the bottom boundary. The use of a half-Gaussian distribution is inspired by classical wall-jet theory, where the presence of the wall suppresses the lower half of the turbulent velocity distribution and forces the maximum velocity to occur directly at the boundary (Schwarz et al., 1961).

In this regime, the velocity profile is expressed as:

$$u(y) \propto exp\left(-\frac{1}{2}\left(\frac{y}{\sigma_{wall}}\right)^{2}\right)$$

thereby producing a maximum velocity directly at the bottom boundary and a decay only in the upward direction. The wall-jet spreading parameter is calculated as:

$$\sigma_{wall} = \frac{A_{jet}}{factor_{eff}}$$

using the same spreading formulation adopted for the free-jet Gaussian reconstruction. In this way, continuity is preserved between the free-jet and wall-jet regimes while allowing the downstream profile to progressively adapt to the bottom-attached configuration observed experimentally. This modification substantially improved the representation of the downstream experimental profiles, particularly at $X = 0.30$ m, where wall-jet behaviour became dominant.

Finally, a moderate entrainment correction was introduced to account for the progressive increase of the effective discharge transported within the jet due to turbulent mixing with the surrounding water (Turner, J.S., 1986). The effective discharge used for reconstructing the velocity profile is expressed as:

$$Q_{eff} = Q_{VO} \cdot f_{entr}$$

where the entrainment factor evolves downstream according to:

$$f_{entr} = 1 + c_e \frac{X}{H_{VS}} \left(\frac{H_{VS}}{H_{ref}}\right)^{\beta_E}$$

An upper limitation equal to $f_{entr,max} = 1.5$ was introduced to prevent unrealistic amplification of the effective discharge at large downstream distances. This upper bound was selected empirically during the calibration phase because larger values generated excessive downstream velocity amplification and unrealistically high momentum levels compared with the experimental measurements. The entrainment correction significantly improved the agreement between the reconstructed and measured peak velocities without excessively narrowing the velocity profiles.

The coefficient $c_e = 0.03$ was selected to provide a moderate downstream increase of the effective discharge. This value produced entrainment levels consistent with the observed behaviour of turbulent plane jets while preserving realistic velocity magnitudes within the reconstructed profiles. Larger values generated excessive amplification of the downstream velocities, whereas smaller values did not sufficiently improve the agreement with the measured peak velocities.

The exponent $\beta_E = 0.5$ was introduced to account for the experimentally observed dependency of the entrainment behaviour on the opening height. The measurements indicated that the smaller openings exhibited relatively stronger entrainment effects compared with the larger openings. A moderate exponent value was therefore selected to include this dependency while avoiding excessive sensitivity of the correction to the gate opening height.

Overall, the modified parametrization preserves the principal conceptual structure of the original VUL_SLUIS schematization while introducing physically motivated corrections directly derived from the MiniShaker experimental observations.

6.2 Calibration without ship

The first stage of the calibration procedure was performed using exclusively the experimental configurations without vessel. The purpose of this initial calibration was to reconstruct the fundamental hydraulic behaviour of the turbulent filling jet independently from the confinement effects generated by the presence of the ship beneath the water surface. In this way, the calibration focuses solely on the intrinsic evolution of the jet itself, namely its downstream spreading, the redistribution of the velocity field, and the progressive sinking toward the bottom boundary.

The calibration was conducted by optimizing the principal parameters governing the modified jet parametrization, namely the spreading coefficients c_2 and c_3, the sinking coefficient $k_{s,0}$, the concentration $factor$ associated with the Gaussian reconstruction, and the opening-dependent correction parameter α. These parameters were determined through comparison with the experimental velocity profiles extracted from the MiniShaker measurements for the different hydraulic and geometrical configurations analysed in the previous chapters.

Rather than calibrating each individual case independently, the optimization procedure was formulated as a global calibration problem. The objective was therefore to identify a single parameter set capable of reproducing consistently the general behaviour of the filling jet across all available experimental configurations. This approach ensures that the resulting parametrization maintains a sufficiently general character and avoids overfitting the model to a limited number of isolated measurements.

The calibration procedure is based on the minimization of a global objective function combining different error contributions associated with the reconstructed velocity field. The comparison between numerical and experimental profiles considers not only the overall shape of the velocity distribution, but also the prediction of the maximum velocity magnitude and the downstream position of the jet core. In this way, the optimization simultaneously evaluates the ability of the model to reproduce the spreading behaviour, the concentration of the jet core, and the sinking trajectory observed experimentally.

To allow a consistent comparison between cases characterised by different hydraulic head differences, all error terms were normalized using a characteristic reference velocity defined as:

$$U_{ref} = \sqrt{2g\Delta H}$$

This normalization ensures that cases with larger hydraulic heads do not dominate the optimization solely because of their larger absolute velocities, thereby allowing all experimental configurations to contribute comparably to the calibration process.

The global calibration error is expressed as:

$$J_{total} = \frac{1}{N_{cases}} \sum_{i=1}^{N_{cases}} J_i$$

where N_{cases} represents the number of experimental configurations included in the calibration and J_i denotes the error associated with the individual case i.

For each experimental configuration, the reconstructed model profiles are compared with the MiniShaker measurements at different downstream locations from the gate. The objective function therefore evaluates the overall agreement between numerical and experimental profiles over the entire dataset rather than at a single measurement section.

This global optimization strategy proved particularly important because the experimental measurements covered different opening heights and hydraulic head differences, resulting in substantially different spreading rates, peak velocities, and sinking behaviours. The use of a single optimized parameter set therefore demonstrates that the proposed parametrization can reproduce the dominant hydraulic mechanisms governing the downstream development of the filling jet under varying operating conditions.

6.2.1 New profiles

The modified jet parametrization was implemented directly within the existing VUL_SLUIS computational framework by replacing the original *vul_sluis_impuls_straal_LvH.m* routine inside the calculation loop. In this way, the general structure of VUL_SLUIS, including the discharge evolution and force calculation procedures, remained unchanged, while the internal reconstruction of the filling jet was replaced by the new parametrized formulation described in the previous section.

Once integrated into the model, the modified routine generates new downstream velocity profiles based on the calibrated parametrization. In the following analyses, several representative examples are plotted together with the corresponding experimental profiles obtained from the MiniShaker measurements. The selected cases correspond to the experimental configurations that contributed most significantly to the calibration process and to the identification of the final parameter set.

The calibrated values obtained through the optimization procedure are reported in Table 14 together with the final value of the global calibration error J_{total}.

Parameter	Value
c_2	0.010256
c_3	1.999999
$k_{s,0}$	0.500000
$factor$	3.000000
α	1.123021
Total calibration error: J_{total}	2.3498*10^-2

Table 14. New calibrated parameters for no-ship configurations.

The objective of the following comparisons is to evaluate the capability of the modified parametrization to reproduce the experimental velocity distributions measured in the physical model tests. For this reason, the reconstructed profiles obtained with the new model are compared directly with the MiniShaker measurements at the same downstream locations from the gate.

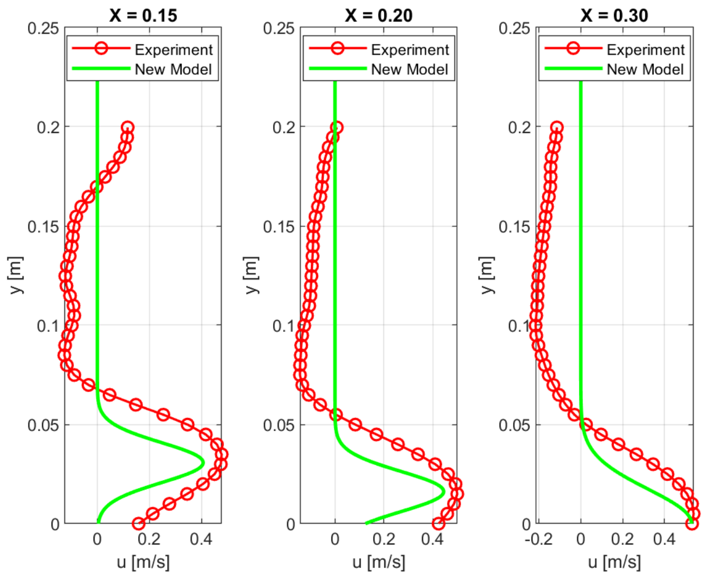

Figure 40. Comparison between new model profiles and experimental data profiles (h_o = 0.03 m, Δh = 0.07 m).

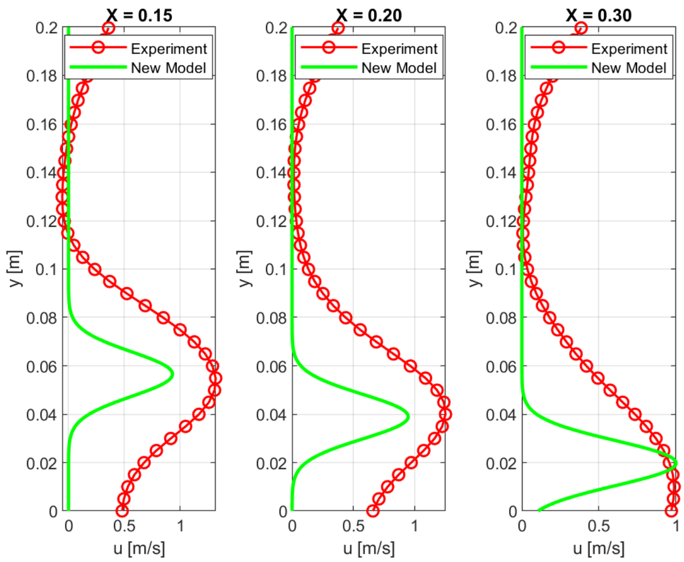

Figure 41. Comparison between new model profiles and experimental data profiles (h_o = 0.06 m, Δh = 0.09 m).

Figure 40 and Figure 41 show that, even without explicitly imposing the jet angle as an input parameter, the modified formulation can reproduce the downstream sinking behaviour of the jet. Furthermore, the reconstructed spreading of the velocity profiles remains reasonably consistent with the experimental observations.

The comparison with the original VUL_SLUIS schematization will be presented in the following section, where the differences between the original and modified jet reconstructions will be analysed directly.

6.3 Calibration with ship

Once the parametrization was calibrated for the no-ship configurations, additional corrections were introduced to reproduce the experimentally observed modifications caused by the presence of the vessel inside the lock chamber. One of the principal motivations behind the development of the new jet schematization was precisely the possibility of introducing the influence of the ship directly within the reconstruction of the filling jet, something that is not considered in the original VUL_SLUIS implementation.

The experimental measurements demonstrated that the presence of the ship modifies the downstream evolution of the jet, particularly its downward deflection beneath the hull. Among the different hydraulic characteristics affected by the vessel, the sinking behaviour proved to be the most sensitive and the most clearly measurable parameter in the MiniShaker experiments. For this reason, the ship-dependent correction was introduced specifically through the parametrization of the sinking coefficient.

To account for the under-keel confinement effects, the sinking coefficient k_s was extended as:

$$k_s = k_{s,base} + a_1 k_c + a_2 X_{bow}$$

The keel clearance is derived directly from the hydraulic and geometrical conditions imposed in each case according to:

$$k_c = z_{water} - z_{bottom} - T$$

where z_{water} is the downstream water level, z_{bottom} is the bottom elevation of the lock chamber, and T is the vessel draught.

Within the VUL_SLUIS implementation, the longitudinal distance X_{bow} corresponds to the parameter X_s defined in the input file. As discussed previously in Chapter 5, X_s represents the effective horizontal distance between the gate and the vessel bow used internally by VUL_SLUIS for the force calculations and for the interaction between the filling jet and the ship geometry.

The additional coefficients a_1 and a_2, governing respectively the influence of the keel clearance and the vessel position on the sinking behaviour, were calibrated using the same optimization philosophy adopted previously for the no-ship configurations. The calibration was therefore based on the minimization of a global objective function evaluating the discrepancy between the reconstructed and experimental velocity profiles for all ship configurations included in the MiniShaker measurements.

The optimization searched for a single pair of coefficients capable of reproducing consistently the experimentally observed modifications of the jet trajectory beneath the vessel for the different combinations of keel clearance and ship position analysed in the present research. The calibrated values obtained for the ship-dependent correction coefficients are reported in Table 15 together with the final value of the global calibration error.

Parameter	Value
a_1	0.013292
a_2	0.024134
Total calibration error : J_{total}	2.1388*10^-1

Table 15. New calibrated parameters for ship configurations.

This modification allows the downstream trajectory of the jet to adapt automatically to the ship configuration. The calibration procedure shows that both the keel clearance and the vessel position influence the downward development of the jet and therefore modify the redistribution of momentum beneath the hull.

An important aspect of this approach is that these dependencies were not imposed but emerged directly from the calibration against the experimental measurements. The optimization procedure revealed that the under-keel confinement generated by the vessel systematically affects the sinking behaviour of the jet and therefore cannot be neglected when reconstructing the downstream velocity field inside the lock chamber.

The adopted correction remains intentionally simple and focuses exclusively on the sinking behaviour. This choice was motivated both by calibration stability and by the experimental observations themselves, which indicated that the downward deflection of the jet is the hydraulic feature most strongly affected by the vessel presence. Introducing additional ship-dependent corrections on spreading or velocity concentration would likely require a substantially larger experimental dataset to obtain sufficiently robust and stable calibration coefficients.

6.3.1 New profiles

The calibrated ship-correction coefficients a_1 and a_2 are subsequently implemented directly within the modified VUL_SLUIS jet routine. The resulting parametrisation allows the jet sinking coefficient k_s to vary as a function of both the under-keel clearance and the gate-to-bow distance. Following the implementation of these additional correction terms, the reconstructed velocity profiles obtained with the modified model are again compared with the experimental MiniShaker measurements to evaluate the quality of the fitting and the capability of the updated formulation to reproduce the measured downstream jet development beneath the vessel.

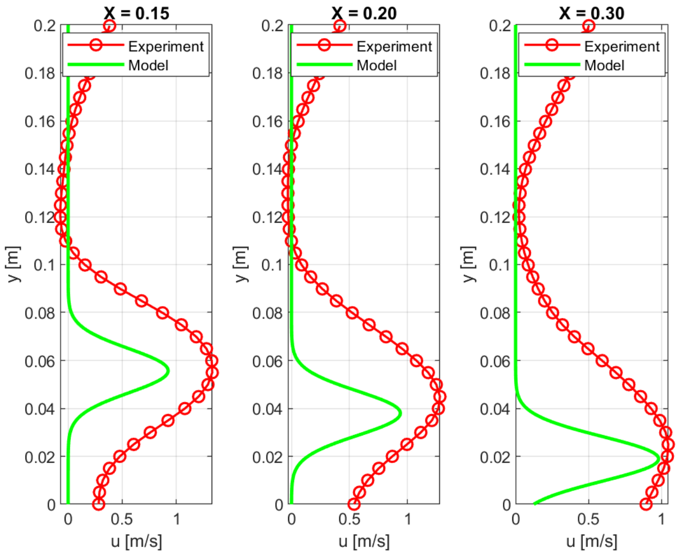

Figure 42. Comparison between new model profiles and experimental data profiles (h_o = 0.06 m, Δh = 0.09 m, k_c = 0.08 m, X_{bow} = 0.65 m).

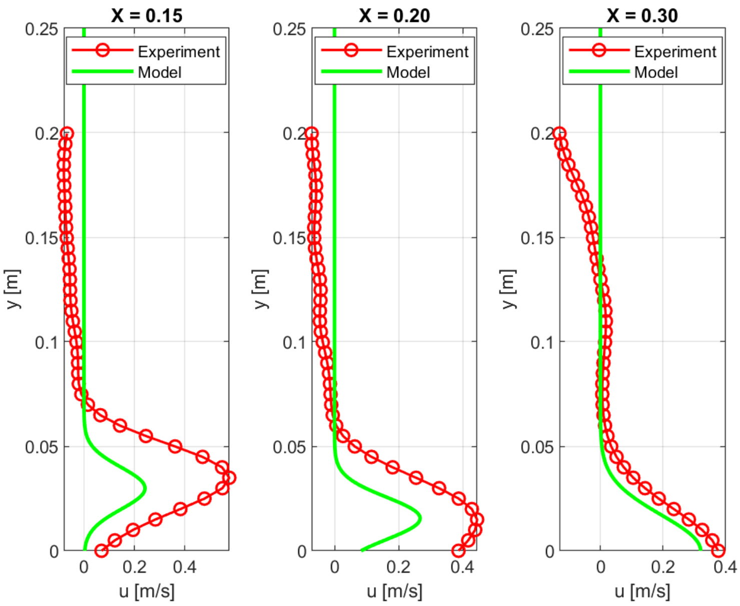

Figure 43. Comparison between new model profiles and experimental data profiles (h_o = 0.03 m, Δh = 0.02 m, k_c = 0.08 m, Xbow = 0.65 cm).

Figure 42 and Figure 43 show that the reconstructed velocities are generally underestimated, similarly to the behaviour already observed in the original version of VUL_SLUIS. Nevertheless, the modified formulation reproduces a significantly more realistic profile shape and downstream jet trajectory. Most importantly, the new parametrisation automatically accounts for the presence and longitudinal position of the vessel inside the lock chamber without requiring a direct experimental input of the jet angle.

The comparison with the original VUL_SLUIS schematization will be presented in the following chapter, where the differences between the original and modified jet reconstructions will be analysed directly.

6.4 New forces calculation

Following the implementation of the modified jet schematization inside the VUL_SLUIS routine, the resulting longitudinal forces acting on the vessel are recalculated to evaluate how the new jet representation affects the hydrodynamic loads predicted by the software. Since the filling jet constitutes one of the principal mechanisms governing the longitudinal flow beneath the vessel, modifications in the downstream velocity distribution, jet spreading, sinking behaviour, and wall interaction are expected to directly influence the calculated forces.

The new parametrisation modifies several aspects of the jet development simultaneously. In particular, the introduction of the delayed sinking formulation, the wall-jet transition near the bottom boundary, the entrainment correction, and the ship-dependent sinking coefficient alters both the local velocity magnitudes and the downstream momentum redistribution beneath the hull. Consequently, the longitudinal force components associated with the filling jet are expected to differ from those obtained with the original VUL_SLUIS schematization.

To quantify these differences, the longitudinal force components calculated with the modified model are directly compared with those produced by the original version of VUL_SLUIS (Table 16). Focus is given to the jet-related force contributions, namely the direct jet force and the impulse-related force components, since these terms are directly influenced by the downstream evolution of the filling jet.

Case	Ship Configuration	h_o [m]	Δh [m]	k_c [m]	X_{bow} [m]	X_s [m]
1	With ship	0.03	0.02	0.03	0.505	0.11
2	With ship	0.03	0.09	0.03	0.505	0.16
3	With ship	0.06	0.02	0.03	0.505	0.125

Table 16. Cases for which comparation with original VUL_SLUIS forces is performed.

Case 1:

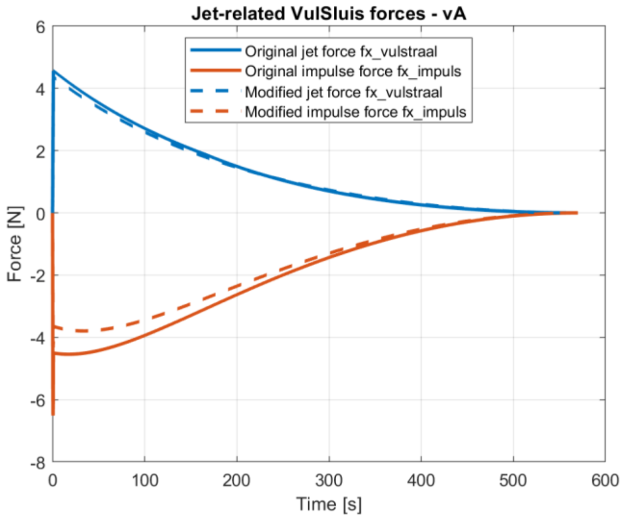

Maximum	$f_{x,\mathrm{vulstraal}}$	$f_{x,\mathrm{impuls}}$
Original	4.562 N	6.510 N
Modified	4.364 N	4.322 N
Change	-4.35 %	-33.61 %

Mean	$f_{x,\mathrm{vulstraal}}$	$f_{x,\mathrm{impuls}}$
Original	1.278 N	1.921 N
Modified	1.245 N	1.682 N
Change	-2.62 %	-12.46 %

Figure 44. Comparison of forces between Original and Modified VUL_SLUIS (Case 1).

Case 2:

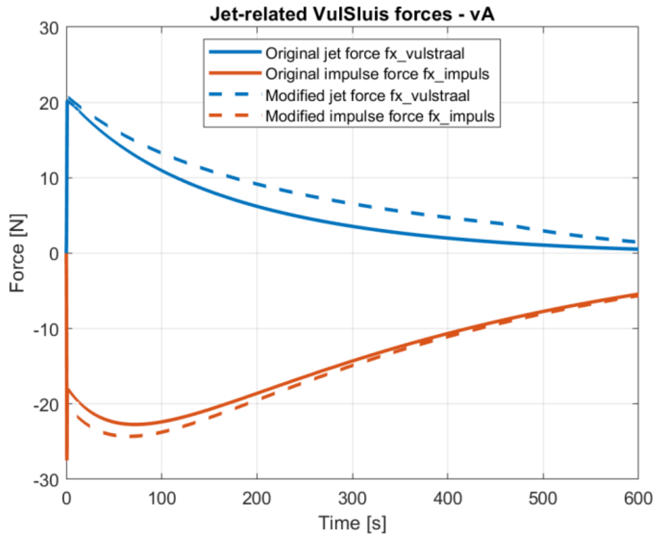

Maximum	$f_{x,\text{vulstraal}}$	$f_{x,\text{impuls}}$
Original	20.24 N	27.50 N
Modified	20.78 N	24.31 N
Change	2.65 %	-11.62 %

Mean	$f_{x,\text{vulstraal}}$	$f_{x,\text{impuls}}$
Original	5.52 N	14.46 N
Modified	7.83 N	15.24 N
Change	41.9 %	5.39 %

Figure 45. Comparison of forces between Original and Modified VUL_SLUIS (Case 2).

Case 3:

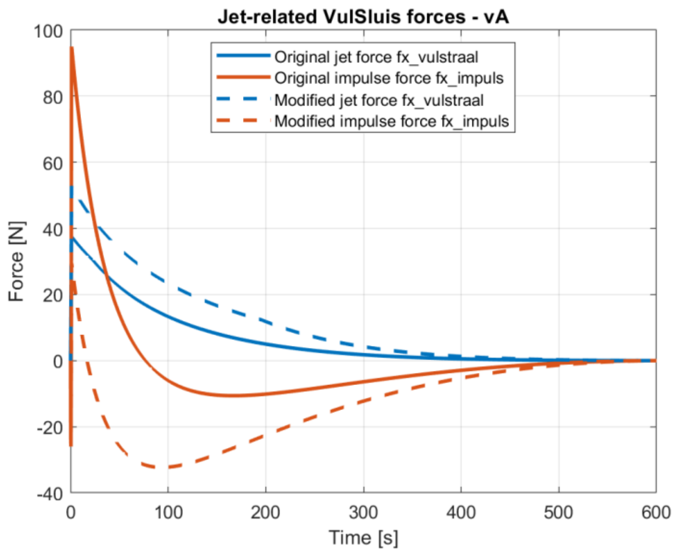

Maximum	$f_{x,\text{vulstraal}}$	$f_{x,\text{impuls}}$
Original	37.58 N	95.02 N
Modified	52.87 N	32.295 N
Change	40.67 %	-66.01 %

Mean	$f_{x,\text{vulstraal}}$	$f_{x,\text{impuls}}$
Original	6.06 N	8.23 N
Modified	10.442 N	13.32 N
Change	72.47 %	61.84 %

Figure 46. Comparison of forces between Original and Modified VUL_SLUIS (Case 3).

The three comparisons show that the modified jet schematization does not influence all cases in the same manner. This behaviour is expected because the modification primarily changes the vertical distribution of the jet velocity field rather than the global discharge itself. Consequently, the force component most directly affected is the jet force $f_{x,\text{vulstraal}}$, while the impulse force $f_{x,\text{impuls}}$ responds more indirectly through changes in the overall momentum distribution within the lock chamber.

In the first comparison (Figure 44), the original and modified curves remain very close to each other. This indicates that, for this specific case, the Gaussian LoMo-inspired reconstruction produces a jet distribution like the original VUL_SLUIS schematization. Consequently, both the direct jet contribution and the impulse contribution remain almost unchanged.

In the second comparison (Figure 45), the behaviour is intermediate. The modified schematization increases the jet force, while the impulse force remains relatively similar to the original case. This is an important observation because it indicates that the modification mainly affects the local velocity distribution beneath the vessel while leaving the global momentum balance comparatively unchanged.

In the third second comparison (Figure 46), the differences become significantly larger. The modified formulation produces a substantially higher jet force and alters the impulse force considerably. This suggests that, in the original schematization, the jet spreading and momentum distribution were likely too diffuse. The modified Gaussian profile preserves a larger amount of concentrated momentum within the region interacting with the vessel, resulting in a stronger direct jet force. Because the global momentum balance is also altered, the impulse force changes accordingly.

Overall, these comparisons demonstrate that the proposed modification primarily affects the local jet-induced loading represented by $f_{x,\mathrm{vulstraal}}$, whereas the impulse force $f_{x,\mathrm{impuls}}$ is more closely related to the integral momentum balance of the entire flow field. The magnitude of the differences depends on the hydraulic conditions, such as gate opening, head difference, vessel position, and under keel clearance.

7 ANALYSIS AND DISCUSSION

The previous chapters presented the experimental investigation of the filling jet through MiniShaker PTV measurements, the analysis of the original VUL_SLUIS jet schematization, and the development of a modified parametrization calibrated against the experimental data. The objective of the present chapter is to discuss the overall outcomes of the research and to evaluate the extent to which the proposed modifications improve the representation of the filling jet inside the lock chamber.

Rather than presenting additional isolated measurements, this chapter focuses on the broader interpretation of the results obtained throughout the work. First, a general comparison between the original and modified schematizations is carried out to highlight the principal differences in the reconstruction of the downstream jet behaviour. In addition, representative experimental cases are presented by directly comparing the experimental velocity profiles with both the original VUL_SLUIS reconstruction and the modified parametrization. For the original VUL_SLUIS implementation, comparisons are shown both with and without the manually imposed jet inclination angle, allowing the influence of the input angle on the downstream reconstruction to be evaluated directly.

Subsequently, the overall contribution and limitations of the research are discussed with reference to the initial objectives defined in the introduction. Finally, the principal conclusions emerging from the analyses are summarized in preparation for the final conclusions and recommendations presented in the following chapter.

7.1 General Comparison

7.1.1 Without ship

The first comparisons are performed for the configurations without vessel to analyse the intrinsic behaviour of the jet reconstruction independently from under-keel confinement effects. The objective of these comparisons is primarily to evaluate the differences in the downstream distribution of the velocity field and the capability of the modified parametrization to reproduce the sinking behaviour of the jet automatically, without imposing an inclination angle within the input parameters.

The comparison between the experimental measurements, the original VUL_SLUIS schematization, and the modified parametrization clearly highlights the principal differences between the three approaches. In general, the results confirm that the modified model reproduces more realistically the downstream evolution of the filling jet, particularly regarding the concentration of the velocity core and the progressive downward movement toward the bottom boundary.

The experimental profiles obtained from the MiniShaker measurements consistently show a concentrated jet core associated with strong velocity gradients and a progressive downward displacement of the maximum velocity region as the distance from the gate increases. In contrast, the original VUL_SLUIS implementation reconstructs profiles that remain excessively symmetric and vertically diffused, especially at larger downstream distances. The spreading of the jet is therefore overestimated, while the sinking behaviour remains insufficient unless an inclination angle is manually imposed.

The modified parametrization instead reconstructs narrower and more concentrated velocity distributions whose downstream evolution is considerably closer to the experimental observations. The introduction of the Gaussian reconstruction together with the exponential sinking formulation allows the jet core to move progressively downward while preserving a more realistic profile shape.

The first comparison (Figure 47), corresponding to the configuration with $h_o = 0.03\ \mathrm{m}$ and $\Delta h = 0.02\ \mathrm{m}$, highlights clearly the limitations of the original VUL_SLUIS implementation. At all downstream locations, the original profiles remain excessively smooth and vertically distributed around an almost symmetric centreline. The new parametrization instead reconstructs a much more concentrated velocity core and reproduces more realistically the progressive downward displacement of the jet observed experimentally. The improvement becomes increasingly evident at $X = 0.20$ m and $X = 0.30$ m, where the experimental measurements already exhibit a pronounced wall-jet tendency close to the bottom boundary.

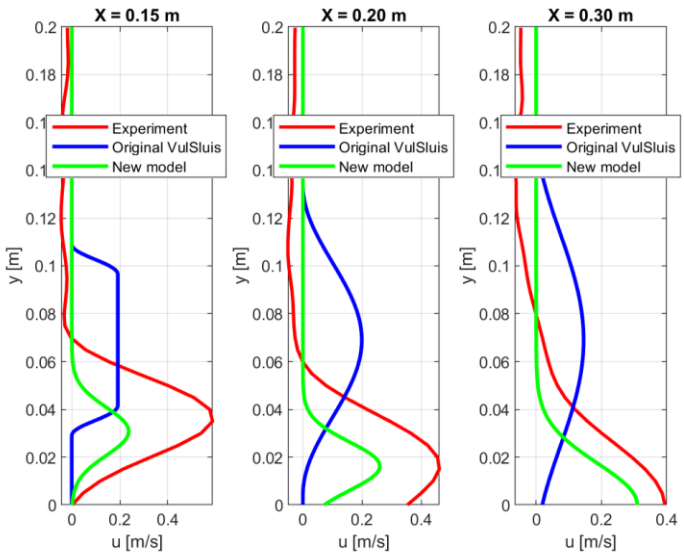

Figure 47. General comparison without ship (h_o = 0.03 m, Δh = 0.02 m).

A similar behaviour is observed for the second configuration (Figure 48), corresponding to $h_o = 0.06\ \mathrm{m}$ and $\Delta h = 0.09\ \mathrm{m}$. Also in this case, the original VUL_SLUIS profiles remain excessively centred within the water column and fail to reproduce adequately the experimentally observed redistribution of the velocity field toward the bottom. The modified model instead captures more effectively the concentration of the jet core and its downstream movement toward the bottom boundary.

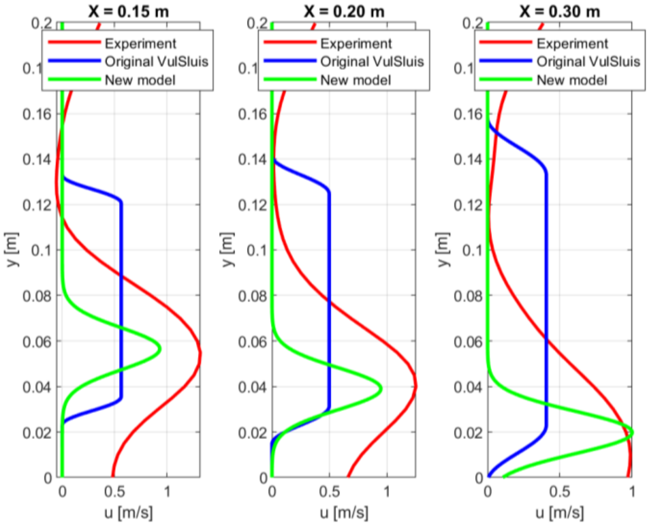

Figure 48. General comparison without ship (h_o = 0.06 m, Δh = 0.09 m).

At the same time, the comparisons also show that discrepancies in the maximum velocity magnitude remain between the reconstructed and experimental profiles. Although the modified parametrization improves substantially the shape and downstream evolution of the velocity distributions, the peak velocities predicted numerically do not yet fully coincide with the experimental measurements for all configurations and downstream locations. This behaviour was already partially present in the original VUL_SLUIS implementation and indicates that, despite the improved geometrical reconstruction of the jet, additional refinements of the entrainment formulation or discharge redistribution mechanisms could further improve the quantitative agreement with the measured velocity magnitudes.

The third comparison (Figure 49) considers the same hydraulic configuration but with a non-zero jet inclination angle imposed within the original VUL_SLUIS input file. This comparison is particularly important because it demonstrates one of the principal conceptual limitations of the original schematization. By manually introducing an inclination angle, the original VUL_SLUIS formulation becomes capable of reproducing part of the downstream sinking behaviour observed experimentally. In particular, the profiles at larger downstream distances move closer to the bottom boundary and become qualitatively more similar to the experimental measurements.

However, the comparison also demonstrates that the reconstructed behaviour remains strongly dependent on the manually imposed input angle. The sinking trajectory is therefore not generated naturally by the model itself but rather prescribed externally through a case-dependent parameter. Moreover, although the imposed angle improves the downstream position of the jet, the velocity distributions remain relatively rigid and do not reproduce accurately the experimentally observed concentration and spreading behaviour.

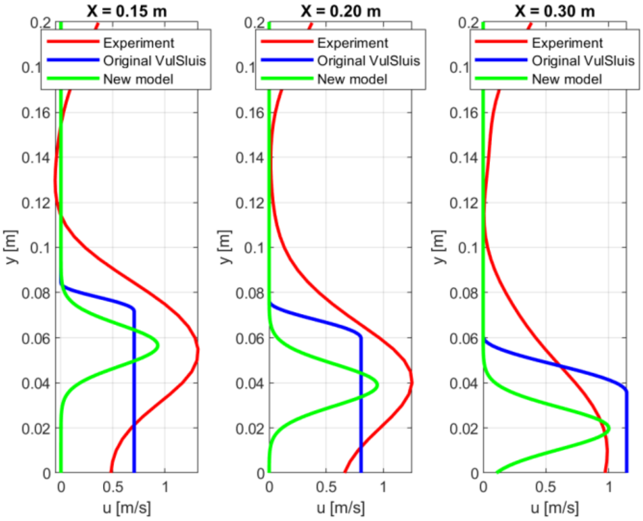

Figure 49 . General comparison without ship (h_o = 6 cm, Δh = 9 cm, Φ = -18°).

The modified parametrization instead reproduces the downward trajectory automatically, without requiring any manually imposed jet angle. The sinking behaviour emerges directly from the calibrated parametrization and evolves continuously as a function of the hydraulic and geometrical conditions. This represents one of the principal conceptual advantages of the proposed approach, since the downstream development of the jet no longer depends on the arbitrary selection of a case-specific inclination angle but becomes part of the internal jet reconstruction itself.

7.1.2 With Ship

For the configurations with ship, the comparisons are intended to evaluate how the modified parametrization changes the reconstruction of the filling jet once the vessel influence is introduced directly within the jet schematization. In all cases, the comparison between the experimental measurements, the original VUL_SLUIS reconstruction, and the new parametrization highlights the different ways in which the downstream jet evolution is represented.

In the first configuration (Figure 50), corresponding to $h_o = 0.03$ m, $\Delta h = 0.02$ m and $k_c = 0.03$ m and $X_{bow} = 0.505\ m$, the original VUL_SLUIS profiles remain relatively smooth and vertically distributed, while the modified model reconstructs a more concentrated velocity core together with a stronger downward evolution of the jet. The new parametrization produces profiles that are qualitatively closer to the experimentally observed wall-jet behaviour, particularly at the larger downstream distances where the experimental maximum velocities move closer to the bottom boundary.

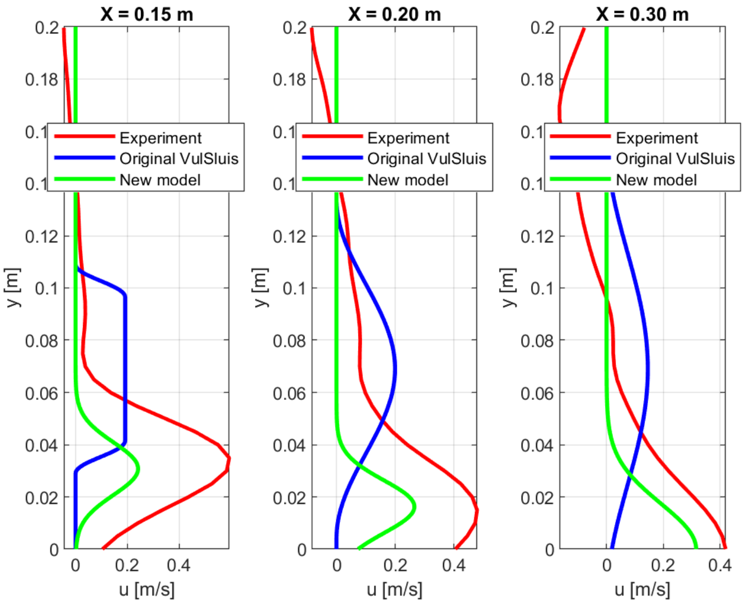

Figure 50. General comparison with ship (ho = 3 cm, Δh = 2 cm, kc = 3 cm, Xbow = 50.5 cm).

The second configuration (Figure 51), corresponding to $h_o = 0.06$ m, $\Delta h = 0.02$ m and $k_c = 0.08$ m and $X_{bow} = 0.65\,m$ confirms the same general behaviour. Also in this case, the original VUL_SLUIS implementation reconstructs profiles that remain excessively centred within the water column and insufficiently influenced by the vessel configuration. The modified model instead generates a more pronounced downward displacement of the velocity core and a downstream evolution that follows more closely the experimental observations. The reconstructed profiles additionally show that the calibrated parametrization adapts the sinking behaviour according to the specific ship configuration rather than maintaining a fixed jet trajectory.

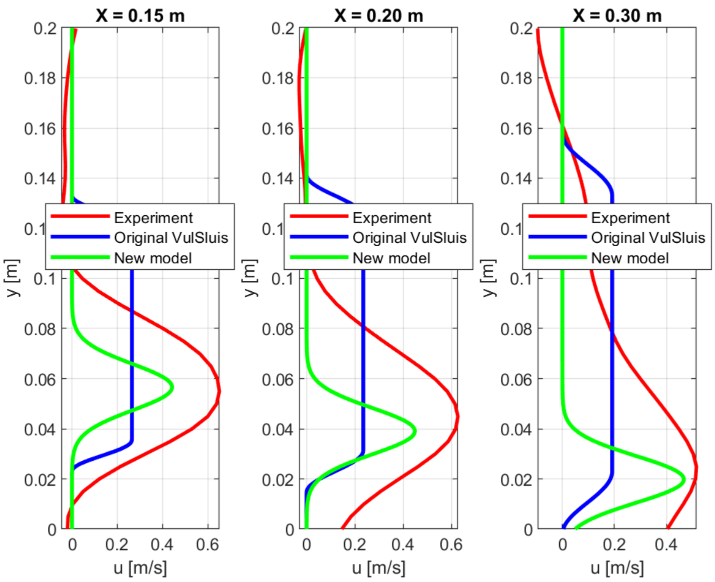

Figure 51. General comparison with ship (ho = 6 cm, Δh = 9 cm, k_c = 8 cm, X_{bow} = 65 cm).

The third comparison (Figure 52) presents the same hydraulic configuration but with a non-zero jet inclination angle manually imposed within the original VUL_SLUIS input file. Introducing the inclination angle allows the original schematization to reproduce part of the experimentally observed sinking behaviour, especially at $X = 0.30$ m where the velocity core shifts closer to the bottom boundary. Nevertheless, the comparison also demonstrates that the downstream trajectory remains highly dependent on the manually selected input angle. The reconstructed behaviour is therefore prescribed externally rather than generated directly by the jet parametrization itself.

The modified model instead reproduces the downward movement automatically through the calibrated dependence on keel clearance and vessel position. The sinking behaviour emerges directly from the parametrized reconstruction and therefore becomes part of the jet model itself. This constitutes one of the principal conceptual developments introduced in the present research, since the vessel now directly influences the reconstructed filling jet rather than affecting only the subsequent force calculations performed by VUL_SLUIS.

At the same time, the comparisons show that discrepancies in the peak velocity magnitudes remain between the reconstructed and experimental profiles. Although the modified parametrization substantially improves the downstream organisation of the jet and its sinking behaviour, differences in the exact velocity magnitude persist for some downstream locations. This indicates that further refinement of the entrainment and discharge redistribution mechanisms could still improve the quantitative agreement with the experimental measurements.

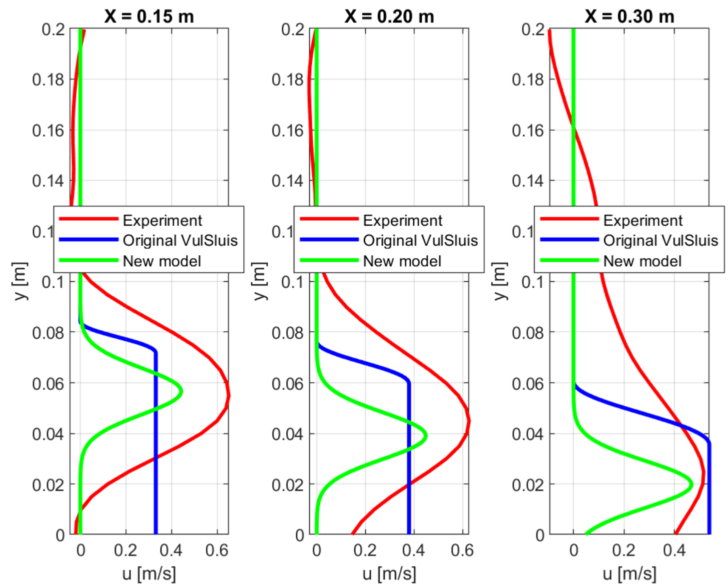

Figure 52. General comparison with ship (ho = 6 cm, Δh = 9 cm, k_c = 8 cm, X_{bow} = 65 cm, Φ = 18 °).

7.2 Analysis

The work developed within the present research demonstrates that experimental velocity measurements can be used successfully to improve the reduced-order schematization of filling jets inside numerical lock-filling models. The MiniShaker measurements provided detailed information regarding the downstream spreading, sinking behaviour, and wall-jet development of the filling jet under different hydraulic and geometrical conditions. These observations made it possible to identify the principal discrepancies of the original VUL_SLUIS implementation and to formulate physically motivated corrections.

One of the most important aspects of the work concerns the introduction of a parametrized jet trajectory directly derived from the experimental observations. The original VUL_SLUIS formulation required the inclination angle $\Phi$to be imposed manually, whereas the modified parametrization reconstructs the downstream sinking behaviour through a continuous empirical relation calibrated against the measured profiles. This constitutes one of the principal conceptual developments introduced in the present work.

The research additionally demonstrated that the presence of the vessel significantly affects the downstream development of the jet, particularly through under-keel confinement effects. The experimental results showed that the jet trajectory beneath the hull cannot be considered independent from the ship configuration. Introducing ship-dependent corrections therefore represents an important extension of the original VUL_SLUIS schematization.

At the same time, several limitations of the present work must also be acknowledged. The calibration was performed using a limited number of experimental configurations and under quasi-steady hydraulic conditions. Although the experimental measurements with vessel clearly indicated modifications in the downstream jet behaviour, the influence of the ship on the sinking trajectory was not always visible with the same level of clarity for all configurations. This was likely influenced by limitations in the camera field of view, which was optimized primarily for resolving the jet structure itself rather than capturing a wider portion of the surrounding flow field.

The experimental profiles additionally showed that significant flow redistribution and recirculation regions develop above the jet core. These recirculation structures were observed consistently within the MiniShaker measurements and represent an important component of the overall hydraulic behaviour inside the lock chamber. However, the present modified schematization focused primarily on the reconstruction of the jet core evolution, including spreading and sinking behaviour, and did not attempt to reproduce the complete recirculation field. Accurately parametrizing these upper-flow recirculation structures would require substantially higher measurement accuracy over the entire water depth together with a more detailed characterization of the surrounding turbulent flow field.

Furthermore, the physical model reproduced only the initial stage of the filling process rather than the complete transient levelling operation occurring inside a real lock chamber. The MiniShaker measurements also focused primarily on the two-dimensional evolution of the jet within the longitudinal vertical plane and therefore did not investigate possible three-dimensional effects across the width of the lock chamber. Consequently, the proposed parametrization should be interpreted as a reduced-order reconstruction of the dominant jet behaviour rather than a complete representation of the full three-dimensional transient hydraulic flow inside a lock chamber.

The ship-dependent calibration was also intentionally restricted to the sinking behaviour of the jet. Although the experiments suggested that the vessel may additionally influence spreading and momentum redistribution, introducing further ship-dependent corrections would require a broader experimental dataset to ensure sufficiently stable and generalizable calibration coefficients.

Nevertheless, the objective of the present research was not to produce a definitive universal jet model, but rather to demonstrate the feasibility of improving the VUL_SLUIS jet schematization through experimentally calibrated parametrizations. From this perspective, the work successfully establishes a methodological framework that can be extended and refined in future studies.

7.3 Conclusion considering the analysis

The analyses presented throughout this thesis demonstrate that the original VUL_SLUIS jet schematization captures the general behaviour of turbulent filling jets but does not reproduce accurately several important hydraulic characteristics observed experimentally, particularly regarding the downstream sinking of the jet and the influence of the vessel on the flow development beneath the hull.

The modified parametrization proposed in the present work substantially improves the agreement between the reconstructed and experimental velocity profiles while preserving the computational simplicity required for engineering-oriented lock-filling calculations. The introduction of a continuous sinking parametrization, Gaussian velocity reconstruction, and wall-jet transition allowed the downstream jet evolution to be represented more realistically than in the original implementation.

The analyses performed in the present work also showed that the vessel should not be considered only during the force calculation stage, but also within the jet schematization itself. The experimental measurements clearly indicated that under-keel confinement modifies the downstream trajectory of the jet, and the proposed ship-dependent correction constitutes a first attempt to incorporate this behaviour directly within the reduced-order modelling framework.

Although further experimental validation and calibration would be required before practical implementation in operational engineering applications, the proposed approach demonstrates that the VUL_SLUIS jet schematization can be extended significantly without abandoning its original reduced-order philosophy. The work therefore establishes a basis for future developments aimed at improving the physical realism of lock-filling simulations while maintaining the computational efficiency necessary for engineering practice.

The force analyses additionally demonstrated that modifications of the jet schematization can significantly influence the local jet-related force components acting on the vessel. In particular, the modified parametrization altered the direct jet force more strongly than the global impulse-related contribution. This behaviour indicates that the proposed modifications primarily affect the local redistribution of momentum beneath the hull rather than the global discharge balance inside the lock chamber.

The results also highlighted that the influence of the modified jet representation on the total longitudinal force depends strongly on the hydraulic configuration. For some cases, the differences between the original and modified formulations remained limited, whereas for other configurations the reconstructed jet concentration and sinking behaviour produced substantial variations in the predicted jet-induced loads. This observation confirms that an accurate reconstruction of the downstream jet trajectory is essential not only for reproducing the measured velocity profiles, but also for obtaining reliable force estimations within reduced-order lock-filling models.

Overall, the analyses suggest that improvements in the physical representation of the filling jet directly contribute to improving the reliability of the predicted hydrodynamic forces acting on vessels. Even though the present work mainly focused on the hydraulic behaviour of the jet itself, the resulting force comparisons demonstrate the practical engineering relevance of the proposed modifications for future lock-filling simulations and operational assessments.

8 CONCLUSIONS

In this chapter, the final conclusions and recommendations of the present research are presented. The conclusions are based on the experimental investigations performed through MiniShaker PTV measurements, the analysis of the current VUL_SLUIS implementation, and the development of a modified jet schematization calibrated against the experimental data. The objective of this thesis was to improve the understanding and numerical representation of filling jets inside navigation locks through a combined numerical and experimental investigation.

More specifically, the research focused on analysing the current jet representation implemented in VUL_SLUIS, investigating the hydraulic behaviour of filling jets through scale model experiments, comparing numerical and experimental velocity fields, and proposing modifications to the existing jet parametrization.

The following research questions were defined at the beginning of the study:

1. How are filling jet velocities currently calculated in VUL_SLUIS?
2. How does the presence of a vessel modify the jet structure and velocity distribution inside the lock chamber?
3. What differences can be identified between the numerical results produced by VUL_SLUIS and the experimental measurements obtained through PTV analysis?
4. How can the current jet schematization in VUL_SLUIS be improved in order to better reproduce the observed hydraulic behaviour?

The conclusions presented in the following sections provide an answer to these research questions and summarize the principal outcomes of the work.

8.1 Conclusions

The present research investigated the hydraulic behaviour of filling jets inside navigation locks through a combined numerical and experimental approach. The study focused on analysing the current jet representation implemented in VUL_SLUIS, investigating the downstream development of filling jets through MiniShaker PTV measurements, comparing numerical and experimental velocity profiles, and proposing a modified jet schematization capable of reproducing more realistically the observed hydraulic behaviour.

The analysis of the current VUL_SLUIS implementation showed that the software reconstructs the filling jet through a simplified turbulent jet formulation derived from Vrijburcht et al. (1988). The downstream development of the jet is represented through predefined geometrical relations, while the sinking behaviour can only be reproduced by manually imposing a jet inclination angle Φ. Although this approach allows computationally efficient calculations of discharge, momentum, and forces acting on the vessel, the comparison with the experimental measurements demonstrated that several important hydraulic characteristics are not reproduced accurately.

The MiniShaker measurements provided detailed information regarding the downstream evolution of the filling jet under different hydraulic and geometrical conditions. The experiments showed that the jet progressively spreads due to turbulent mixing while simultaneously moving downward toward the bottom boundary, eventually developing into a wall jet. The measured velocity profiles additionally demonstrated that the jet core remains considerably more concentrated than predicted by the original VUL_SLUIS schematization and that the downstream redistribution of momentum differs substantially from the numerical reconstruction.

The experiments also confirmed that the presence of the vessel modifies the downstream jet behaviour beneath the hull. In particular, the under-keel confinement influences the sinking trajectory and the redistribution of the velocity field. The original VUL_SLUIS implementation does not account for this interaction directly within the jet schematization, since the vessel only affects the subsequent force calculations.

The comparison between the numerical and experimental profiles therefore revealed systematic discrepancies between the original VUL_SLUIS reconstruction and the physical measurements. The original profiles remain excessively symmetric and vertically diffused, especially at larger downstream distances, while the reconstructed sinking behaviour depends strongly on the manually imposed jet angle.

To address these limitations, a modified jet parametrization was proposed and implemented within the VUL_SLUIS framework. The new formulation preserves the reduced-order computational philosophy of the original model while introducing physically motivated corrections derived directly from the experimental observations. The modified schematization combines a LoMo-inspired spreading law, an exponential sinking parametrization, and a Gaussian reconstruction of the velocity profiles calibrated against the MiniShaker measurements.

The comparisons performed throughout this thesis demonstrated that the modified parametrization reproduces more realistically the downstream concentration of the jet core, the progressive sinking toward the bottom boundary, and the transition toward wall-jet behaviour. In addition, the modified formulation introduces, for the first time within this framework, a direct dependency between the jet reconstruction and the vessel configuration through calibrated parameters linked to keel clearance and ship position.

The present research therefore demonstrated that experimentally calibrated parametrizations can significantly improve the representation of filling jets inside reduced-order engineering tools such as VUL_SLUIS while preserving the computational efficiency required for practical lock-filling simulations. The proposed methodology establishes a first framework capable of linking physical model measurements with engineering-oriented jet schematizations and represents a first step toward a more physically realistic representation of filling jets inside navigation locks.

8.2 Recommendations

Several recommendations for future research and possible improvements of the proposed parametrization follow directly from the findings of the present study.

The most important recommendation concerns the extension of the experimental database used for calibration. The present calibration was performed using a limited number of hydraulic and geometrical configurations under quasi-steady conditions corresponding mainly to the initial stage of the filling process. A broader experimental campaign including additional gate openings, hydraulic heads, vessel geometries, keel clearances, and ship positions would likely improve the robustness and generality of the calibration coefficients.

Future experimental investigations should additionally consider a wider measurement domain. In the present work, the MiniShaker setup was optimized primarily for resolving the jet core evolution. Although the measurements clearly demonstrated modifications in the downstream jet behaviour caused by the vessel, the influence of the ship on the sinking trajectory was not always visible with the same level of clarity for all configurations. A larger field of view would allow a more detailed characterization of the surrounding recirculation regions and the global redistribution of momentum inside the lock chamber.

The experimental profiles additionally showed the development of recirculation structures above the jet core. These regions were not included within the modified parametrization because the present research focused primarily on the reconstruction of the jet core behaviour, namely spreading and sinking. A more accurate parametrization of the complete recirculation field would require substantially higher measurement precision over the entire water depth together with a broader characterization of the turbulent flow field.

Another important recommendation concerns the transient nature of real lock-filling operations. The present experiments reproduced quasi-steady hydraulic conditions rather than the complete transient levelling operation occurring inside a real lock chamber. Future investigations could therefore analyse the temporal evolution of the jet during the complete filling process to evaluate the behaviour of the parametrization under continuously varying hydraulic conditions.

The present work additionally adopted a two-dimensional approach focused on the longitudinal vertical plane of the lock chamber. Although this assumption remains consistent with the reduced-order philosophy of VUL_SLUIS, possible three-dimensional effects across the width of the lock chamber were not investigated and could contribute to further refinements of the jet schematization.

Concerning the numerical implementation itself, future improvements could refine the entrainment formulation and the discharge redistribution mechanisms in order to improve the agreement with the experimentally measured peak velocities. Although the modified parametrization improved substantially the downstream jet evolution and the sinking behaviour, discrepancies in the exact velocity magnitudes remained for some configurations and downstream locations.

Finally, the principal recommendation for VUL_SLUIS concerns the direct integration of ship-dependent jet behaviour within the standard jet schematization framework. The present research demonstrated that the vessel modifies the downstream development of the filling jet and that this influence can be represented through calibrated parametrizations linked to keel clearance and ship position. The methodology introduced in this thesis therefore provides a basis for future developments aimed at improving the physical realism of engineering-oriented lock-filling simulations while maintaining the computational efficiency necessary for practical engineering applications.

REFERENCES

Albayrak, I., E. J. Hopfinger, and U. Lemmin. 2008. 'Near-Field Flow Structure of a Confined Wall Jet on Flat and Concave Rough Walls'. *Journal of Fluid Mechanics* 606:27–49. doi:10.1017/S0022112008001444.

Belzner Fabian, Simons Franz, and Thorenz Carsten (2018). 'An Application-Oriented Model for Lock Filling Processes'. In proceedings 34th PIANC-World Congress. Pp. 19.

Deltares (2016), 'Lockfill, user and technical manual', Technical Report, Delft.

Launder, B. E., and W. Rodi. 1983. 'The Turbulent Wall Jet Measurements and Modeling'. *Annual Review of Fluid Mechanics* 15(1):429–59. doi:10.1146/annurev.fl.15.010183.002241.

LaVision (2019), 'FlowMaster Shake-The-Box (4D PTV), Product Manual'.

Rajaratnam, N., & Subramanya, K. (1968). *Plane Turbulent reattached wall jets*. Journal of the Hydraulics Division, 94(1), 95-112.

Rijkswaterstaat. (2020). Waterway Guidelines. Transport and Environment (WVL) BNSV Department https://www.marin.nl/api/marin/downloads/getdownload/5943/0/2421/block_files_4ikukoi9ko6t /sstlD8-cFMk_X9lmlXmi_ivKzNc=/Waterway%2520Guidelines%25202020.pdf.

Schwarz, W.H. and Cosart, W.P. (1961) 'The two-dimensional turbulent wall-jet', *Journal of Fluid Mechanics*, 10(4), pp. 481–495. doi:10.1017/S0022112061000299.

Swamee P.K., (1992), 'Sluice-Gate Discharge Equations', https://doi.org/10.1061/(ASCE)0733-9437(1992)118:1(56).

Turner, J.S. (1986) 'Turbulent entrainment: the development of the entrainment assumption, and its application to geophysical flows', *Journal of Fluid Mechanics*, 173, pp. 431–471. doi:10.1017/S0022112086001222.

Van Loon, O., (2017). 'Improving the filling jet schematization trough a lock door by taking into account the presence of a ship', MSc Thesis, Delft University of Technology.

Vercruysse, J.;Verelst, K.;Peeters, P.;Mostaert, F. (2016). Klasse Vb sluis te Sint-Baafs-Vijve: Advies nivelleeropeningen en openingswet hefschuiven. Versie 4.0. WL Adviezen, 16_042. Waterbouwkundig Laboratorium: Antwerpen, België

Verelst, K.; De Mulder, T.; Schindfessel, L.; Peeters, P.; Mostaert, F. (2014). Numerieke modellering van sluisvulling via openingen in deuren: Deelrapport 1 : Opmaak en eerste validatie van het programma vul_sluis. Versie 3_0. WL Rapporten, 00_077. Waterbouwkundig Laboratorium: Antwerpen, België.

Verelst K.; Schindfessel, L.; De Mulder T.; Peeters, P.; Mostaert F. (2016). Numerieke modellering van sluisvulling via openingen in deuren: Deelrapport 2 – Verder testen en ontwikkelen programma vul_sluis. Versie 4_0. WL Rapporten, 00_077. Waterbouwkundig Laboratorium: Antwerpen, België.

Vrijburcht, A. (1988). Het vulproces van een schutsluis met een langsvulsysteem: invloed translatiegolven, vulstraaleffekten en dichtheidsverschillen op de langskrachten. Verslag berekeningen. Q176 deel II augustus 1988. Waterloopkundig Laboratorium = Delft Hydraulics Laboratory: Delft.

APPENDIX

A. Setup pictures

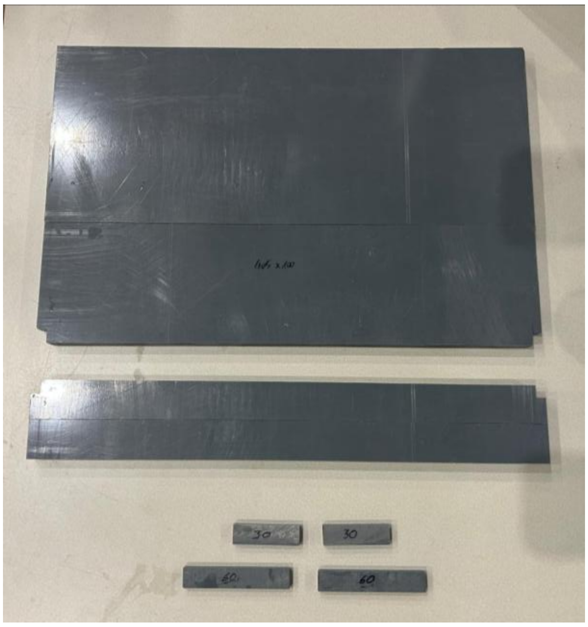

Figure A1. Designed gate with two different opening heights.

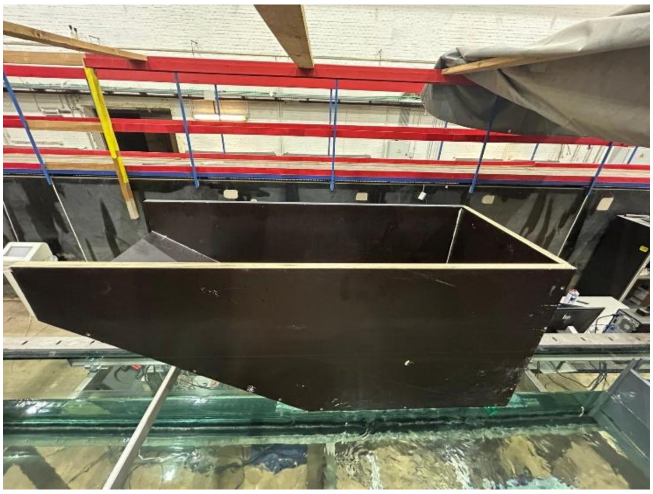

Figure A2. Designed ship.

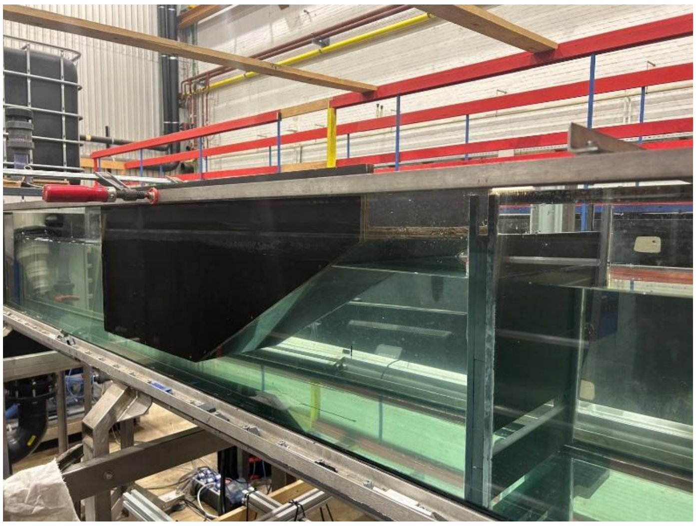

Figure A3. Setup flume with gate and ship.

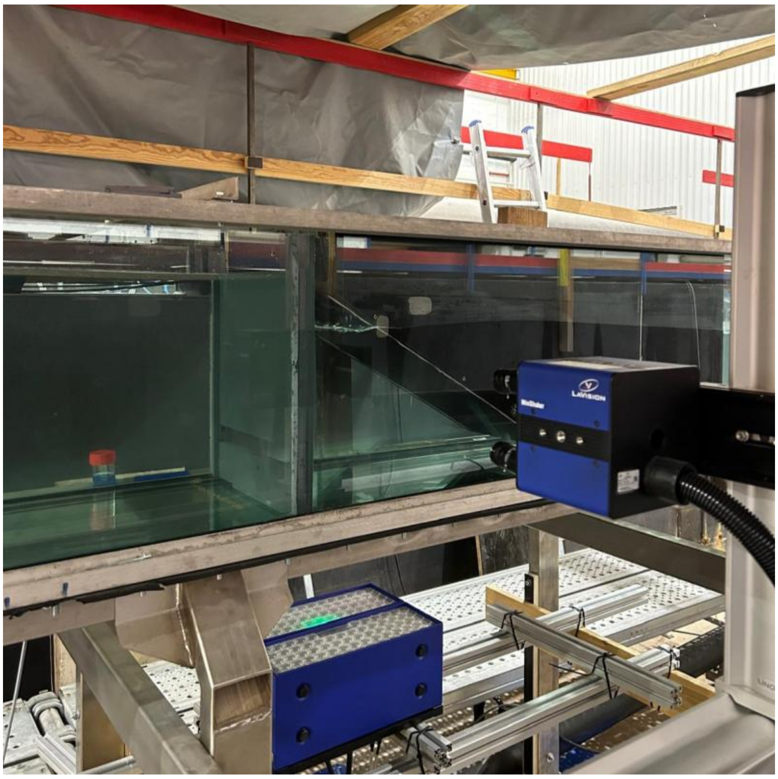

Figure A4. Setup flume with MiniShaker devices (Camera and LED-Flashlights).

B. Measurements Accuracy

To verify the consistency of the results obtained for the lock-filling configurations with gate and vessel, additional steady-state measurements were performed in the flume without gate and without vessel. The objective of these measurements was to assess the consistency between the experimentally measured velocity profiles and the independently measured discharge provided by the flow meter.

The steady-state velocity profiles were obtained directly from the experimentally velocities acquired with PTV measurements. The corresponding discharge was subsequently reconstructed by integrating the measured velocity distribution over the wetted cross-section.

For a flume width B and local vertical velocity distribution $U(y)$, the discharge is given by:

$$Q = B \int_0^h U(y)\, dy$$

where h denotes the measured water depth. Water level was measured at different locations along the flume length, resulting in an average flow depth of approximately $0.27\ \mathrm{m}$. The flow meter indicates a flow rate of $Q = 0.0053\ \mathrm{m\hat{}3}/s$.

The discharge reconstructed from the integrated velocity profiles resulted in:

$$Q = 0.0054\ \mathrm{m}^3/\mathrm{s}$$

This value showed very good agreement with the independent flow-meter measurement, confirming the consistency of the experimental velocity measurements and the reconstructed velocity profiles.

The Reynolds number was evaluated using the hydraulic-radius formulation for open-channel flow:

$$Re = \frac{U_{mean} R_h}{\nu}$$

where R_h denotes the hydraulic radius, A the cross-section area and P the wetted perimeter. Using the reconstructed discharge from the profile U_{mean} can be calculated (Table B1).

Parameter	Formula	Value
R_h	$\frac{A}{P}$	0.115 m
A	Bh	0.108 m^2
P	$B + 2h$	0.94 m
U_{mean}	$\frac{Q}{Bh}$	0.05 m/s

Table B1. Calculated values

Assuming water at approximately $20°\mathrm{C}$, with kinematic viscosity $\nu \approx 10^{-6}\ \mathrm{m}^2/s$, the Reynolds number is approximately:

$$Re \approx 5.7 \times 10^3$$

indicating turbulent steady-flow conditions within the flume. Consequently, the measured velocity profiles exhibited the characteristic concave shape associated with turbulent open-channel flow, with lower velocities near the bed and higher velocities toward the free surface ().

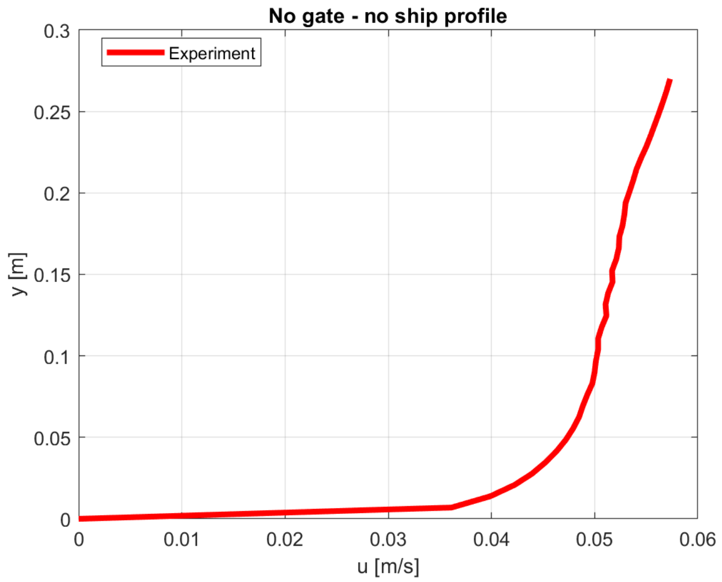

Figure B1. Vertical velocity profile in the flume without gate and ship.

C. Overview of measurements performed

Here, all the values used for the measurements without the ship can be found. Two values (Δh and h_0) are treated as variables, while the others (Q, h_{up}, and h_{down}) are measured accordingly, for the reasons explained in the main text.

Without Ship					
	Δh [m]	h_o [m]	Q [m^3/s]	h_{up} [m]	h_{down} [m]
1	0.02	0.03	0.0052	0.28	0.26
2	0.045	0.03	0.0074	0.29	0.245
3	0.07	0.03	0.0090	0.30	0.23
4	0.09	0.03	0.0100	0.31	0.22
5	0.02	0.06	0.0097	0.28	0.26
6	0.045	0.06	0.0144	0.285	0.24
7	0.07	0.06	0.0175	0.29	0.22
8	0.09	0.06	0.0200	0.30	0.21

Table C1. Performed measurements without ship.

Here is the same but for cases with ship but now variables are four, including also k_c and X_{bow}.

With Ship							
	Δh [m]	h_o [m]	Q [m^3/s]	h_{up} [m]	h_{down} [m]	k_c [m]	X_{bow} [m]
9	0.02	0.03	0.0053	0.28	0.26	0.03	0.505
10	0.045	0.03	0.0068	0.29	0.245	0.03	0.505
11	0.09	0.03	0.0095	0.31	0.22	0.03	0.505
12	0.02	0.03	0.0052	0.275	0.255	0.08	0.505
13	0.045	0.03	0.0068	0.285	0.24	0.08	0.505
14	0.09	0.03	0.0098	0.295	0.205	0.08	0.505
15	0.02	0.06	0.0095	0.28	0.26	0.03	0.505
16	0.045	0.06	0.0138	0.305	0.26	0.03	0.505
17	0.09	0.06	0.0200	0.34	0.25	0.03	0.505
18	0.02	0.06	0.0095	0.27	0.25	0.08	0.505
19	0.045	0.06	0.0135	0.275	0.23	0.08	0.505
20	0.09	0.06	0.0200	0.29	0.20	0.08	0.505
21	0.02	0.03	0.0052	0.285	0.265	0.03	0.650
22	0.09	0.03	0.0097	0.315	0.225	0.03	0.650
23	0.02	0.03	0.0053	0.27	0.25	0.08	0.650
24	0.09	0.03	0.0099	0.295	0.205	0.08	0.650
25	0.02	0.06	0.0097	0.27	0.25	0.08	0.650
26	0.09	0.06	0.0203	0.29	0.20	0.08	0.650
27	0.02	0.06	0.0097	0.29	0.27	0.03	0.650
28	0.09	0.06	0.0208	0.345	0.255	0.03	0.650

Table C2. Performed measurements with ship